CEMCAP

Co-funded by the European Union

Grant Agreement Number:
641185

Action acronym:
CEMCAP

Action full title:
CO_2 capture from cement production

Type of action:

H2020-LCE-2014-2015/H2020-LCE-2014-1

Starting date of the action: 2015-05-01
Duration: 42 months

D12.2
Results of entrained flow carbonator/ calciner tests

Due delivery date: 2017-04-30
Actual delivery date: 2017-04-04

Organization name of lead participant for this deliverable:
AGENCIA ESTATAL CONSEJO SUPERIOR DE INVESTIGACIONES CIENTIFICAS

Project co-funded by the European Commission within Horizon2020		
Dissemination Level		
PU	Public	X
CO	Confidential , only for members of the consortium (including the Commission Services)	

Deliverable number:	D12.2
Deliverable title:	Results of entrained flow carbonator/ calciner tests
Work package:	WP12 x Calcium Looping (CaL) capture
Lead participant:	USTUTT

Author(s)		
Name	**Organisation**	**E-mail**
Borja Arias	CSIC	borja@incar.csic.es
Sandra Turrado	CSIC	s.turrado@incar.csic.es
Mónica Alonso	CSIC	mac@incar.csic.es
Gregorio Marbán	CSIC	greca@incar.csic.es
Carlos Abanades	CSIC	abanades@incar.csic.es

Abstract

This document reports the progress to date in the investigation of reactor components in integrated Calcium Looping systems designed to use entrained bed reactors for the step of CO_2 capture by carbonation (Romano et al. 2013), (Spinelli et al. 2016), after the generation of a sufficient flow of active CaO by calcination of a Ca-rich raw material.

New experimental work in a thermogravimetric analyser has been carried out, at the limits of detection of this equipment, in an attempt to elucidate the role of belite formation during fast calcination of different raw meals as this parallel reaction was found to deactivate the calcined material towards CO_2 capture (see MS12.2). The new tests have revealed great differences in behaviour among raw meals depending on the level of aggregation of Ca and Si elements. CO_2 activities towards CO_2 as low as 0.1 have been measured for a marl-type raw meal after a first calcination of the material in less than 1 minute, in rich CO_2 and $H_2O_{(v)}$ atmospheres at just over 900ºC. In contrast, other raw meals containing mixed $CaCO_3$ grains in the micrometre scale are able to sustain activities of CaO towards CO_2 over 0.6 (i.e. very similar those of parent limestones).

On the other hand, in order to carry out CO_2 capture test with gas/solid contact times in the range of those expected in entrained reactor systems, a new retrofit has been completed of the 30 kW_{th} Calcium looping pilot used earlier for the CFBC test (see D12.1). Many challenges related to the feeding of a continuous flow of calcined powdered solids to the system, or with the operation of gas/solid contact under differential conditions, have been found and partially solved. Tests with different activity material have been carried out, measuring experimental conversion of gas (CO_2 concentration profiles) for gas/solid contact times between 0.5-6 seconds. Results follow trends that can be interpreted with a simple plug flow reactor model when changing solid flow rates, gas flow rates (residence time of gas and solids in the reactor) and CO_2 concentration at the inlet of the reactor. These results should allow for a suitable tuning of kinetic expressions for the carbonation reaction (in progress for MS12.5) expected to support the reactor design of the "integrated CaL" process.

This project has received funding from the European Union's Horizon2020 Research and Innovation Programme under Grant Agreement No 641185

TABLE OF CONTENTS

Page

This project has received funding from the European Union's Horizon2020 Research and Innovation Programme under Grant Agreement No 641185

1 SCOPE AND INTRODUCTION

This document reports the progress achieved within the CEMCAP project (up to April 2017) investigating the performance of reactors components in Calcium looping systems designed to use entrained bed reactors for the step of CO_2 capture by carbonation, after the generation of active CaO by calcination of a range of Ca-rich materials. According with the schedule of deliverables and milestones in the project work programme, it must be noted that there are two additional documents closely linked to this deliverable, and that are expected to be delivered in the next few months: D8.3 "Assessment of calciner test results" in WP8 (M30) and MS12.5 "Completion of CaL entrained flow tests" (M32). Therefore, the information presented in this deliverable D12.2 will be refined and expanded when drafting these later documents. In particular milestone MS12.5, expected to support with the latest experimental information the reactor design of the "integrated CaL" process (Romano et al. 2013, Spinelli et al. 2016) under development in CEMCAP (see also MS12.1, "Experimental matrices for fluidized bed and entrained flow" and "CaL process model for first WP4 process design and integration study").

One of the central ideas behind the integrated CaL configuration is the use in the CO_2 capture step of typical particle sizes of cement plants (≈10-20 μm on average), which makes the adoption of entrained flow CaL reactors the preferred design option (Romano et al. 2013, Spinelli et al. 2016). Furthermore, because of the large make up flows of calcium characteristic of CaL in cement plants, the ratio of fresh calcium entering the system per unit of CO_2 captured is necessarily very high (up to two orders of magnitude higher than the typical values for other postcombustion applications of CaL). This should lead to higher activity materials in the calcium loop, which will allow for an effective CO_2 capture even with the short gas-solid contact times characteristic of entrained bed reactors.

On the other hand, some uncertainties about the activity of the calcined material (or CO_2 carrying capacity, defined as the fraction of active CaO able to react with CO_2 in a "fast reaction mode") were identified in previous deliverables when investigating sorbent deactivating reactions by belite formation (see MS12.2). Therefore, an update of the current of understanding of these kinetic limitations is provided in this deliverable. As will be discussed below (see section 3), the problem of deactivation by belite formation in the calciner is currently being narrowed down to a certain type of raw meals (like marls) where there is a proximity, perhaps at atomic level, between the reacting Ca and Si species. A more comprehensive kinetic study on this topic is expected in MS12.5.

On the other hand, and to our knowledge, there is no previous experimental information published on the carbonation of fine CaO particles in entrained bed conditions. These reactors should be operated under conditions as close as possible to those expected in CaL systems capturing CO_2 from cement plant (i.e., gas-solid contact times in the range of seconds, high CO_2 concentration, highly active sorbent in the solid circulation loop, fine particle sizes to facilitate clinker reactions in the rotary kiln etc.). Therefore, the main specific target of this Deliverable 12.2 has been to experimentally investigate this reactor configuration using as a basis the existing high temperature reactor facilities for CaL at INCAR-CSIC (see D12.1). These have been extensively retrofitted to accommodate suitable feeding and sampling methods of gases and solids to monitor the progress of reaction when operating in entrained mode. The necessary retrofits to achieve this target, have been much more problematic than expected, mainly because the complex fluid-dynamics of the fine solids when fed to the reactors, and because of the many

This project has received funding from the European Union's Horizon2020 Research and Innovation Programme under Grant Agreement No 641185

difficulties experienced with the actual feeding system of a small, disperse flow of active solids to the reactors (see section 2 below and Appendix), for which no commercial equipment has been found. Despite these difficulties, many successful series of experimental results have been achieved, as discussed in section 4 of this deliverable. The interpretation of results with reactor models adapted to the experimental set up will be further refined towards MS12.5.

This project has received funding from the European Union's Horizon2020 Research and Innovation Programme under Grant Agreement No 641185

2 EXPERIMENTAL FACILITIES AND MATERIALS

2.1 Thermogravimetric test

As discussed in M12.2 ("Reaction rates under new carbonation and calcination conditions for integrated CaL") thermogravimetric (TG) analysis of carbonation and calcination reactions has been a suitable technique for calcium looping applications for many years. There is a vast literature on kinetics studies of carbonation and calcination reactions relevant for standard CaL applications (where particles residence times are in the order of the minutes) (Martínez et al. 2016). However, the application of the TG analysis to kinetic problems relevant for the entrained bed reactors in the integrated CaL process under development in CEMCAP is much more challenging. This is because many important phenomena may be occurring in time scales of a few seconds, which will be also the time scale of many of the changes in the TG experimental set up (for example the "fast switch" of temperature and gas compositions around the sample may no longer be "fast" if this change is taking place under similar times scales than those of the main reactions). Indeed, the most relevant reactions for the entrained bed reactor configurations under development in the CEMCAP project fall in this category: the calcination reactions of fine particles (like raw meals) at temperatures over 900ºC, carbonation reactions under rich atmospheres of CO_2 and $H_2O_{(v)}$, or the belite formation reactions at these high temperatures can all be sufficiently fast to push the detection limits of the TG analysis.

Therefore, a first task for the TG analysis conducted in this deliverable with different raw meals has been to recalibrate the TG experimental set up of INCAR-CSIC, which is shown in Figure 2.1. This is an in-house design extensively used for long multicycle carbonation/calcination testing and shown to be less affected by errors detected when using other commercial equipment (Alonso et al. 2014). It contains a precise microbalance (CI Instruments) that continuously measures the weight of the sample, which is suspended in a platinum basket. The TG analyser currently consists of a mullite tube (2.54×10^{-2}m o.d.) placed inside a two-zone furnace capable of working at temperatures of up to 1000ºC and at different temperatures in each furnace zone. For the tests described in this work, the sample pan was located in the upper furnace position. The bottom part of the oven was used to preheat the mixture of steam and air before they reached the sample. The temperature of the sample is measured with a thermocouple placed 5 mm below the pan and continuously recorded by a computer. The calibration of the thermocouple is needed to ensure the reliability of measurements. The calibration of the thermocouple in this TG is carried out by using two reference points: the temperature of the decomposition of $CaCO_3$ to CaO in pure CO_2 (i.e. at 900 ºC, (Baker 1962)) and the temperature of the decomposition of $Ca(OH)_2$ to CaO in pure steam (i.e. at 519 ºC, (Barin 1993)), both at atmospheric pressure. The difference between these temperatures and those measured by the thermocouple during the calibration tests allows for the correction of thermocouple's measurements. The permanent gases (air and CO_2) used during the tests come from bottles whereas the steam is generated from distilled water contained in pressurized cylinders (4 bar). The flowrate of water is controlled through a Bronkhorst liquid mass flow controller. Liquid water is vaporized downstream by means of 2 heating tapes of 700 W each one. The temperature of the heating tapes is adjusted by means of a temperature controller. A continuous and steady flow of steam is generated during the test. A three-way pneumatic valve connected to the heated pipeline allows a continuous flow of steam during the change from steam conditions to non-steam conditions (or vice versa).

This project has received funding from the European Union's Horizon2020 Research and Innovation Programme under Grant Agreement No 641185

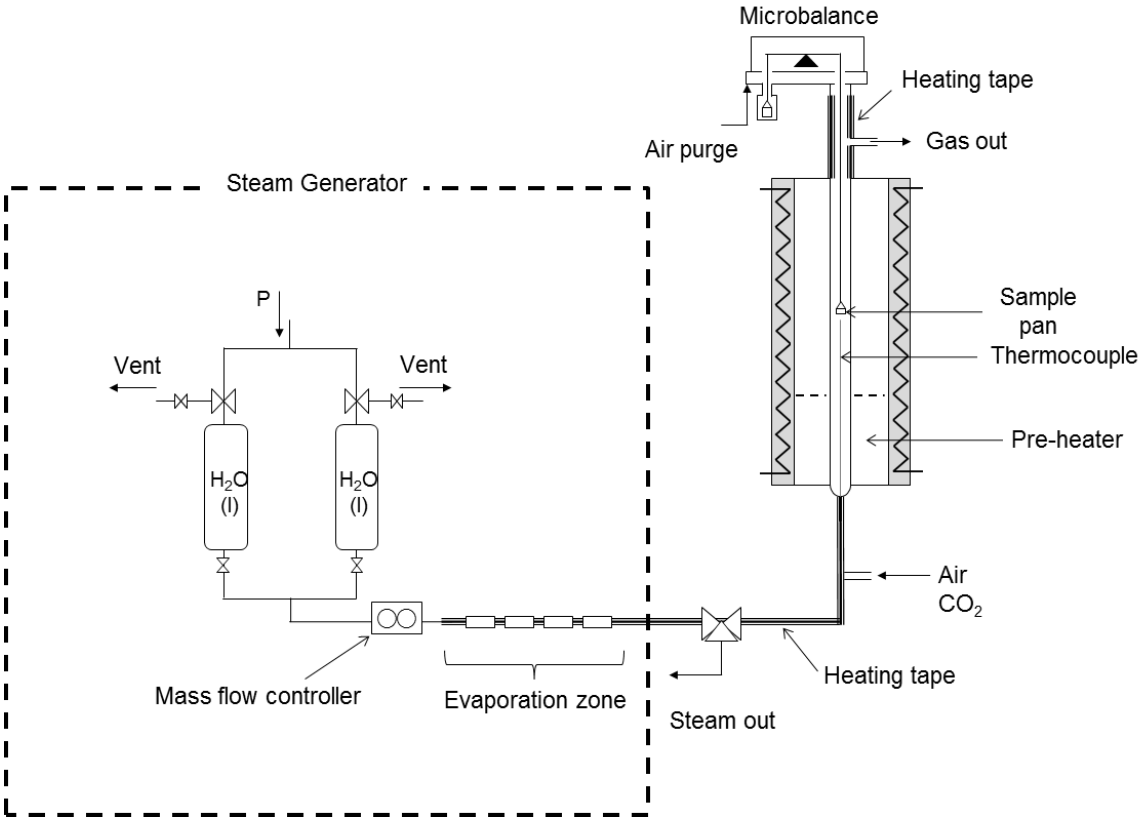

Figure 2.1 Scheme of the multicycle TGA at INCAR-CSIC highlighting the new steam generator.

As described in M12.2, the external diffusion resistances have been minimised during diffusional calibration tests, by operating with initial sample weights around 3 mg of raw meals and a total gas flow of $7.22 \cdot 10^{-6}$ Nm^3/s (this means that the results are not affected by further reductions in sample mass or by further increases in the gas flow rate). A typical test of carbonation starts after a calcination step where the sample has been completely calcined. Then, the sample is cooled down from the calcination temperature to the carbonation temperature (i.e. 650 ºC) in air atmosphere. Once a stable temperature and a stable weight measurement are reached, the reacting atmosphere is changed to 10 vol.% CO_2 in air while maintaining the gas velocity around the sample for at least 5 minutes. There is initially a rapid increase in the weight of the samples due to the kinetic control step of the carbonation reaction. After that, the reaction rate decreases abruptly because the diffusional resistance of CO_2 across the calcium carbonate product layer becomes the control step (Curran et al. 1967, Barker 1973). The reaction rate can be estimated from the change in the CaO conversion (i.e. defined as moles of CO_2 absorbed per initial mol of CaO) with time. Figure 2.2 shows two examples of carbonation tests over a limestone and the raw meal RM1 (natural marl) after the calcination step. As can be seen in this Figure, the change from kinetic control to diffusional control can be easily determined by the change of the slope of the curve. Moreover, the reaction rate during the kinetic control step can be easily estimated as it is the slope of the curve in the first seconds of the reaction.

This project has received funding from the European Union's Horizon2020 Research and Innovation Programme under Grant Agreement No 641185

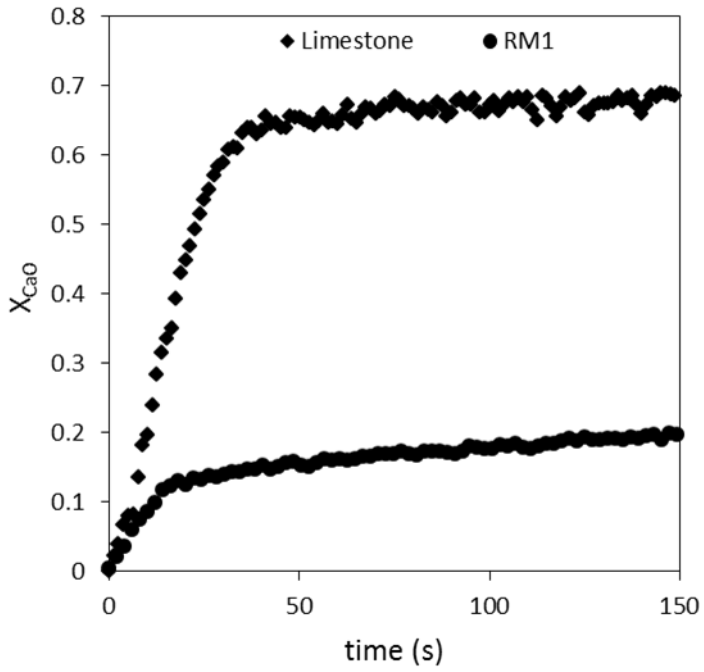

Figure 2.2 Example of carbonation tests in the TGA.

All carbonation tests presented in this deliverable were carried out following the experimental procedure described above.

2.2 Analysis of raw materials and solid samples

Three different raw meals from different cement plants in Spain and Italy (RM1-3) have been tested. They present similar chemical compositions (see Table 2.1) but very different particle size distributions (see Figure 2.3). An X-Ray Fluorescence Spectrometer (SRS 3000 Bruker) was used to determine the chemical composition of the samples following the fused cast-bead method (PERLX'3 Philips). The particle size distributions were measured by a Beckman-Coulter LS 13320 laser diffraction particle size analyser in wet mode, in which ethanol was used as a dispersant agent. Apart from that, a reference limestone from Spain in powder form (see Fig 2.1) was used to prepare two "synthetic raw meals" that have also been used in some tests. Both synthetic raw meals were prepared by mixing 84 wt./wt % of the limestone with Aerosil 380 ® (Evonik Co., fumed silica, 380 m^2/g, 7 nm of particle diameter). One of them (called SRM-DM) was prepared in a dry mode using a laboratory mixer, whereas the other one (called SRM-WM) was prepared in a wet mode using deionized water. The prepared solution was subsequently centrifuged and dried during one night in an oven at 110 ºC.

This project has received funding from the European Union's Horizon2020 Research and Innovation Programme under Grant Agreement No 641185

Table 2.1 Chemical composition of the raw meals and limestone measured by XRF

Oxide (%wt.)	RM1	RM2	RM3	Limestone
CaO	42.7	36.3	42.3	54.2
Al_2O_3	4.1	3.9	2.6	0.4
SiO_2	13.4	18.4	15.5	0.9
Fe_2O_3	1.9	2.2	1.6	0.4
K_2O	0.9	1.1	0.5	
MgO	0.7	1.3	0.9	0.8
MnO		0.1	0.1	
SrO			0.1	
TiO_2	0.2	0.2	0.2	
SO_3	1.0	1.4	0.2	0.1
LOI*	35.0	35.2	35.9	43.2

*Loss On Ignition

Figure 2.3 shows the particle size distributions of the commercial raw meals (RM1-3) and the reference limestone obtained by means of laser diffraction. Although the tested materials have a similar average particle size (i.e. d50 between 8 and 9 μm), the results reveal that raw meals RM2 and RM3 seem to be mixtures of separate compounds, as different volumetric fractions are observed clearly separated for certain particle size ranges. However, RM1 and the limestone present more homogeneous particle size distributions.

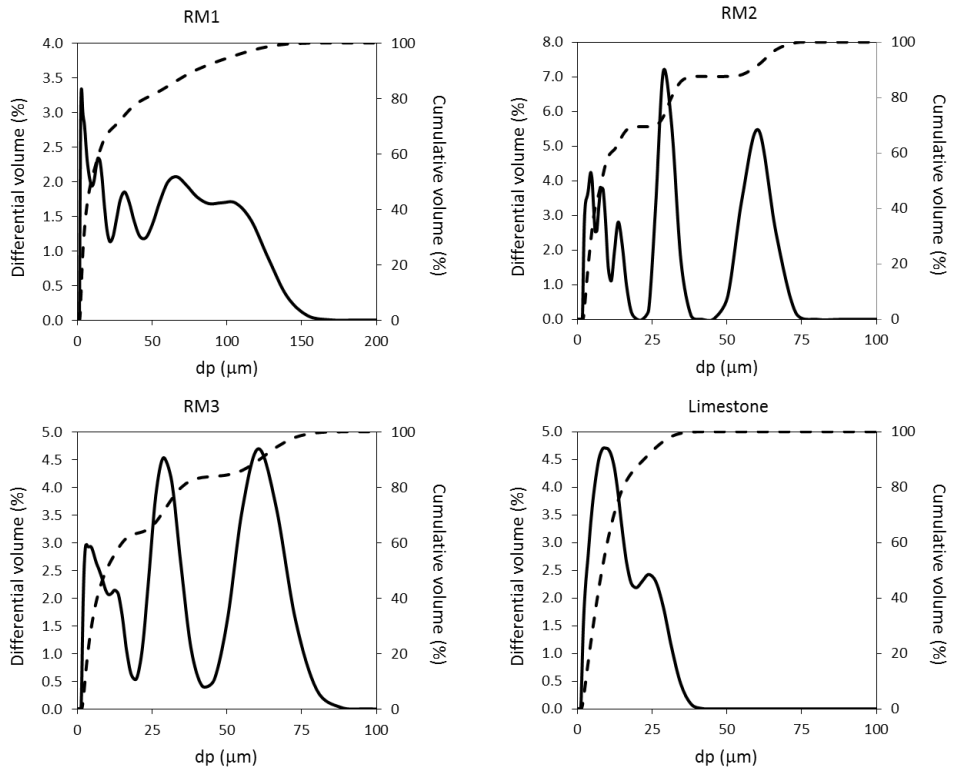

Figure 2.3 Particle size distributions of the commercial raw meals and limestone obtained by means of laser diffraction.

This project has received funding from the European Union's Horizon2020 Research and Innovation Programme under Grant Agreement No 641185

Scanning electron microscopy (SEM, Quanta FEG 650 microscope) equipped with an energy-dispersive X-Ray (EDX) analyser (Ametek-EDAX with an Apollo X detector) was used to evaluate the level of aggregation of the Ca/Si elements in the materials tested. However, these analyses only have shown to be conclusive when working with mixtures of the limestone and SiO_2 particles (i.e. the synthetic raw meals). Figure 2.4 shows examples of SEM images obtained by using back-scattered electrons (BSE) for the SRM-WM and SRM-DM samples. This technique shows those compounds with higher density in brighter colours, which facilitates the detection of possible changes in the chemical compositions (through changes in the molecular weight) or texture (i.e. apparent density) of the particles observed in the samples.

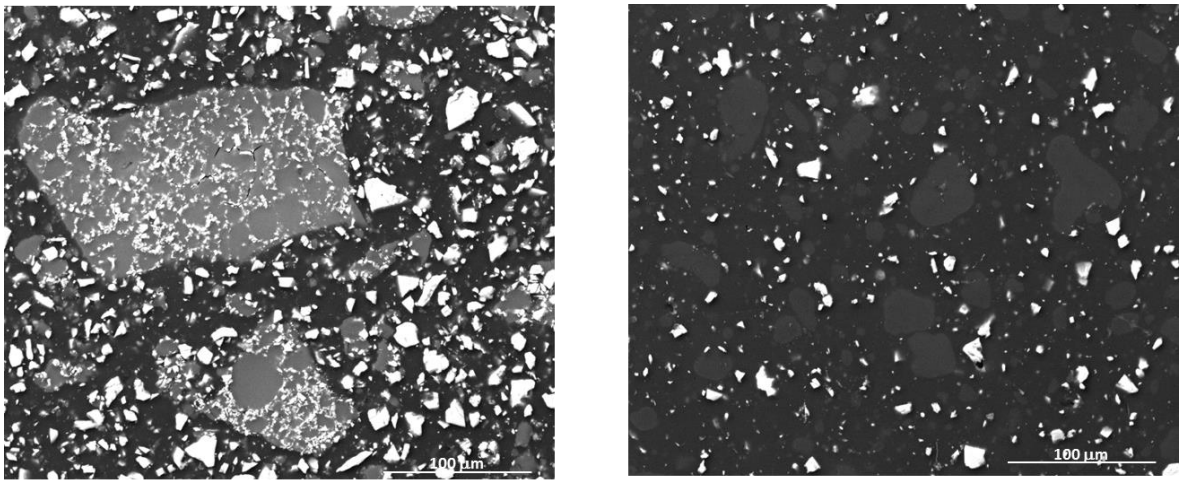

Figure 2.4 SEM-BSE images of synthetic raw meals. Left: SRM-WM. Right: SRM-DM.

As can be seen in Figure 2.4, silica particles observed in the wet mixture (Figure 2.4 Left, large light grey particles) are larger and with higher apparent density than silica particles observed in the dry mixture (Figure 2.4 Right, medium size, dark grey particles). In both figures, the $CaCO_3$ rich particles are the smallest and brightest. The particle size of the SiO_2 particles is just 7 nm. Therefore, it is clear from both figures (but especially in Figure 2.4 left) that there is a very high tendency of these silica nanoparticles to form agglomerates of several hundred microns. Another indication of this is that, although the weight fraction of limestone in both raw meals is the same (84 wt.%), the area fraction of limestone looks lower due to the large size of the silica agglomerates. As a result, due to the presence of these large agglomerates, little level of aggregation between limestone (white particles) and silica was observed in the dry mixture, despite the nominally low size of the individual particles of both $CaCO_3$ and SiO_2. This situation still persists in the wet mixture, but clearly improves, as the silica agglomerates seem to be better covered by limestone particles. This should translate into a higher level of aggregation between both components that will enhance the rate of formation of belite as will be discussed below.

In order to identify the main chemical species present in the sorbents before and after calcination and carbonation tests, X-Ray diffraction (XRD) tests were performed using a Bruker D8 powder diffractometer equipped with a CuKα monochromatic X-Ray tube, a Göbel mirror in the incident beam and a parallel-slits analyzer in the diffracted beam. Diffraction data were collected by step scanning using a step size of 0.02º, a scan step of 1 s and a scan range of 5º to 60º 2θ. An example of these observations is shown in Figure 2.5.

This project has received funding from the European Union's Horizon2020 Research and Innovation Programme under Grant Agreement No 641185

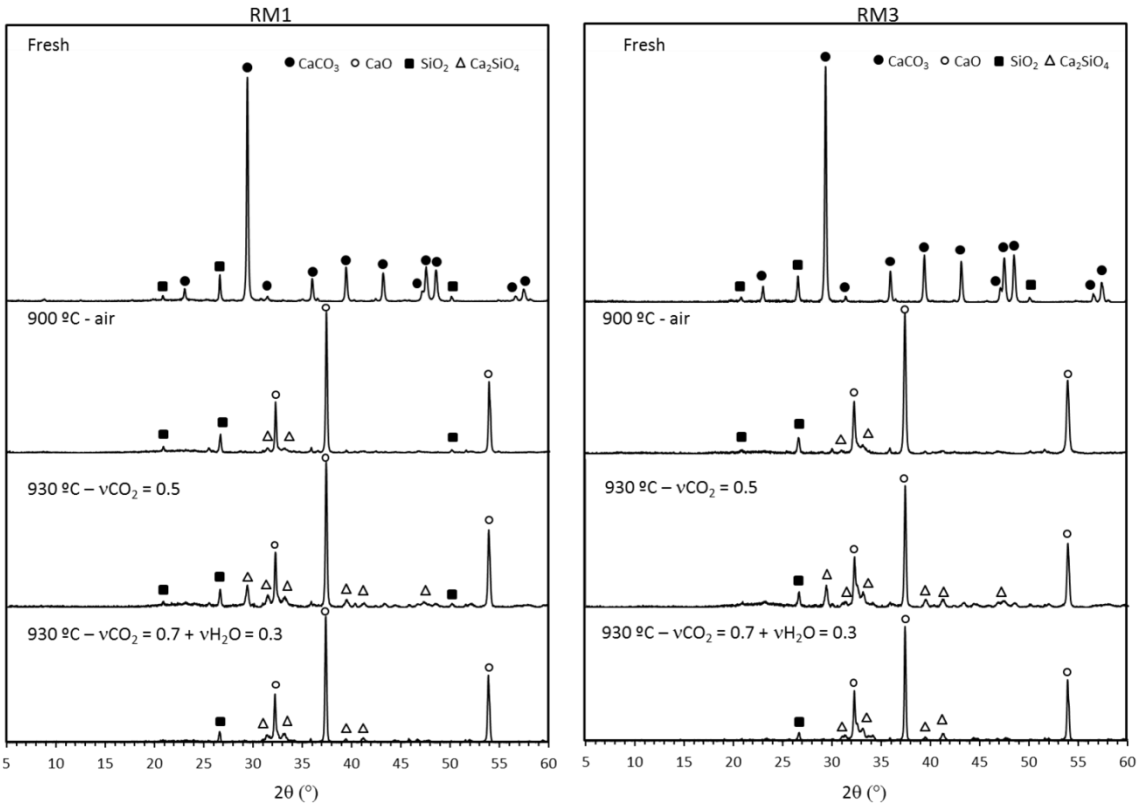

Figure 2.5 Example of XRD patterns of fresh and calcined samples (obtained under different calcination atmospheres) of RM1 and RM2 raw meals.

As can be seen in Figure 2.5, the calcium silicate (Ca_2SiO_4, or belite) could form during the calcination of both raw meals carried out in air at 900 ºC. The increase in the temperature and the presence of CO_2 and steam during the calcination seemed to promote the formation of belite, as the number and/or the intensity of the peaks owing to belite increased under these conditions.

2.3 Description of the entrained carbonator pilot set up

The entrained bed carbonation tests have been carried out using as a basis the high temperature reactors available at INCAR-CSIC for circulating fluidized CaL systems (rated at 30 kW_{th}). This included the new heating elements installed in these reactors (see D12.1), which allow a more even temperature distribution over a large fraction of the 6.2 m length of the reactors. However, since this kind of lab scale longitudinal dimension is very small compared to the 40-80 m expected in industrial applications, it is not possible to fully reproduce gas and solid residence time and contact mode of an industrial system. A certain sacrifice is compulsory on some key operating variables (i.e. gas velocity, gas/solid ratios etc.).

On the other hand, to facilitate data analysis and scalability of results, we have chosen to conduct all the experiments in "differential conditions" respect to the gas. This means that only modest changes in CO_2 concentration are allowed during the carbonation test, so that all particles entering the reactor will experience, ideally, a similar, controlled and measurable reaction environment. As in other G/S reaction systems, this kind of set up allows access to experimental data that can reveal reaction kinetics and other reaction phenomena in very short

This project has received funding from the European Union's Horizon2020 Research and Innovation Programme under Grant Agreement No 641185

gas solid contact times (few seconds) of no easy access from other experimental set ups (i.e. thermogravimetric analysis as described in the previous section 2.1).

The operation of the a carbonator reactor in such entrained mode, with very low solid loading to allow differential conditions respect to the gas, requires a very careful control of temperature profiles in the reactor. This is because, in the absence of the huge heat transfer capabilities of solid circulation streams in the reactor (as it is the case during CFB CaL test campaigns), large difference in temperature could observed between the bottom and the top of the reactor, especially when there is reactions. To balance heat losses (especially in the top 3 m of the reactor set up), the carbonator was equipped with five ovens with an individual capacity of 3.0 kW_e installed in the first 2.5 m of the reactor. Four additional heating elements (1.5 kW_e) have been installed in the upper part of the carbonator with their individual temperature control system to facilitate the control of the carbonator temperature profile in the interior of the reactor.

The upper part of the risers is isolated using ceramic refractory fibre. In the Appendix A1, there is description of the different experimental set ups that have been used for entrained reactor testing and the rationale behind the decisions to introduce new retrofits on the pilot, in order to achieve the results as described below in section 3. The final configuration yielding most of the valuable experiments reported in this deliverable is represented in Figure 2.6.

This project has received funding from the European Union's Horizon2020 Research and Innovation Programme under Grant Agreement No 641185

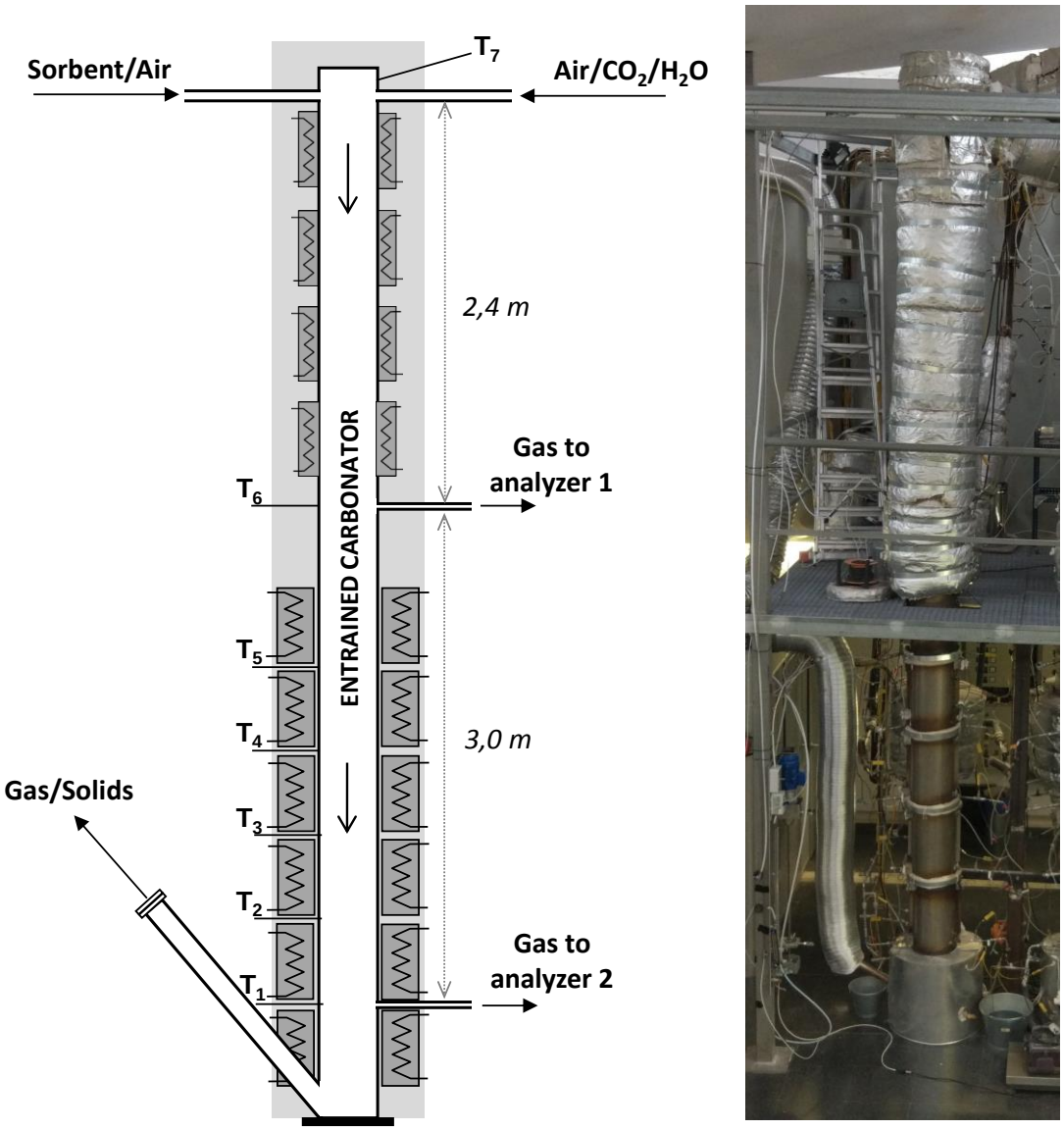

Figure 2.6 Scheme and picture of the down-flow carbonator reactor set up used during carbonation test in entrained mode (gas and solids moving downwards).

In this configuration, gas and solids are injected at the top of the carbonator and move downwards. As discussed on Appendix A2, several feeding systems and modifications have been tried to feed and disperse the fine powders tested during these experiments. The most successful configuration is shown in Figure 2.7. It consists in a cylindrical reservoir where the fine solids are loaded at the beginning of each experiment. In a typical experiment, a batch of 150-450 g of calcined CaO-rich material is loaded in the cylinder depending on the bulk density of the solids.

This project has received funding from the European Union's Horizon2020 Research and Innovation Programme under Grant Agreement No 641185

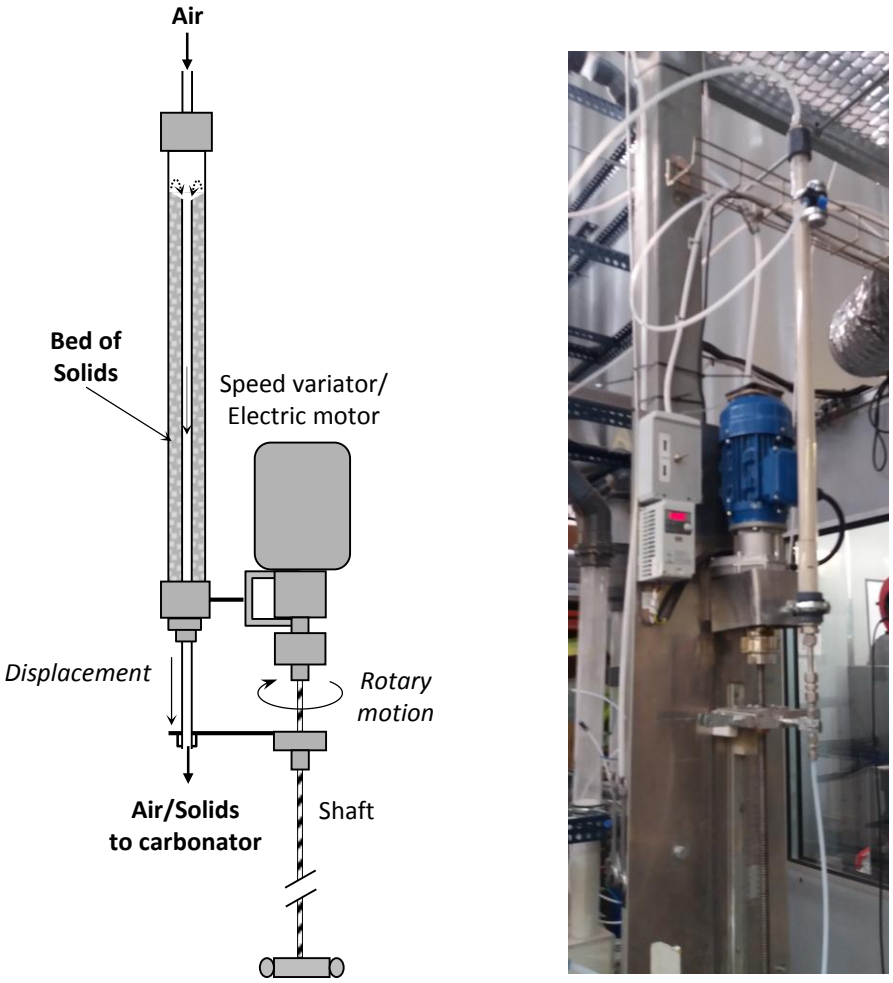

Figure 2.7 Scheme of the solid feeding system used in most the carbonation test in entrained mode (gas and solids moving downwards).

Inserted in the bed of solids, there is a drain tube that can be moved downwards in order to remove the solids from reservoir. The rate of removal of solids from the reservoir is proportional to the vertical displacement velocity of the tube which is connected to a mechanical system. This system consists in a shaft connected to an electric motor equipped with a speed variator to control the rotary speed. The maximum rate of displacement is 5.6 m/h which allows for solids feeding rate up to 8 kg/h. A vibration device installed in the reservoir helps to level the profile of solids in the discharge point and to maintain a uniform solid flow rate.

An adjustable conveyor air flow is injected into the reservoir through the top, in order to disperse and transport the solids through a pipe to the inlet of the carbonator. The air flow rate is adjusted manually with a needle valve and measured using a rotameter. Typical gas velocities in the pipe are around 30-40 m/s and 0.5 m/s in the reservoir of solids.

The simulated flue gas for carbonation is fed to the reactor by mixing air, CO_2 and steam (when relevant). Air supply to the reactor comes from a blower with a maximum capacity 90 m^3/h respectively. Air supply to the solid feeder comes from a compressor at 5 bar. A liquid Deward of CO_2 is used to feed this gas into the carbonator. Air and CO_2 flow rates are adjusted

This project has received funding from the European Union's Horizon2020 Research and Innovation Programme under Grant Agreement No 641185

using mass flow controllers to generate a synthetic combustion flue gas. A small steam generator has also been installed to supply a continuous flow of water vapor to the carbonator up to 2.0 kg H_2O/h. In the down flow configuration shown in the Figure 2.6, the mixture of air/CO_2/H_2O is pre-heated at temperatures around 250-300 ºC before being fed into the entrained carbonator by using the second riser of the 30 kW_{th} pilot facility (not shown in the Figure for simplicity).

A very high efficiency cyclone (from Air Classify for PM10 sampling) has been used in some experiments to capture solid samples at different times. These solid materials have been characterized to measure rate of reaction towards CO_2 and CO_2 maximum carrying capacity as well as particle size distribution and $CaSO_4$ content in some cases.

Most of the experiments were carried out by measuring the gas composition at 5.4 m from the solids injection points. However, some experiments were conducted by measuring simultaneously the gas composition at two different heights (2.4 and 5.4 m respectively). For this purpose, two gas analyzers (ABB EL3020, ABB AO2000) were used. Each gas sampling port is equipped with a particulate filter and a gas sampling dryer system in order to protect the analyzers from the sorbent particles and moisture (in the case of the experiments carried out with steam). Seven ports along the reactor are used to measure the temperature profile. Each oven has its own independent controller in order to adjust the temperature in each zone of the reactor. All the electric signals from the thermocouples, pressure transducers, gas analyzers, and mass flow controllers are collected in a computer using a data logger.

This project has received funding from the European Union's Horizon2020 Research and Innovation Programme under Grant Agreement No 641185

3 EXPERIMENTAL RESULTS AND DISCUSSION

This section reports the experimental results when investigating the carbonation kinetics of CaO particles in reactor components of the "integrated Calcium Looping systems", designed to use entrained bed reactors for CO_2 capture by carbonation in cement plants (Romano et al. 2013, Spinelli et al. 2016). It must be noted that this process concept has lower TRL than the standard CaL concept involving interconnected circulating fluidised bed reactors (or "tail end" postcombustion CaL process described in MS12.4 and by Hornberger et al (Hornberger et al. 2016). Then later has been widely tested within the CEMCAP project at TRL 4 (see D12.1 and (Arias et al. 2017) and validated at TRL 6 (Hornberger et al. 2016). However, the former requires further tuning of some kinetic information at particle level (first subsection 3.1 below) and more proof of concept data at TRL4. In this regard, section 3.2 reports for the first time some experimental results from the pilot at INCAR-CSIC, when retrofitted to operate under entrained bed conditions as described in section 2.3.

3.1 CO_2 capture rates of calcined solids when taking into account Belite formation

In an attempt to elucidate the role of belite formation during fast calcination of different raw meals, new experimental work in thermogravimetric analyser has been carried out as described in section 2.1. The role of belite formation, as a parallel reaction during calcination competing for the "active CaO" needed for CO_2 capture, was detected in previous experiments described in MS12.2 (see also Figure 3.1)

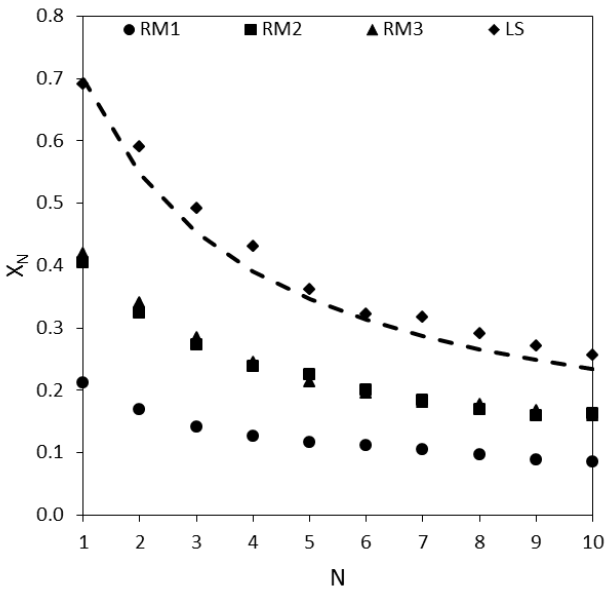

Figure 3.1 Evolution of the maximum molar conversion with the number of cycles for three raw meals (RM1-3) and limestone in TGA (calcination at 900 ºC in air for 10 min; carbonation at 650 ºC, 10 vol.% CO_2 in air for 10 min).

The impact of Belite formation on CO_2 carrying capacities (X_N) is self-explanatory in a typical plot of a carbonation-calcination TG test. In addition to the typical decay curve along cycling of

This project has received funding from the European Union's Horizon2020 Research and Innovation Programme under Grant Agreement No 641185

the parent limestone (LS points and discontinuous line in Figure 3.1) it is clear that the formation of belite promotes an additional deactivation of the CaO in the raw meals. The CaO deactivation due to belite formation mainly occurs during the first cycle. From that point onwards, the evolution of the maximum CaO conversion is similar to what is expected for pure CaO particles starting from the same value of CO_2 carrying capacity. It was also noted in M12.2 that the raw materials with a very intimate Ca-Si aggregation level, as it happens in the natural marl RM1 in Figure 3.1, the formation of belite is favoured, compared with raw meals that are mixtures of limestone-rich minerals such as RM2 and RM3.

In light with the previous comments, most of the new tests discussed below were focused on the first carbonation cycle only, after a single calcination step. All the experiments were carried out with the raw meals and synthetic mixtures of limestone and silica listed in Table 2.1. Figure 3.2 (left) shows the evolution with time of the CaO molar conversion for five raw meals during a carbonation test after a first calcination stage carried out in air at 900 ºC for 10 min. As can be seen, the maximum molar conversion of the CaO varied between 0.2 for the natural marl (RM1) and 0.55 for the synthetic raw meal in dry mixture (SRM-DM). The synthetic raw meal in wet mixture (SRM-WM), with a Ca-Si aggregation level higher than that of the dry mixture (see Figure 2.4), achieved a molar conversion of 0.4, which is similar to those achieved by the raw meals that are mixtures (RM2 and RM3). Therefore, these results confirmed great differences in behaviour among raw meals depending on the level of aggregation of Ca and Si elements when calcination times are around 10 min long.

When the calcination time is shortened to about 1 minute, which is the limit allowed by the TG equipment, the results are plotted in Figure 3.2 Right). CaO activities towards CO_2 higher than 0.5 can be observed for the raw meals that are mixtures of individual fine particles of $CaCO_3$ and SiO_2, including the synthetic raw meals. In contrast, the marl-type raw meal is only able to sustain activities of CaO towards CO_2 around 0.2 (i.e. similar to the previous test). These results demonstrate that longer calcination times promote the formation of belite, especially in those materials with higher Ca-Si aggregation, which deactivates a larger fraction of CaO. However, as long as particles rich in Ca and Si are separated at micrometric scale, and remain at calcination temperatures for less than 1 minute, the activity of the material towards CO_2 can remain close to the one expected for a calcined solid with the same fraction of pure limestone.

This project has received funding from the European Union's Horizon2020 Research and Innovation Programme under Grant Agreement No 641185

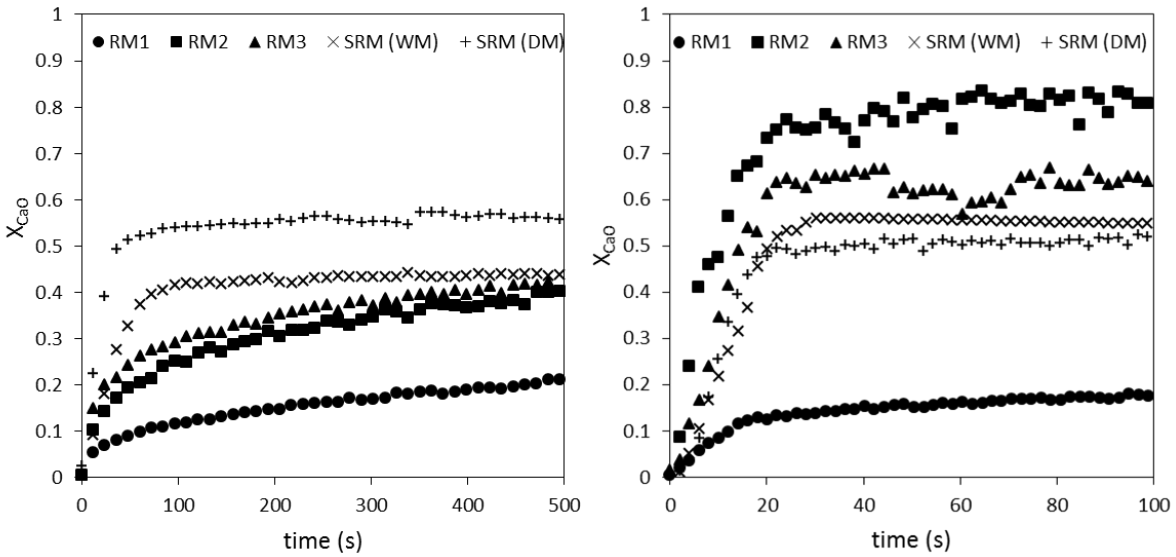

Figure 3.2 Evolution of CaO molar conversion in the first cycle. (carbonation at 650 ºC, 10 vol.%CO_2). Left: Calcination at 900 ºC in air for 10 min. Right: Calcination at 900 ºC in air for 1min.

The influence of the aggregation level between the Ca and Si compounds on belite formation has been confirmed with other tests in which the calcination time and calcination temperature were modified. Figure 3.3, Left shows the evolution of CaO conversion in RM1 after calcination stages carried out for 1 minute at temperatures from 810 ºC to 910 ºC. For RM1, which is a marl-type raw meal, the maximum molar conversion of CaO was lower than 0.4 at all temperatures tested in spite of the very low calcination time. In contrast, for a mixture-type raw meal as RM3, higher CaO molar conversions can be achieved after calcination periods of 10 minutes (carried out at temperatures lower than 900 ºC (see Figure 3.3 Right)). These results demonstrate that CaO conversions similar to those achieved with CaO of limestone are feasible with mixture-type raw meals by performing at lower calcination temperatures and longer calcination times or at higher calcination temperatures during shorter calcination times (see Figure 3.2 Right). In view of these results, the use mixture-type raw meals as CO_2 sorbents for Ca-looping in entrained bed applications is clearly more desirable than the use of marl-type raw meals.

This project has received funding from the European Union's Horizon2020 Research and Innovation Programme under Grant Agreement No 641185

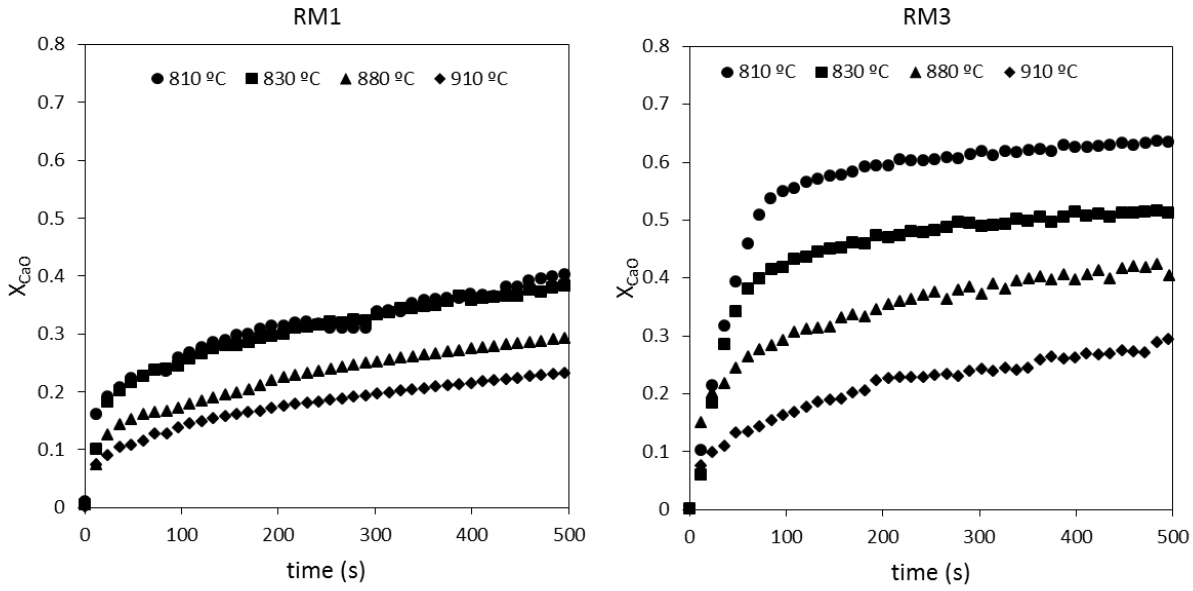

Figure 3.3 Evolution with time of CaO molar conversion during first cycle at different calcination temperatures in air (Carbonation, 650 ºC, 10 vol.%CO_2). Left. RM1, calcination time 1 min. Right. RM3, calcination time 10 min.

In all previous results, the calcination was carried out in air. However, CO_2 and steam are always present in realistic calcination environments. It is well known that CO_2 and steam have positive sintering effects on the nascent specific surface of CaO (Borgwardt 1989), leading to a fast decrease with time of the specific surface. The effect of the presence of CO_2 and steam during calcination on CaO conversion during the carbonation stage was studied and the results are plotted in Figure 3.4. As can be seen, the maximum CaO molar conversion achieved by RM2 after a first calcination at 945 ºC for 2 min in presence of 70 vol.% of CO_2 was 0.25, which is 50 % lower than the CaO conversion achieved in air conditions. However, the presence of steam seemed not to have further deactivation effect at these conditions. The drop in the carrying capacity of the solids observed due to the presence of CO_2 during the calcination could be due to an increase in the reaction rate of belite formation. So, as high CO_2 concentration in the calciner is unavoidable and taken into account the previous results, a further attempt to reduce calcination times was carried out, by increasing at the same time the calcination temperatures in the TG equipment.

This project has received funding from the European Union's Horizon2020 Research and Innovation Programme under Grant Agreement No 641185

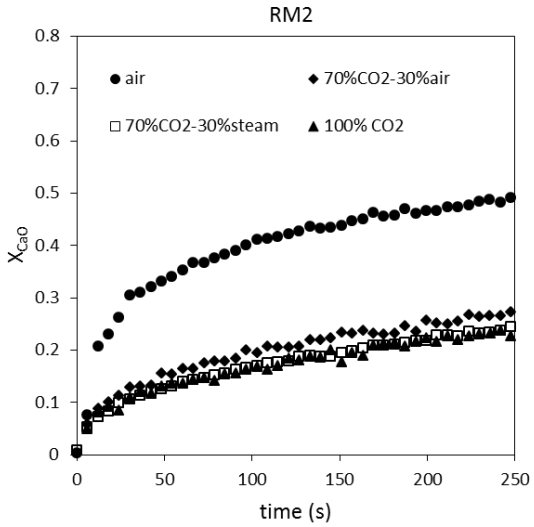

Figure 3.4 Effect of CO_2 and/or steam during calcination on the maximum molar conversion of CaO of RM2. (Calcination temperature 945 ºC, calcination time 2 min, Carbonation temperature, 650 ºC in 10 vol.%).

Figure 3.5 shows the evolution with time of CaO conversion for all raw meals and synthetic mixtures when the calcination was carried out at 930 ºC during 30s in 70 vol%. CO_2 and 30 vol.% steam. When the calcination time is as low as 30 s, the synthetic raw meals that seemed to have the lower Ca-Si aggregation level achieved a maximum molar conversion of 0.5, which is a similar value of that achieved by CaO from limestone at the same conditions. However, if the calcination time is increased to 10 min (white circles symbols), the synthetic raw meal achieved a maximum conversion similar to that of the marl-type raw meal (RM1), which is 50 % lower than the value achieved by CaO from limestone. It can also be noted that the mixture-type raw meals showed an intermediate behavior between synthetics and marl-type.

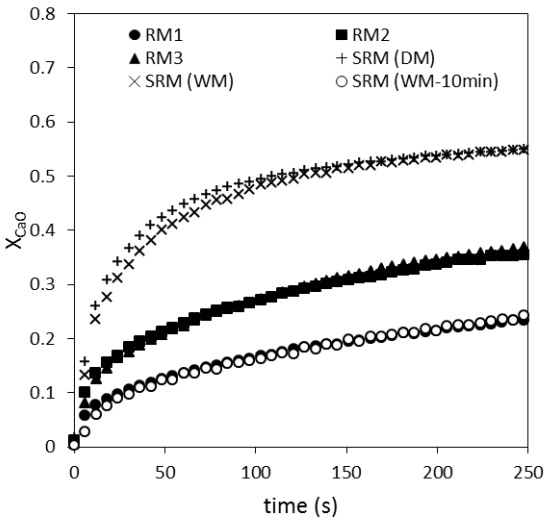

Figure 3.5 Evolution of molar conversion of the three raw meals and the synthetic mixtures after a calcination in 70 vol.%CO2 and 30 vol.% steam at 930 ºC for 30s.

This project has received funding from the European Union's Horizon2020 Research and Innovation Programme under Grant Agreement No 641185

In summary, the new TG test conducted under differential conditions and shorter reaction times clearly indicate that for Calcium looping applications it is preferable to use mixture-type raw meals instead of marl-type. In all cases, the calcination temperature and time should be as low as possible in order to prevent the belite formation that deactivates a large fraction of CaO in marl-type raw meals. Since belite forms from a solid-solid reaction, the aggregation level between Ca-Si strongly affects the kinetics of this reaction and hence the final value of free and active CaO available for carbonation reaction. Since the kinetics of belite formation will be different for different raw meals (due to the different aggregation level of Ca-rich and Si particles), it should be important to carry out specific kinetic studies for the target raw meals to support carbonator and calciner reactor designs.

3.2 Capture of CO_2 in entrained bed reactor

Section 2.3 described the final stage of a new retrofit of the 30 kW_{th} Calcium looping pilot (TRL4) used to carry out CO_2 capture test with gas/solid contact times in the range of those expected in entrained reactor systems. Other variants of the experimental set up and their challenges and experimental results are described in the Appendix A. Therefore, in the next paragraphs only experimental results with "down flow" of solids and gases are discussed, as this was the only set up and conditions in which a reasonable understanding of the solid flow pattern in the reactor (i.e. a plug flow respect to both the solids and the gas) could be validated. For this kind of experiments, it is possible to observe trends in the experimental results that are consistent with our current understanding of the kinetics of the carbonation reaction of materials with a certain fraction of active CaO (i.e. the fraction of free CaO that is able to react in the fast carbonation regime as discussed in M12.2). When these experimental observations are fitted to a suitable reactor model (this work is in progress towards delivery in M32 for the MS12.5), a useful and more reliable tool to support the reactor design of the "integrated CaL" process will be available.

Before discussing the results obtained, it is important to describe the experimental methodology followed to carry out these carbonation tests. A typical experiment starts with the preheating of the carbonator reactor. For this purpose, the temperature of the ovens is progressively increased to achieve the reaction temperature. An example of the heating up of the carbonator is shown in Figure 3.6a. Typically, around two hours are needed to increase the temperature from ambient conditions up to carbonation conditions, of around 650 ºC in the example.

A typical temperature profile during steady state conditions is shown in Figure 3.6 b. As can be seen the installation of the addition al elements improved the longitudinal temperature profile especially between 2.4 and 5.4 m which presents a maximum temperature dispersion of 50ºC. There is a lower temperature zone at the top of the carbonator reactor due to injection of the solids, the entry of carrier air a ambient temperature and the relatively low temperature of the preheated CO_2/air/H_2O mixture. As discussed below, this has implications in the analysis of the results, as the kinetics of the carbonation reaction at the top of the reactor would be too low to be considered part of the reaction zone. It is therefore necessary to estimate an effective reactor length as will be discussed below.

This project has received funding from the European Union's Horizon2020 Research and Innovation Programme under Grant Agreement No 641185

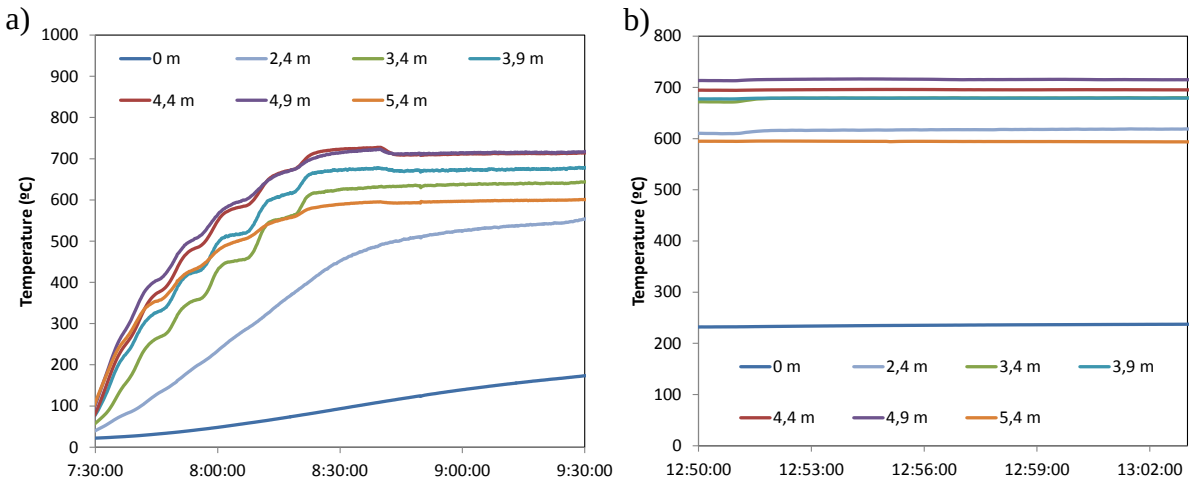

Figure 3.6 Examples of the pilot plant preheating before a carbonation test (a) and a temperature profile (b) during a carbonation test (distances referred from the solid injection point).

As described in Appendix A, our initial approach during the first series of carbonation tests was to collect solid samples in order to estimate the extent of the carbonation reaction from the chemical analysis of the sorbent particles, as well as from the signal obtained from the gas analysers. However, this approach proved difficult to be put in practice as the carbonation of the sorbent was detected to take place in the solids collection pot of the cyclone (due to the relative long residence times compared with the reaction time in the carbonator). Therefore, it was decided to use the measurement of the CO_2 concentration in the gas phase as the best source of information to follow the extent of the carbonation reaction and in turn the carbonation conversion of the calcined solids injected into the reactor. This approach was proven to be reasonably successful, as described in this section. This methodology requires the detection of small variations of the CO_2 concentrations in the gas phase. Thus, special care was taken to ensure reliable gas composition measurements (by very frequent calibration of equipment and entry concentration) in order to estimate as accurate as possible the amount of CO_2 disappearing from the gas phase and be able to close the carbon mass balances yielding solid conversion data (see below).

Figure 3.7 presents an example of the methodology followed during the carbonation tests and the CO_2 concentration measurement during different periods of a typical experiment. In this figure, CO_{2in} corresponds to the CO_2 concentration of gas fed into the carbonator and CO_{2out} corresponds to the experimental concentrations measured using two analyser installed in both gas sampling ports of the carbonator (at 2.4 and 5.4 m from the injection point respectively). The routine starts with feeding the mixture of air/CO/H_2O into the carbonator (Period 1). The mass flow rates of air and CO_2 fed into the carbonator with the mass flow controllers are verified by the measuring the gas composition with both gas analysers. Then, the conveyor air is fed into the reactor and the air mass flow rate is also validated with the measurement of the gas analysers (Period 2).

This project has received funding from the European Union's Horizon2020 Research and Innovation Programme under Grant Agreement No 641185

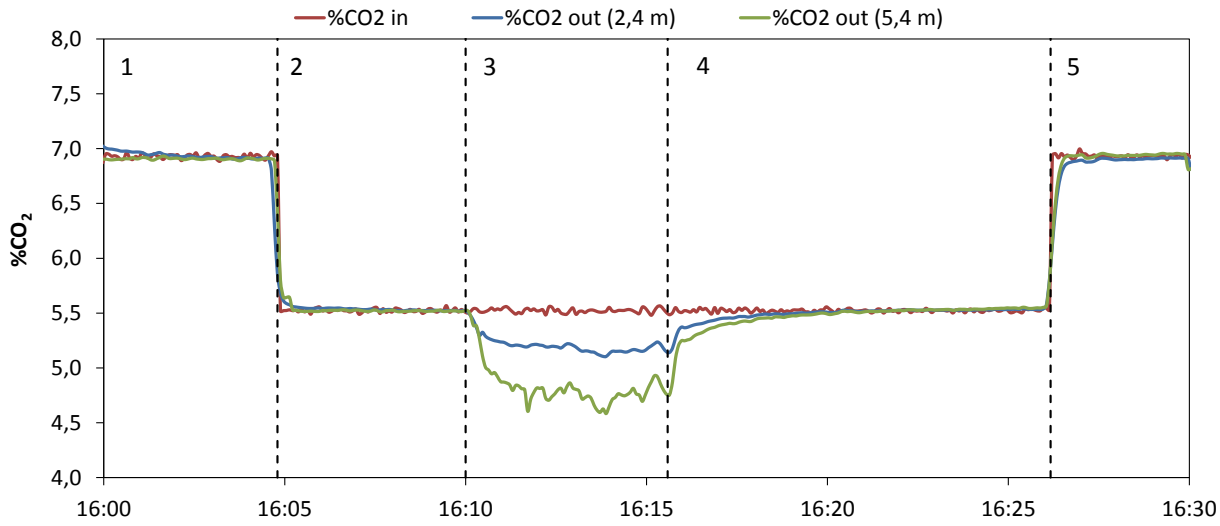

Period	Time	Description
1	16:00	Feeding the preheated mixture through the reactor
2	16:05	Injection of air feeding system to the carbonator
3	16:10	Feeding of sorbent
4	16:16	Stopping the feeding of sorbent
5	16:26	Stopping the air from the solid feeding system

Figure 3.7 Example of the typical experimental procedure during a carbonation test (average carbonator temperature=670 ºC, gas velocity=0.9 m/s, solid feed rate= 3.2 kg/h).

For this specific test, the reaction conditions are 5.5%$_v$ of CO_2. Once ensuring the experimental conditions along the reactor are stable, the solid feeding system is turned on and the sorbent is injected into the carbonator (Period 3). After a transition period of around 2 minutes, the CO_2 concentration reached a value of 5.16 and 4.75 at a height of 2.4 and 5.4 m, respectively. At 16:16, the feeding of sorbent is stopped (Period 4). At this point, the CO_2 concentration increases rapidly up to a transition point from which the concentration shows a slower increase until it reached the initial value. This second period has been attributed to the relatively slow carbonation of the sorbent particles collected in the filters installed in the gas analyser sampling ports. The residual carbonation in the filter has been taken into account and discounted from the CO_2 measurements to calculate the CO_2 captured in the carbonator reactor.

During this period, it is also important to check that initial the concentration of CO_2 is recovered after and before feeding the sorbent in order to verify that no problems have taken place (i.e. air infiltration in the lines of the CO_2 analysers). Moreover, the stability of the air and inlet mass flow rates during each experiment is validated by removing the conveyor air and measuring the CO_2 concentration at the inlet of the reactor (Period 5).

The main operation variables tested during the entrained carbonator reactor experiments is summarized in Table 3.1.

This project has received funding from the European Union's Horizon2020 Research and Innovation Programme under Grant Agreement No 641185

Table 3.1 Operating conditions and main variables during entrained carbonation test.

Carbonator temperature (ºC)	T_{carb}	590-720
Carbonator inlet velocity (m/s)	u_{carb}	0.5-2.0
Inlet CO_2 volume fraction to the carbonator	ν_{CO2}	0.05-0.30
Inlet Steam volume fraction to the carbonator	ν_{H2O}	0-0.25
Maximum CO_2 carrying capacity	X_{ave}	0.15-0.70
Solids flowrate (kg/h)		0.3-8.0
Average particle size of the sorbents used (µm)	d_{p50}	35-60

The main sets of experimental results obtained in the down flow configuration and presented in this section refer to CO_2 capture test carried out with a sorbent derived from calcined limestone. This has been obtained in the 30 kW_{th} pilot facility operating under the standard configuration with both circulating fluidized bed interconnected (see D12.1 for more details). An average CO_2 carrying capacity of 0.41 has been measured for this sorbent in a TG equipment following a standard procedure (carbonation conditions in TG: T_{carb}=650ºC, p_{CO2}=0.10, mass of sample=20 mg, reaction time=10 min). This is quite representative of the activity of raw meals described in section 3.1. Additional test with calcined raw meals from real cement plants can be attempted in the future if there is an interest in testing more realistic materials, although the results of section 3.1 indicate that the carrying capacity of the material in the first carbonation cycle fully determines the reactivity of the material towards CO_2 capture. Figure 3.8 shows the particle size distribution of this sorbent, which present average diameters of 50 µm.

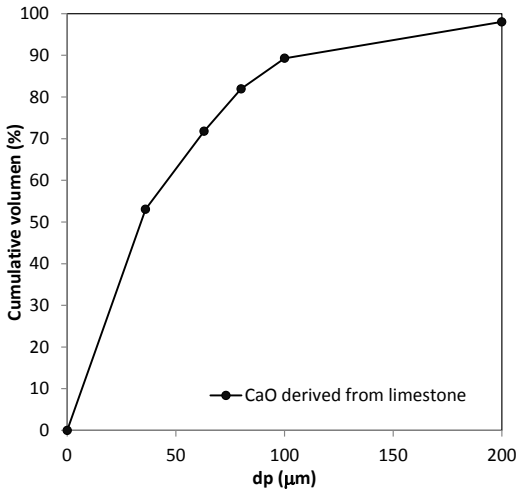

Figure 3.8 Particle size distribution the CaO sorbent used during entrained bed test and obtained from calcination test in the 30 kW_{th} pilot facility.

From the experimental information obtained in each test, the following CO_2 mass balance can be solved:

$$\begin{pmatrix} CO_2\ removed\ from \\ the\ gas\ phase \end{pmatrix} = \begin{pmatrix} CaCO_3\ formed\ in\ the \\ stream\ of\ CaO \end{pmatrix} \quad (3.2.1)$$

or

This project has received funding from the European Union's Horizon2020 Research and Innovation Programme under Grant Agreement No 641185

$$F_{CO2in} - F_{CO2out} = F_{Ca}(X_{carb} - X_{calc}) \quad (3.2.2)$$

The molar flow rates of CO_2 at the inlet and outlet of the carbonator, F_{CO2in} and F_{CO2out} respectively, can be determined from the air and CO_2 flows coming into the reactor and from the measurement of the composition of the gas phase leaving the reactor. As indicated above, the mass flow rate of sorbent fed into the carbonator is adjusted with the rotary speed of the motor and the rate of displacement of the drain tube by knowing the bulk density of solids in the reservoir. However, the mass of solids in the reservoir is weighted before and after each test in order to determine the actual flow rate. Together with the composition of the sorbent, this is used to calculate the experimental molar flow of CaO (F_{Ca}) and in turn the increment of the carbonate content (X_{carb}-X_{calc}) of the sorbent as follows:

$$Increment\ of\ carbonate\ conversion = (X_{carb} - X_{calc}) = \frac{F_{CO2in} - F_{CO2out}}{F_{Ca}} \quad (3.2.3)$$

One important aspect to be discussed is the reaction time of the particles inside the carbonator reactor. Assuming that particles are effectively dispersed by the feeding systems and taking into account the average particle diameter of 50 µm, it has been calculated that the terminal velocity of the sorbent particles is about 0.05 m/s under the conditions used during these tests. As indicated in Table 3.1, gas velocities in the carbonator were one order of magnitude higher (between 0.5-2.0 m/s) than this value. Therefore, it can be approximated that the particle residence time in the reactor is given the gas velocity and can be modified with the mass flow rates fed into the carbonator.

Regarding the particle reaction time, it is important to take into account that there is a low temperature region at the top of the reactor (see for example the temperature profile shown Figure 3.6.b). Due to the configuration of the entrained carbonator, it is not possible to measure the gas composition or the temperature in this region which would allow determining the height at which the carbonation reaction starts. In order to interpret the results presented in this report, a reasonable assumption has been adopted considering that sorbent carbonation starts at 1 meter from the injection point where the gas/solid mixture is being preheated.

This project has received funding from the European Union's Horizon2020 Research and Innovation Programme under Grant Agreement No 641185

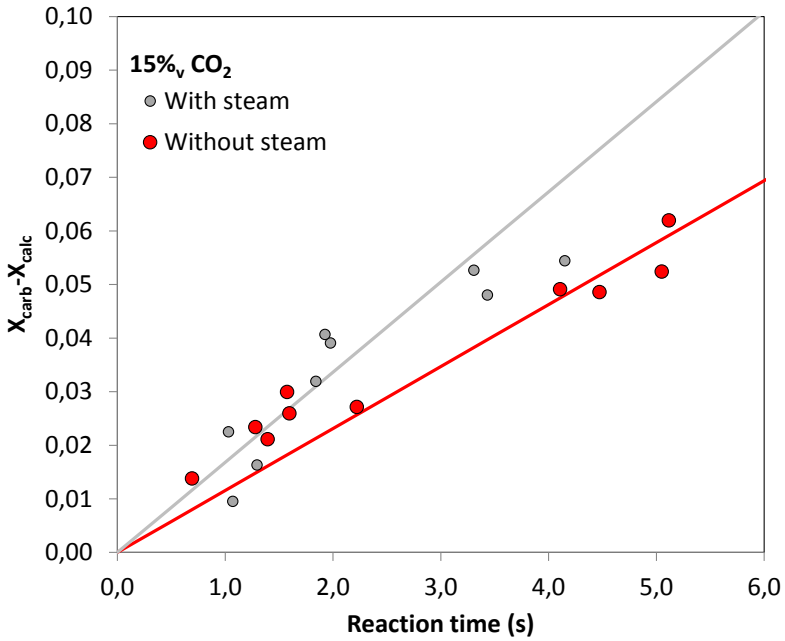

Figure 3.9 Evolution of the sorbent conversion with the reaction time under a reaction atmosphere with a 15%v CO_2.

As example of the results obtained following the experimental methodology and assumptions described above, Figure 3.9 shows the increment of $CaCO_3$ conversion of the CaO sorbent for different particle reaction times under a reaction atmosphere with a 15%v CO_2. In this figure, it can be seen that the linear increase of the carbonate content with the particle reaction time corresponding to the fast kinetic regime of the carbonation reaction (Barker 1973). This figure also includes the results of the tests were carried out by adding steam to the synthesis flue gas (15%v CO_2 and 20%v H_2O). As can be seen, the increment of carbonate conversion achieved during these tests is slightly higher during those experiments carried out with steam in the synthetic flue gas. The positive effect of the presence of steam on the CaO carbonation conversion has been already observed in several studies in TG and pilot plant by several authors (Sun et al. 2008, Yang and Xiao 2008, Symonds et al. 2009, Manovic and Anthony 2010, Arias et al. 2012, Donat et al. 2012, Dieter et al. 2014) including the results presented in D12.1 "Results from 30 kW_{th} CaL CFB experiments".

As indicated above, these results presented in this report will be used to derive data for a suitable tuning of kinetic expressions for the carbonation reaction. This analysis will be presented in MS12.5 as support for the designing of the carbonator reactor in the "integrated CaL" process. However, an initial analysis of the kinetics rates has been included in this report. For this purpose, a simple particle reaction model has been assumed which considers a constant rate until the maximum CO_2 carrying capacity is achieved (X_{ave}) and then the reaction rate becomes zero (Alonso et al. 2009). This simple carbonation model is consistent with the experimental results available from thermogravimetric tests (see for example (Grasa et al. 2008)) and allows a simple interpretation of the results obtained in the entrained carbonator. According to this model, the particle reaction rate can be calculated as a function of the X_{ave} and the average CO_2 concentration in the carbonator as follows:

This project has received funding from the European Union's Horizon2020 Research and Innovation Programme under Grant Agreement No 641185

$$\left(\frac{dX}{dt}\right)_{reactor} = ks\varphi X_{ave}\left(\overline{\vartheta_{CO2} - \vartheta_{CO2eq}}\right) \quad (3.2.4)$$

where k_s is the sorbent constant reaction rate and the term φ is a gas-solid contacting factor as defined in previous works (Rodriguez et al. 2011). Thus, the increment of carbonate content of the sorbent in the entrained carbonator can be calculated as function of the reaction time (t_r) according to:

$$(Increment\ of\ CaCO_3) = \left(\frac{dX}{dt}\right)_{reactor} t_r \quad (3.2.5)$$

By combining Eqs 3.2.3 and 3.2.4 into 3.2.5, the following expression can be obtained.

$$\left(\frac{F_{CO2in} - F_{CO2out}}{F_{Ca}}\right) = k_s\varphi X_{ave}\left(\overline{\vartheta_{CO2} - \vartheta_{CO2eq}}\right)t_r \quad (3.2.6)$$

The apparent reaction rate constant (ks φ) can be calculated as a fitting parameter by comparing both terms of this equation. Figure 3.10.a shows the results obtained for the experiments carried out with different CO_2 concentrations and no steam in the flue gas. For this set of experiments, the calculated reaction rate constant has a value of 0.23 s^{-1} which is consistent with that obtained in previous works (Charitos et al. 2011, Rodriguez et al. 2011, Arias et al. 2013, Arias et al. 2017).

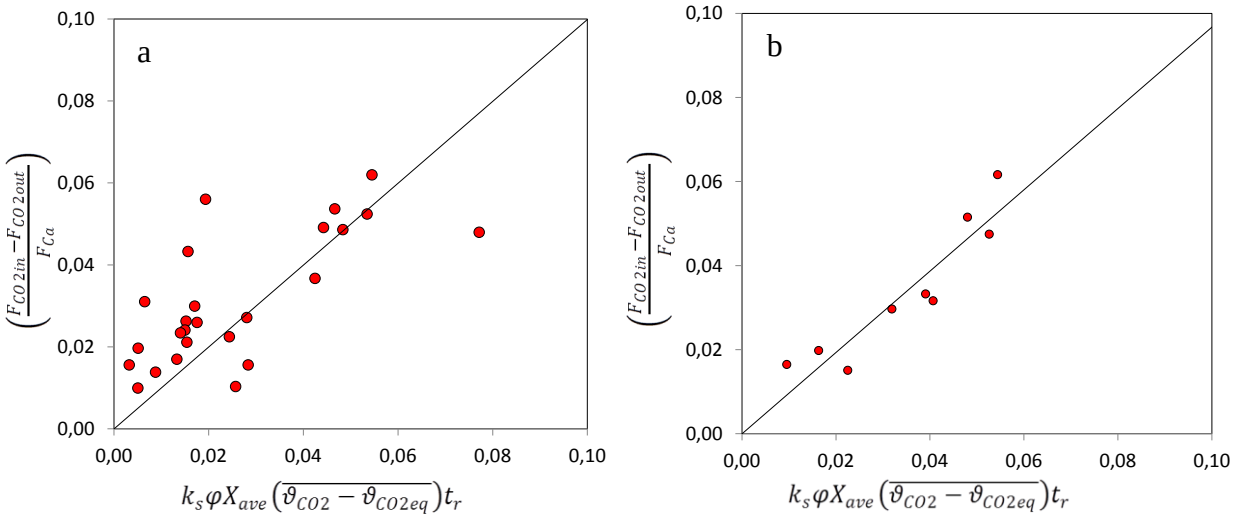

Figure 3.10 Comparison between the experimental increment of the $CaCO_3$ conversion of the sorbent and that calculated. a. Experimental data without steam. b. Experimental data with steam

This project has received funding from the European Union's Horizon2020 Research and Innovation Programme under Grant Agreement No 641185

Despite the reduced number of experiments carried out with the presence of stream in the synthetic flue gas, Figure 3.10b presents a similar analysis for this set of experiments. As expected from Figure 3.9, the calculated apparent reaction rate constant is slightly higher with a value of 0.34 s^{-1}. However, this value needs to be confirmed by carrying more tests under these conditions.

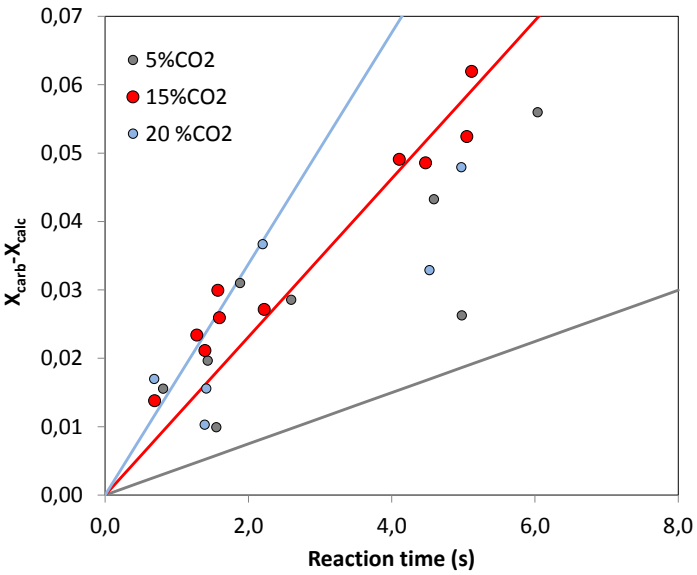

Figure 3.11 Effect of CO_2 concentration on sorbent conversion (solids lines calculated with Eq. 3.2.5 and a $k_s\varphi$ of 0.23 s^{-1} for the three CO_2 concentrations).

Finally, Figure 3.11shows the effect of the CO_2 concentration in the flue gas on the increase of sorbent conversion. As can be seen in this figure, the results obtained do not follow the trends expected for a first order reaction order respect to the CO_2 concentration (marked as solids lines). This is somehow surprising because the first order for the carbonation reaction is well established in the literature (see review by Martínez et al (Martínez et al. 2016)). The current level of information does not permit to discuss in deeper detail the reason behind this unexpected trend. However, as indicated in the introductory parts of this report, a more elaborated analysis of these results should be presented in MS12.5.

This project has received funding from the European Union's Horizon2020 Research and Innovation Programme under Grant Agreement No 641185

4 CONCLUSIONS

The 30 kW_{th} pilot at INCAR-CSIC has been extensively retrofitted in order to operate as an entrained carbonator. The new setup of the experimental facility allowed carrying out several series of carbonation experiments under relevant conditions for entrained reactor system (i.e. short reaction time with contact times of around 0.5-6 seconds). The reaction rate of the sorbents has been analyzed by measuring CO_2 concentration profiles. A valuable data base of results has been obtained for modeling purposes. A basic particle reaction model has been applied to obtain a preliminary interpretation of the experimental results. An apparent carbonation constant rate of 0.23 s^{-1} has been calculated from the experimental results presented in this report. Some tests have been carried out with steam in the synthetic flue gas fed into the carbonator showing its positive effect on carbonation rates in agreement with previous experimental results. These results are consistent with reaction rates found in previous works using different experimental facilities, as long as the initial fraction of active CaO in the solids (able to react in the fast carbonation regime is known). For the typical gas environments in the calciner (i.e. with high content of CO_2 and/or H_2O_v) this parameter is highly affected by the level of aggregation of the solids in the raw meals and by the calcination temperature (especially above 900ºC).

Despite the limitations noted during both the TG and entrained bed reactor test, the experimental results presented and discussed in this deliverable tend to support the viability of the entrained bed carbonator reactor concept for a CaL system, specially when using sufficiently short calcination times (less than 30 seconds) and disaggregated raw meals (i.e. with separated particles at micrometer level of Ca- and Si-rich compounds) to yield calcined materials with a high fraction of active CaO to capture CO_2 in the carbonator.

This project has received funding from the European Union's Horizon2020 Research and Innovation Programme under Grant Agreement No 641185

5 NOTATION

F_{Ca}	mol/m^2s	Ca molar flow circulating between reactors
F_{CO2in}	mol/m^2s	molar flow of CO_2 entering the carbonator
F_{CO2out}	mol/m^2s	molar flow of CO_2 leaving the carbonator
k_s	s^{-1}	constant reaction rate
t	s	Particle residence time in the carbonate
T_{carb}	ºC	average carbonator temperature
u_{carb}	m/s	carbonator gas velocity
X_{ave}		average CO_2 carrying capacity
X_{calc}		initial molar carbonate content of the solids
X_{carb}		molar carbonate content of the solid in the carbonator
φ		gas-solid contacting effectivity factor

This project has received funding from the European Union's Horizon2020 Research and Innovation Programme under Grant Agreement No 641185

6 REFERENCES

Romano, M. C., M. Spinelli, S. Campanari, S. Consonni, G. Cinti, M. Marchi and E. Borgarello (2013). The calcium looping process for low CO2 emission cement and power. ICAE2014, Energy Procedia. **37:** 7091-7099.

Spinelli, M., I. Martinez, E. De Lena, G. Cinti, M. Hornberger, R. Spörl, J. C. Abanades, S. Becker, R. Mathai, K. Fleiger, V. Hoenig, M. Gatti, R. Scaccabarozzi, S. Campanari, S. Consonni and M. Romano (2016). Integration of Ca-looping systems for CO_2 capture in cement plants. 13th Conference on Greenhouse Gas Control Technologies (GHGT-13). Lausanne (Switzerland), Energy Procedia. **In press**.

Martínez, I., G. Grasa, J. Parkkinen, T. Tynjälä, T. Hyppänen, R. Murillo and M. C. Romano (2016). "Review and research needs of Ca-Looping systems modelling for post-combustion CO_2 capture applications." International Journal of Greenhouse Gas Control **50**: 271-304.

Alonso, M., Y. A. Criado, J. C. Abanades and G. Grasa (2014). "Undesired effects in the determination of CO2 carrying capacities of CaO during TG testing." Fuel **127**: 52-61.

Baker, E. H. (1962). "The calcium oxide-calcium dioxide system in the pressure range 1-300 atmospheres." Journal of the Chemical Society: 464-470.

Barin, I. (1993). Thermochemical data of pure substances. Weinheim, VCH Verlagsgesellschaft.

Curran, G. P., C. E. Fink and E. Gorin (1967). CO_2 acceptor gasification process. Studies of acceptor properties. Advances in Chemistry Series. J. Schora, F.C. New York, American Chemical Society. **69:** 141-161.

Barker, R. (1973). "Reversibility of the reaction $CaCO_3$ <–––––>$CaO + CO_2$." J Appl Chem Biotechnol **23**(10): 733-742.

Hornberger, M., R. Spörl and G. Scheffknecht (2016). Calcium looping for CO2 capture in cement plants - pilot scale test. 13th Conference on Greenhouse Gas Control Technologies (GHGT-13). Lausanne (Switzerland), Energy Procedia. **In Press**.

Arias, B., M. Alonso and C. Abanades (2017). "CO2 Capture by Calcium Looping at Relevant Conditions for Cement Plants: Experimental Testing in a 30 kWth Pilot Plant." Industrial & Engineering Chemistry Research **56**(10): 2634-2640.

Borgwardt, R. H. (1989). "Calcium-Oxide sintering in atmospheres containing water and carbon-dioxide." Industrial & Engineering Chemistry Research **28**(4): 493-500.

Sun, P., J. R. Grace, C. J. Lim and E. J. Anthony (2008). "Investigation of attempts to improve cyclic CO2 capture by sorbent hydration and modification." Industrial & Engineering Chemistry Research **47**(6): 2024-2032.

Yang, S. and Y. Xiao (2008). "Steam catalysis in CaO carbonation under low steam partial pressure." Industrial & Engineering Chemistry Research **47**: 4043.

Symonds, R. T., D. Y. Lu, R. W. Hughes, E. J. Anthony and A. Macchi (2009). "CO2 Capture from Simulated Syngas via Cyclic Carbonation/Calcination for a Naturally Occurring Limestone: Pilot-Plant Testing." Industrial & Engineering Chemistry Research **48**(18): 8431-8440.

Manovic, V. and E. J. Anthony (2010). "Carbonation of CaO-Based Sorbents Enhanced by Steam Addition." Industrial & Engineering Chemistry Research **49**(19): 9105-9110.

This project has received funding from the European Union's Horizon2020 Research and Innovation Programme under Grant Agreement No 641185

Arias, B., G. Grasa, J. C. Abanades, V. Manovic and E. J. Anthony (2012). "The Effect of Steam on the Fast Carbonation Reaction Rates of CaO." Industrial & Engineering Chemistry Research **51**(5): 2478-2482.

Donat, F., N. H. Florin, E. J. Anthony and P. S. Fennell (2012). "Influence of High-Temperature Steam on the Reactivity of CaO Sorbent for CO2 Capture." Environmental Science and Technology **46**(2): 1262-1269.

Dieter, H., A. R. Bidwe, G. Varela-Duelli, A. Charitos, C. Hawthorne and G. Scheffknecht (2014). "Development of the calcium looping CO2 capture technology from lab to pilot scale at IFK, University of Stuttgart." Fuel **127**: 23-37.

Alonso, M., N. Rodriguez, G. Grasa and J. C. Abanades (2009). "Modelling of a fluidized bed carbonator reactor to capture CO2 from a combustion flue gas." Chemical Engineering Science **64**(5): 883-891.

Grasa, G. S., J. C. Abanades, M. Alonso and B. Gonzalez (2008). "Reactivity of highly cycled particles of CaO in a carbonation/calcination loop." Chemical Engineering Journal **137**(3): 561-567.

Rodriguez, N., M. Alonso and J. C. Abanades (2011). "Experimental Investigation of a Circulating Fluidized-Bed Reactor to Capture CO2 with CaO." AIChE Journal **57**(5): 1356-1366.

Charitos, A., N. Rodriguez, C. Hawthorne, M. Alonso, M. Zieba, B. Arias, G. Kopanakis, G. Scheffknecht and J. C. Abanades (2011). "Experimental Validation of the Calcium Looping CO_2 Capture Process with Two Circulating Fluidized Bed Carbonator Reactors." Industrial & Engineering Chemistry Research **50**(16): 9685-9695.

Arias, B., M. E. Diego, J. C. Abanades, M. Lorenzo, L. Diaz, D. Martínez, J. Alvarez and A. Sánchez-Biezma (2013). "Demonstration of steady state CO2 capture in a 1.7MWth calcium looping pilot." International Journal of Greenhouse Gas Control **18**: 237-245.

This project has received funding from the European Union's Horizon2020 Research and Innovation Programme under Grant Agreement No 641185

A APPENDIX

A.1 Other experimental set ups used for entrained reactor testing in the 30kW$_{th}$ pilot.

The two high temperature circulating fluidized bed reactors (CFB) for CaL systems available at INCAR-CSIC are the basis of all the experimental setups used for entrained reactor testing. As it has been explained in section 2.3, the most successful configuration consisted in the use of one of CFB as a gas pre-heater and the other as the entrained down-flow reactor. However, another setup was extensively used during initial campaigns and discussed in some project coordination meetings. Figure A1.1 shows the schematics of this second experimental setup.

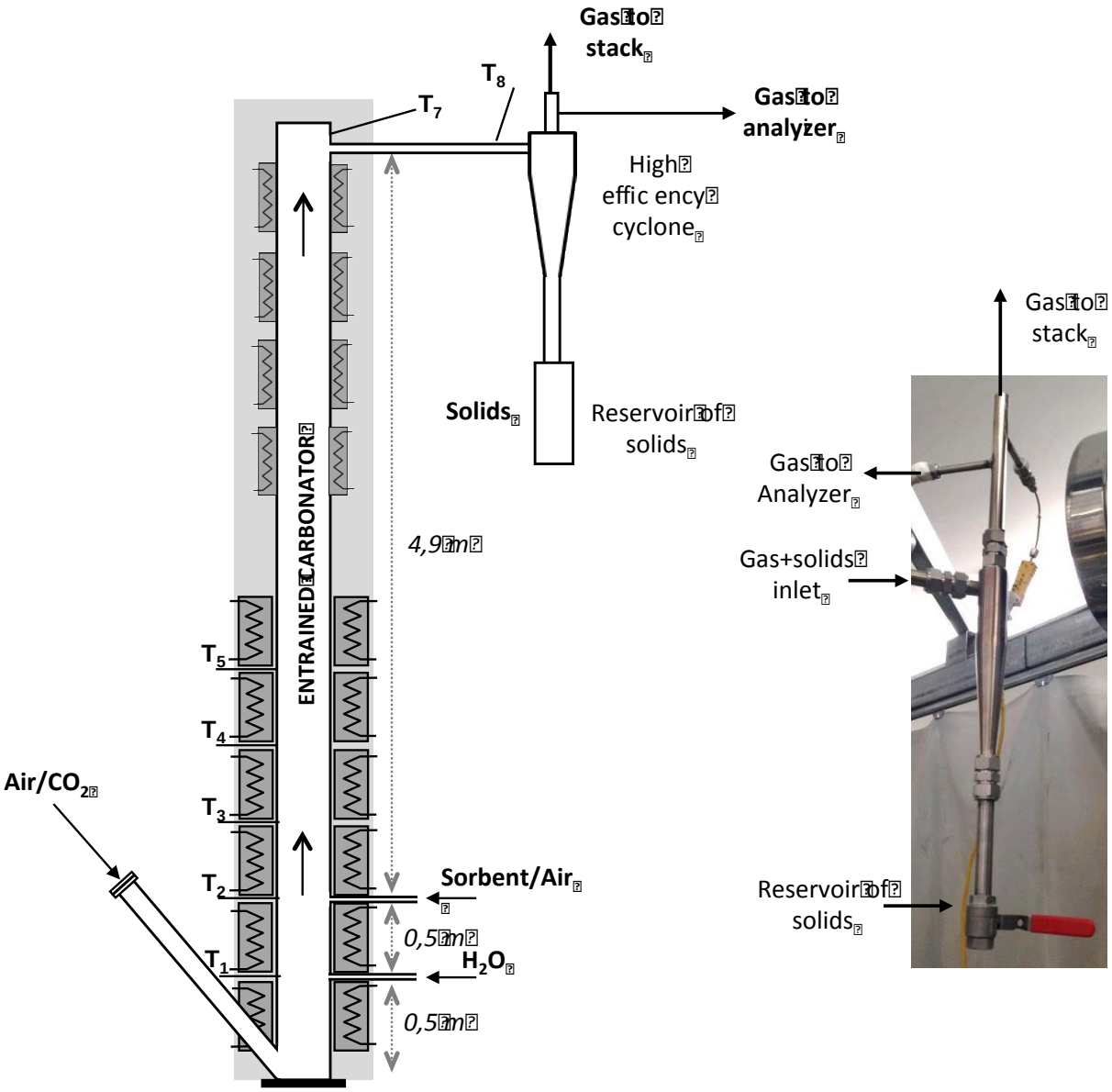

Figure A.1.1. Scheme re of the up-flow carbonator reactor set up used during carbonation test in entrained mode (gas and solids moving upwards).

This project has received funding from the European Union's Horizon2020 Research and Innovation Programme under Grant Agreement No 641185

The simulated flue gas was a mix of air, CO_2 and steam (when relevant). The air was fed into the reactor by a blower with a maximum capacity of $90m^3/h$ and also by the compressor at 5 bar that supply the solid feeding system. The CO_2 was supplied by a liquid Deward or CO_2 bottle and the steam by a small water vapour generator that provides a continuous flow of 2.0 kg/h. The CO_2 and air flows were adjusted using mass flow controllers. For this configuration, the air/CO_2 mixture is injected at the bottom of the reactor. In this case, an additional oven located in this zone with an individual capacity of 3.8 kWe is used to preheat the mixture. At a height of 0.5 m from the bottom, there is an inlet for the steam used in some experimental campaigns. Moreover, the sorbent and the carrier air were injected at 1 m to be driven upwards to its outlet. As indicated, during the initial campaigns the chemical analysis of solids samples was used to measure the sorbent carbonation conversion. For this purpose, a high efficiency cyclone installed in the outlet was used to recover fine particles. The cyclone (from Air Classify with a cut diameter of 5 microns) set in the outlet was equipped with a solid reservoir for sampling of solids at different times during an experiment. In this configuration, the gas sampling to the analyser was located at the exit of this cyclone.

A.2 Experimental set ups used for solid feeding system

The solid feeding system was one of the critical aspects during these tests due to the difficulties on handling fine and cohesive particles. For this purpose, four different feeding systems shown in Figure A.2.1 were tested. One of them is a commercial system designed for the dispersion of fine powders and the others are three in-housed built systems.

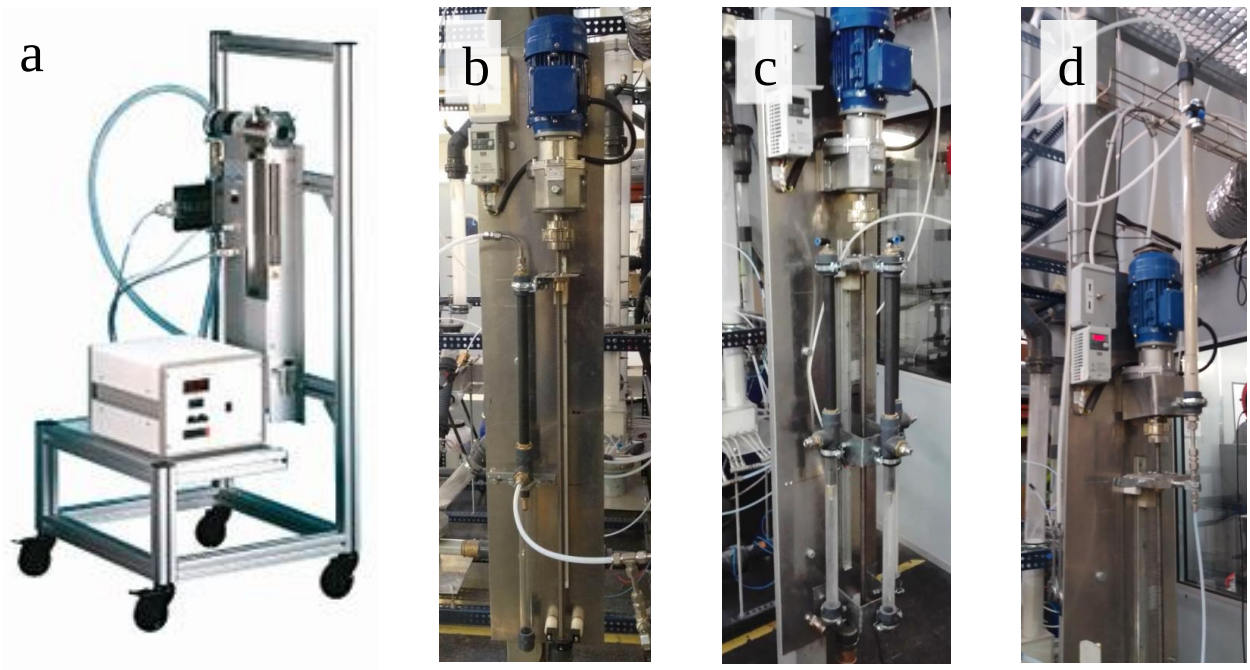

Figure A.2.1. Different solid feeding systems used during the entrained reactor testing. a) Commercial device; b) In-house device 1; c) In-house device 2; d) In-house device 3.

This project has received funding from the European Union's Horizon2020 Research and Innovation Programme under Grant Agreement No 641185

a) Commercial device

The commercial solid feeding system from Palas GmbH was used during an initial series of test to calibrate reactor performances. This device is specifically designed for the dispersion of small flows of fine powders. In this system, the solids are loaded into a cylindrical reservoir. Then, a moving piston at the bottom of this reservoir pushes the particles onto a rotating brush at a precisely controlled feed rate. Then, a dispersion airflow is fed into the head of the feeding system in order to pull the particles out of the brush. The main advantage of this system is the fine dispersion of the particles into the carrying air and therefore in the entrained carbonator. However, some feeding problems were found with some sorbents that were prone to stick into the head of the system. Moreover, another important disadvantage of this device is the low feeding rate of solids (<0.3 kg/h) that does not allow enough solid loading into the carbonator in order to capture a measurable amount of CO_2 from the gas phase.

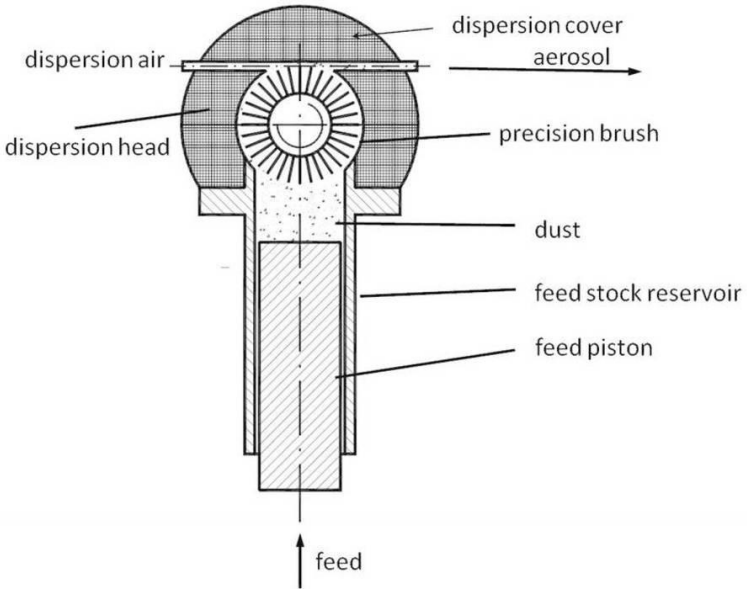

Figure A.2.2. Schematic of the commercial feeding system (from www.palas.de)

b) In-house designed feeding system: Configuration 1

Since the commercial device was only able to feed solid flows of around 0.3kg/h, it was not suitable to carry out experiments where the measurement of the CO_2 concentration in the gas phase is used as method to determine the extent of the carbonation reaction. Therefore, it was decided to build an in-house system capable of feeding higher mass flow rates of solids. Another purpose of this new device was the possibility of feeding a wide range of cohesive solids. The schematic of this device is shown in Figure A.2.3. It consisted in a cylindrical reservoir made of methacrylate to detect any blockage inside the system where the solids are loaded at the beginning of each experiment. A moving piston inserted into the reservoir though its upper part is used to control the solid flow rate. The piston is a cylindrical PVC piece with pointed and drilled end in order to inject the carrying air into the reservoir. The air is supplied from a compressor and the mass flow rate is adjusted manually with a needle valve. The operating mechanism was as follows: the piston is moved downwards inside the reservoir by a mechanical system, so that the solids dragged by the air that comes through the piston and conveyed at high

This project has received funding from the European Union's Horizon2020 Research and Innovation Programme under Grant Agreement No 641185

velocity out of the reservoir to be fed into the reactor through a pipe. The mechanical system that moved the piston consisted in a shaft connected to an electric motor equipped with a speed variator to control the rotary speed.

This device allowed increasing the mass flow rate of solids. Minor problems related with this device were related with the blockage of the piston when feeding sticky solids. However, the main disadvantage of this feeding system was some uncontrolled air leakages in the sealing of the moving piston. This introduces uncertainties in the analysis of the CO_2 concentration in the gas phase and therefore difficulties to calculate the solid carbonation.

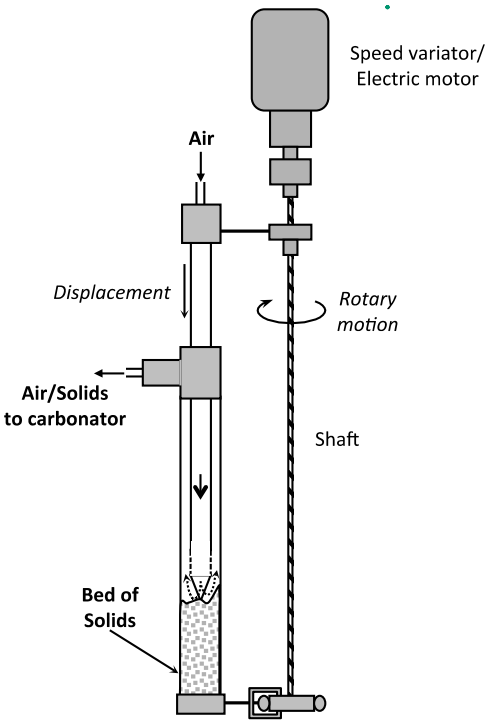

Figure A.2.3. Schematics of the in-house designed feeding system (Configuration 1)

A.2.3 In-house designed feeding system: Configuration 2

This is a modification of the Configuration 1 designed to operate with higher mass flow rates of solids. For this purpose, three pistons feeding solids (similar to those shown in Figure A.2.3) were installed to feed solids into the carbonator. The mechanical system used in Configuration 1 was modified in order to move three pistons at the same time and speed. The sealing of the moving part was also modified to reduce the air leakage. This system was successful to increase the load into the carbonator but minor problems with air leakages were still present.

A.2.4 In-house designed feeding system: Configuration 3

This system was the most successful configuration and is described in detail in Section 2.3 of this report.

This project has received funding from the European Union's Horizon2020 Research and Innovation Programme under Grant Agreement No 641185

A.3 Sorbents tested in the entrained carbonator.

Five different Ca-sorbents were tested the entrained reactor: three different calcined limestones and two sorbents derived from $Ca(OH)_2$. Their properties can be seen in the Table A.3.1:

Sorbent	Precursor	Average CO_2 carrying capacity (X_{ave})	d_{p50} (µm)
A	Limestone	0.25	40
B	Limestone	0.34	80
C	Limestone	0.41	50
D	$Ca(OH)_2$	0.70	36
E	$Ca(OH)_2$	0.16	36

Sorbents A and B were prepared by calcination of batches of fresh limestone in a muffle (calcination time=20min at 900 ºC in air). These samples were used only during initial tests due to the low amount of sample available. Sorbent C was used for test described in Section 3.2 of this report. As indicated, it was obtained in calcination tests carried out in the $30kW_{th}$ pilot facility of the INCAR-CSIC. Sorbent D was used mostly during some tests aimed to characterize the entrained carbonator in the down-flow configuration. Sorbent E was prepared by calcination of $Ca(OH)_2$ in a muffle (calcination time=20min at 900 ºC in air). However, none of the feeding systems used during the experimental campaign was able to give a stable flow for this specific sorbent.

A.4 Entrained reactor characterization

Some experiments were carried out to characterize the reactor with the objective validating the plug flow under the conditions used during the experimental campaigns. The mixture of air/CO_2/steam coming from the preheater enters into the entrained carbonator perfectly mixed due to the number of elbows, pipes and restrictions between the mixing point and the reactor inlet. However, CO_2 profiles inside the carbonator may exits due to the injection of the conveying air at the top of the reactor. For this purpose, several blank tests were carried out by injecting the conveying air at different rates into the carbonator while the air/CO_2 mixture was fed into the carbonator. Then, the CO_2 concentration inside the carbonator at different radial positions was measured. As example, Figure A.4.1. shows the CO_2 profiles inside the carbonator at two different inlet CO_2 concentrations. As it can be seen in the figures, the CO_2 concentration measured is almost constant along the radius of the carbonator.

This project has received funding from the European Union's Horizon2020 Research and Innovation Programme under Grant Agreement No 641185

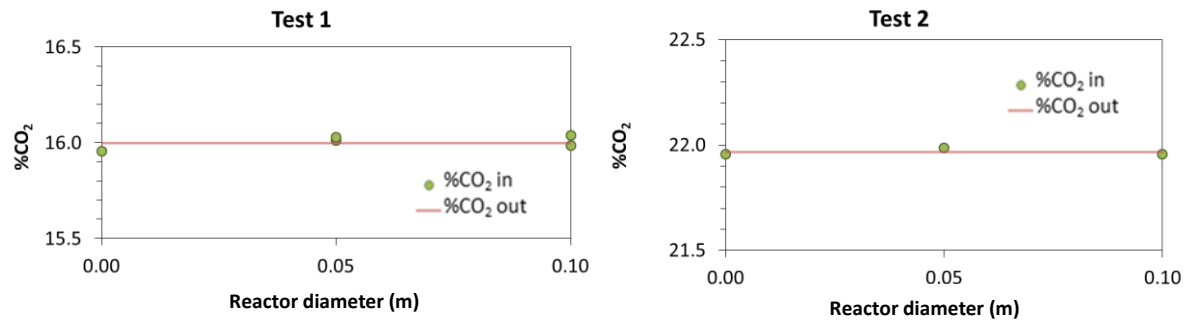

Figure A.4.1. Tests of measurement of CO_2 concentration at different positions all along the reactor section, done at different inlet CO_2 concentrations: a) 16%$_v$; b) 22%v (0.00 and 0.10 m corresponds to the reactor walls and 0.05 m to the centre).

In addition, other tests were carried out to characterize mixing of air and CO_2 inside the carbonator. For this purpose, changes on the CO_2 flow and on the solids feeding system airflow were carried out. Figure A.4.2 shows an example of two steps changes introduced in the conveying air fed at the top of the carbonator. Thus, the red line corresponds to the calculated CO_2 concentration expected according to airflow changes and the green line corresponds to the measured CO_2 concentration with the analyzer (%CO_2 out).

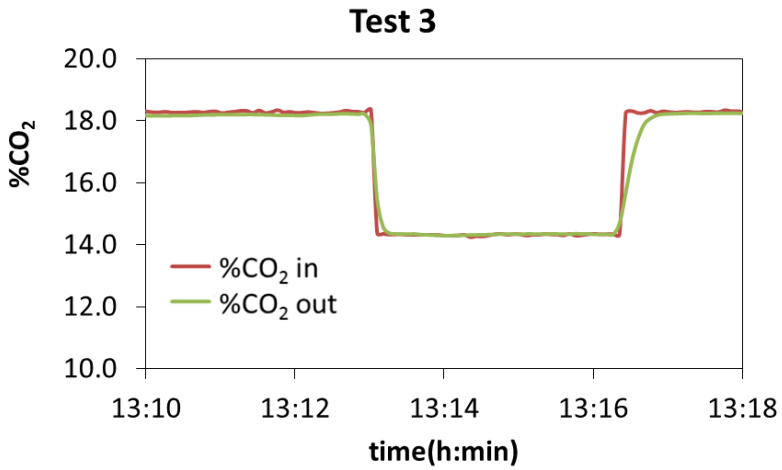

Figure A.4.2. Study of the analyzer response to changes in the feeding system air flow.

As can be seen in this figure, there is fast change of the CO_2 concentration measure in the carbonator according to the step changes introduced in the system. It has to be mentioned that these tests were also used to measure the response time of the gas line.

This project has received funding from the European Union's Horizon2020 Research and Innovation Programme under Grant Agreement No 641185

A.5 Experimental results of carbonation using down-flow of solids and gas in the entrained reactor.

This section of the Annex includes the experimental data sets corresponding to the campaigns carried out in the entrained carbonator. The experimental campaigns are presented in chronological order. A brief discussion for each campaign is included in order to explain the main objectives, problems encountered and results obtained. For each test a table with the main variable is included together with a plot showing the evolution of the CO_2 concentration at the inlet and at the outlet of the carbonator.

A.5.1 Campaign 1: entrained 'up-flow' testing using the commercial solid feeding system

These tests were carried out with the equipment configured as an entrained 'up-flow' reactor (see section A.1). The solid feeding system used was the commercial device described in section A.2.1. The objective during these tests was to measure the extent of the sorbent carbonation conversion by taking solid particles. For this purpose, solids were recovered using the high efficiency cyclone set at the outlet of the carbonator after being in contact with the CO_2-rich gas all along the riser. All these tests carried out with the presence of steam in the reacting mixture.

As indicated in Section 2.1, the main problems of this experimental approach were related with the difficulty of taking representative samples from the cyclone reservoir. The samples were not representative because of the high residence in the cyclone reservoir in contact with the reacting mixture respect to that in the reactor.

Three experiments were carried out maintaining the solid flow, CO_2 flow and air flow constant, but varying the type of solid used and the amount of steam injected. In the first two experiments, calcined limestone with an average CO_2 carrying capacity of around 0.25 was used, while in the third one, the calcined limestone used had an average CO_2 carrying capacity of 0.34. The temperature was kept constant in the riser at around 600°C.

This project has received funding from the European Union's Horizon2020 Research and Innovation Programme under Grant Agreement No 641185

Experiment 1

Solid fed	CaO
Xave	0.25
T (°C)	600
u_{gas} (m/s)	2.33
CO_2 in (vol%)	19.8
Solid flow (kg/h)	0.3
Total gas flow (m^3/h)	20.6
H_2O (vol%)	9.8

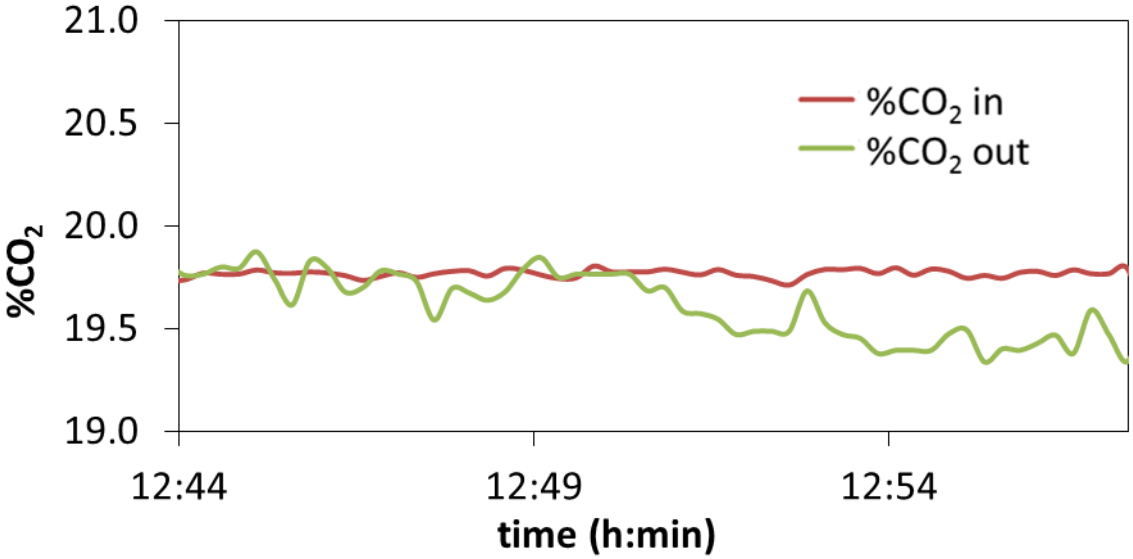

Experiment 2

Solid fed	CaO
Xave	0.25
T (°C)	584
u_{gas} (m/s)	2.07
CO_2 in (vol%)	21.6
Solid flow (kg/h)	0.3
Total gas flow (m^3/h)	18.7
H_2O (vol%)	0.0

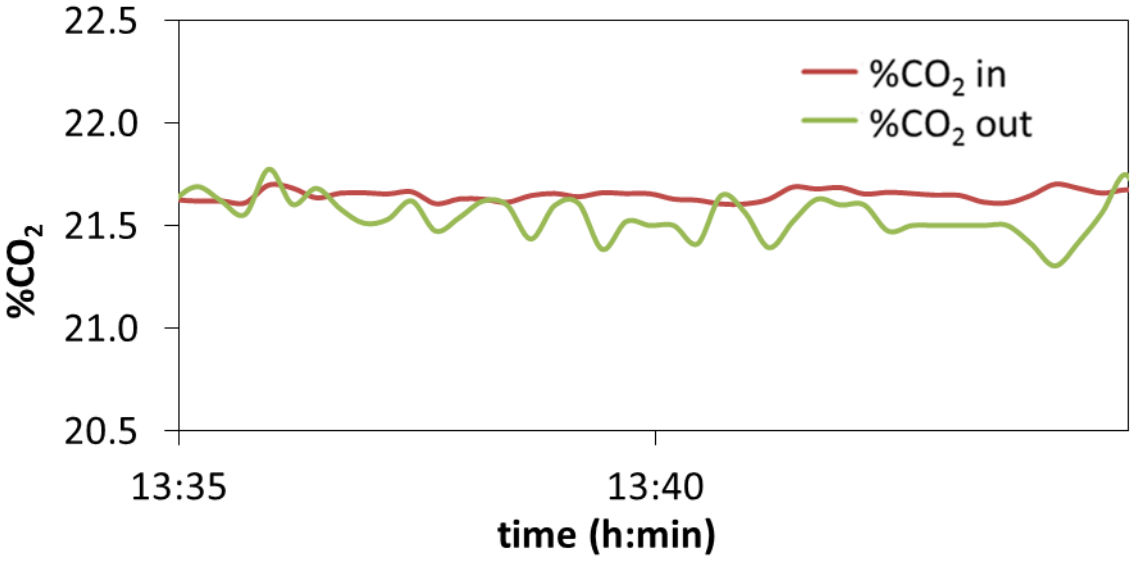

This project has received funding from the European Union's Horizon2020 Research and Innovation Programme under Grant Agreement No 641185

Experiment 3

Solid fed	CaO
Xave	0.34
T (°C)	597
u_{gas} (m/s)	2.33
CO_2 in (vol%)	19.6
Solid flow (kg/h)	0.4
Total gas flow (m^3/h)	20.7
H_2O (vol%)	9.8

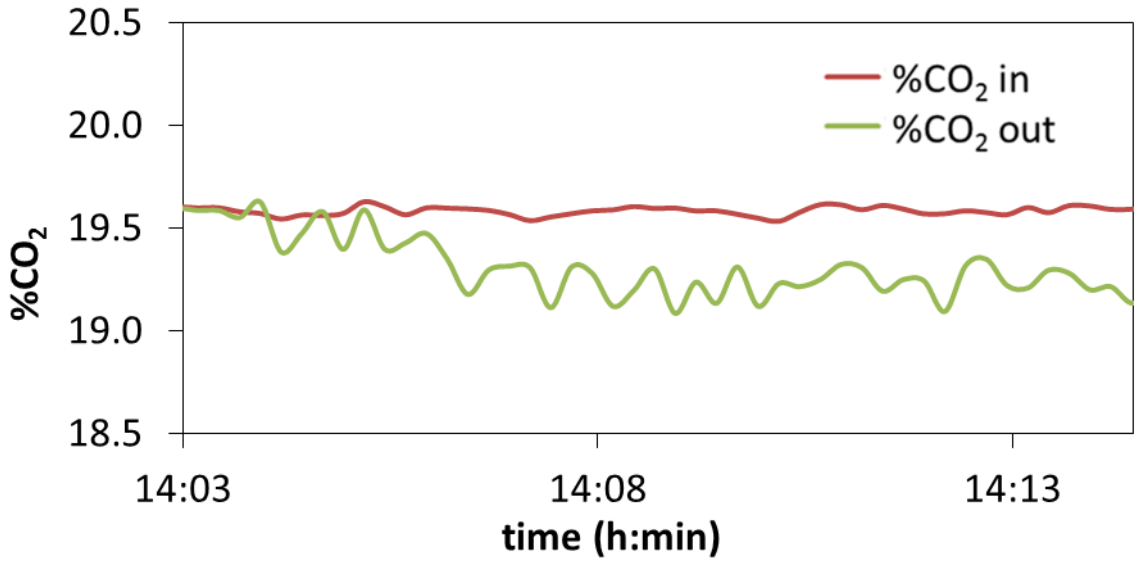

This project has received funding from the European Union's Horizon2020 Research and Innovation Programme under Grant Agreement No 641185

A.5.2 Campaign 2: entrained 'up-flow' testing using the in-house design feeding system (Configuration 1)

During this experimental campaign, a different experimental approach was followed trying to measure the CO_2 removed from the gas phase and the carbonate content formed in the sorbent fed into the carbonator in order to close the CO_2 mass balance. Since the commercial device only allowed us to inject low solid flows (around 0.3 kg/h), it was decided to design a build a new in-hose solid feeding system (see section A.2.2) able to feed a higher flow.

During the tests, some problems were found with the solid feeding system such as the blockage of the piston, the unstable solid feeding or the existence of uncontrolled air leakages in the system. Furthermore, it was still not possible to take representative solid samples in the cyclone reservoir since they could be contaminated with solids from former experiments or being more carbonated due to its stay on the reservoir. That made difficult to obtain relevant results.

The solids used were calcined limestones of two different average CO_2 carrying capacities, 0.25 and 0.34. There were made 5 experiments, the first two were made with an inlet CO_2 concentration of $5\%_v$ and a gas velocity in the riser around 2.1 m/s, while the last three were made with an inlet concentration of $15\%_v$ and setting the gas velocity around 1.25 m/s. The temperature was kept constant at around 660°C.

This project has received funding from the European Union's Horizon2020 Research and Innovation Programme under Grant Agreement No 641185

Experiment 1

Solid fed	CaO
Xave	0.34
T (°C)	662
u_{gas} (m/s)	2.12
CO_2 in (vol%)	5.6
Solid flow (kg/h)	0.5
Total gas flow (m^3/h)	17.5
H_2O (vol%)	13.5

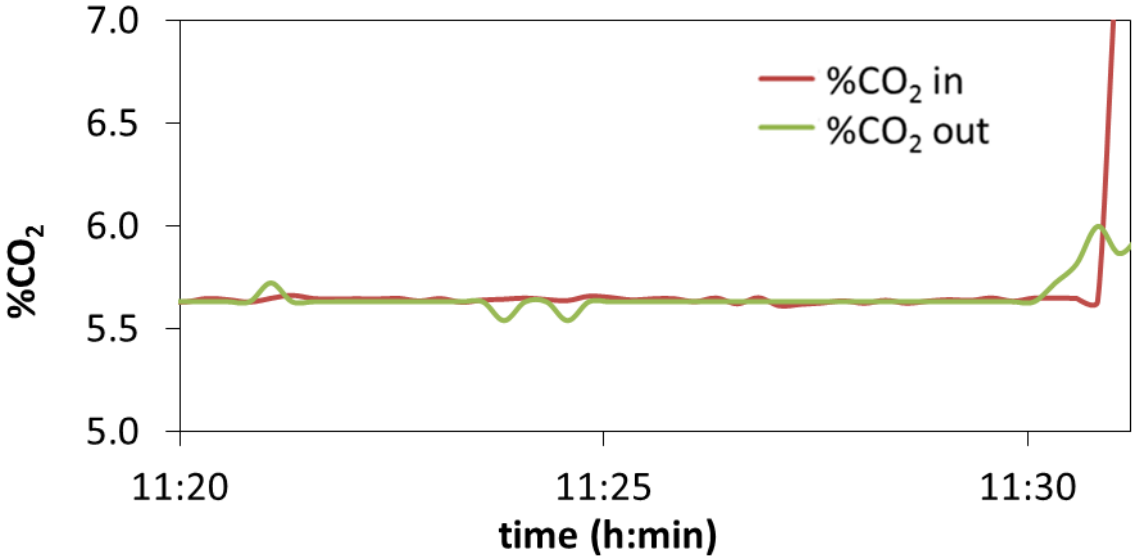

Experiment 2

Solid fed	CaO
Xave	0.25
T (°C)	668
u_{gas} (m/s)	2.17
CO_2 in (vol%)	5.6
Solid flow (kg/h)	0.8
Total gas flow (m^3/h)	17.8
H_2O (vol%)	13.3

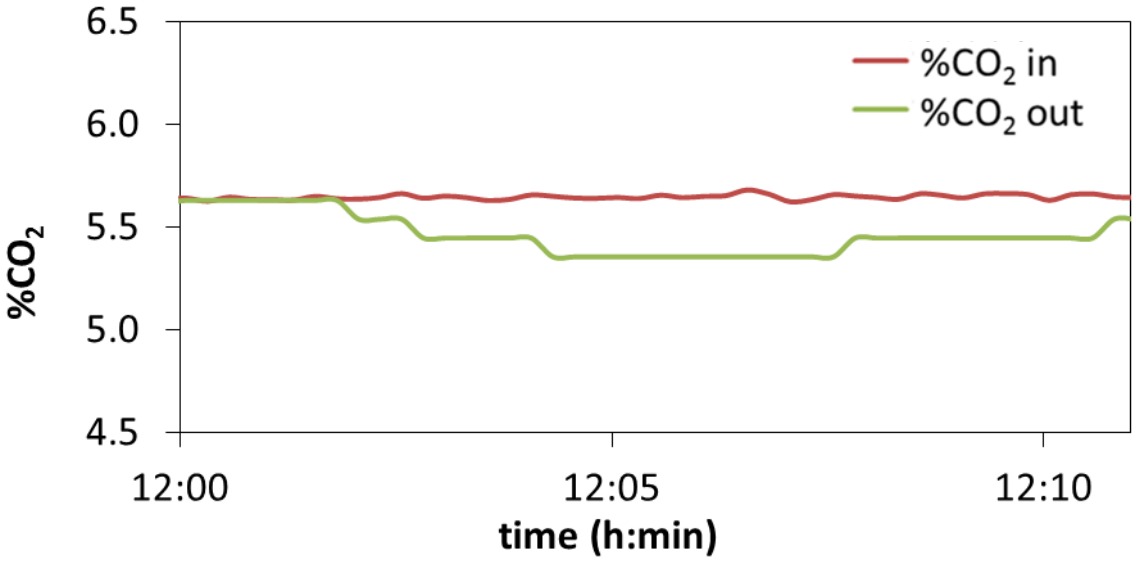

This project has received funding from the European Union's Horizon2020 Research and Innovation Programme under Grant Agreement No 641185

Experiment 3

Solid fed	CaO
Xave	0.34
T (°C)	664
u_{gas} (m/s)	1.25
CO_2 in (vol%)	15.5
Solid flow (kg/h)	1.6
Total gas flow (m^3/h)	10.3
H_2O (vol%)	23.0

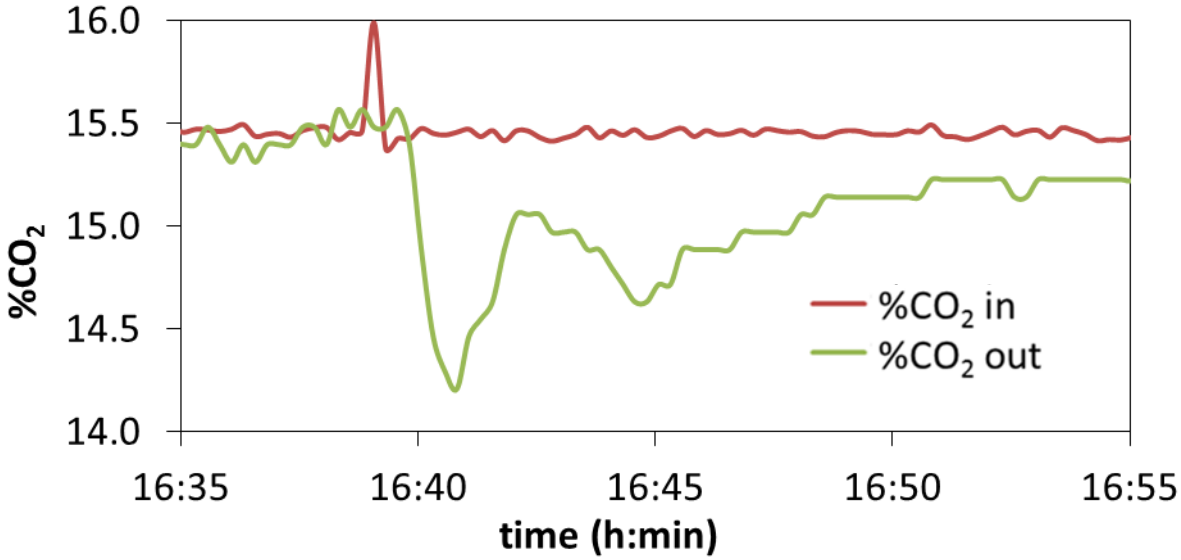

Experiment 4

Solid fed	CaO
Xave	0.34
T (°C)	662
u_{gas} (m/s)	1.25
CO_2 in (vol%)	15.4
Solid flow (kg/h)	1.9
Total gas flow (m^3/h)	10.3
H_2O (vol%)	22.8

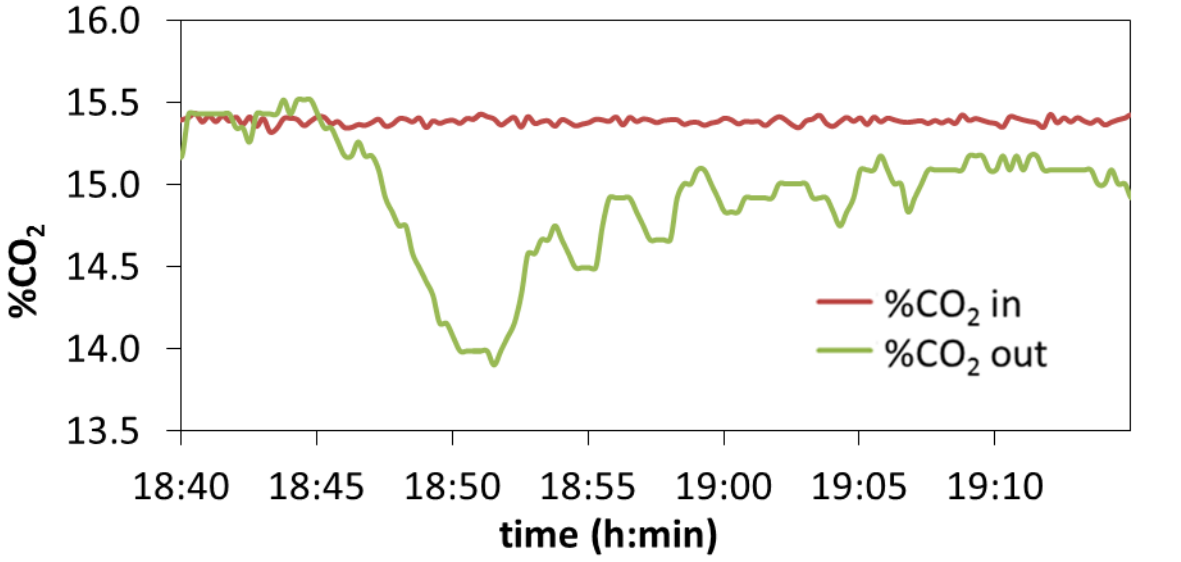

This project has received funding from the European Union's Horizon2020 Research and Innovation Programme under Grant Agreement No 641185

Experiment 5

Solid fed	CaO
Xave	0.34
T (°C)	661
u_{gas} (m/s)	1.28
CO_2 in (vol%)	15.1
Solid flow (kg/h)	1.9
Total gas flow (m^3/h)	10.5
H_2O (vol%)	22.4

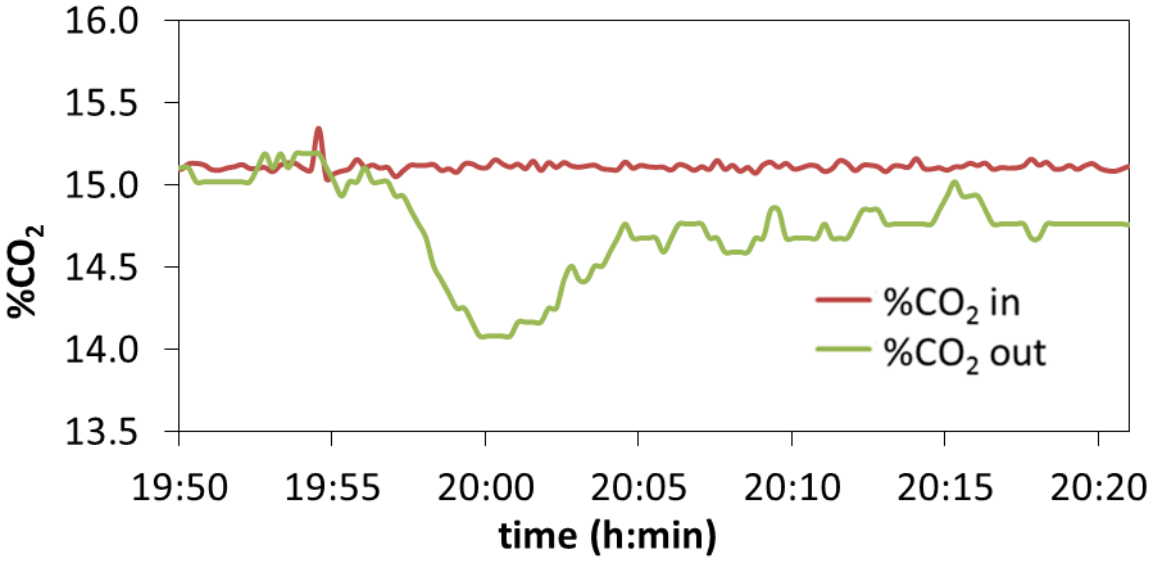

This project has received funding from the European Union's Horizon2020 Research and Innovation Programme under Grant Agreement No 641185

A.5.3 Campaign 3: entrained 'up-flow' testing using the in-house feeding systems (Configuration 2)

During this campaign, the focus was to increase the loading of sorbent into the carbonator in order to increase the change of the CO_2 concentration measurements and obtain more reliable data about the CO_2 removed from the gas phase.

Thus, solids were fed using the in-house solid feeding system (Configuration 2) described in section A.2.3 that allows for high mass flow rate of solids. This new solid feeding system did not have such as important problems of blockage as the previous one and was able of feeding higher solid flows. Therefore, it was possible to follow the carbonation not only by the recovered solids, but also by the CO_2 variations in the gas phase. In spite of that, there were still some air leakages during its working that caused the variations in the CO_2 inlet concentration seen in the graphs of all the experiments and thus, the complexity of treating the gas phase data.

Despite to the difficulties on analyzing the experimental data, it was detected that the entrained up-flow configuration created an accumulation of solids in the bottom part of the carbonator that captured CO_2 and made not entirely true the plug flow assumption for the solid phase. In addition, the problems with the representativeness of the samples taken in the cyclone reservoir continued. That made difficult to obtain relevant results.

Nine different experiments were made keeping the gas velocity constant around 2 m/s in all of them but changing the CO_2 and air flows, so as to study the CO_2 capture capacity of the solids under same residence times but different CO_2 concentrations (from $5\%_v$ to $30\%_v$). The sorbent used was calcined limestone with an average CO_2 carrying capacity of around 0.26. The temperature was kept constant at around 650°C.

This project has received funding from the European Union's Horizon2020 Research and Innovation Programme under Grant Agreement No 641185

Experiment 1

Solid fed	CaO
Xave	0.25
T (°C)	646
u_{gas} (m/s)	1.77
CO_2 in (vol%)	17.4
Solid flow (kg/h)	8.0
Total gas flow (m^3/h)	14.8
H_2O (vol%)	0.0

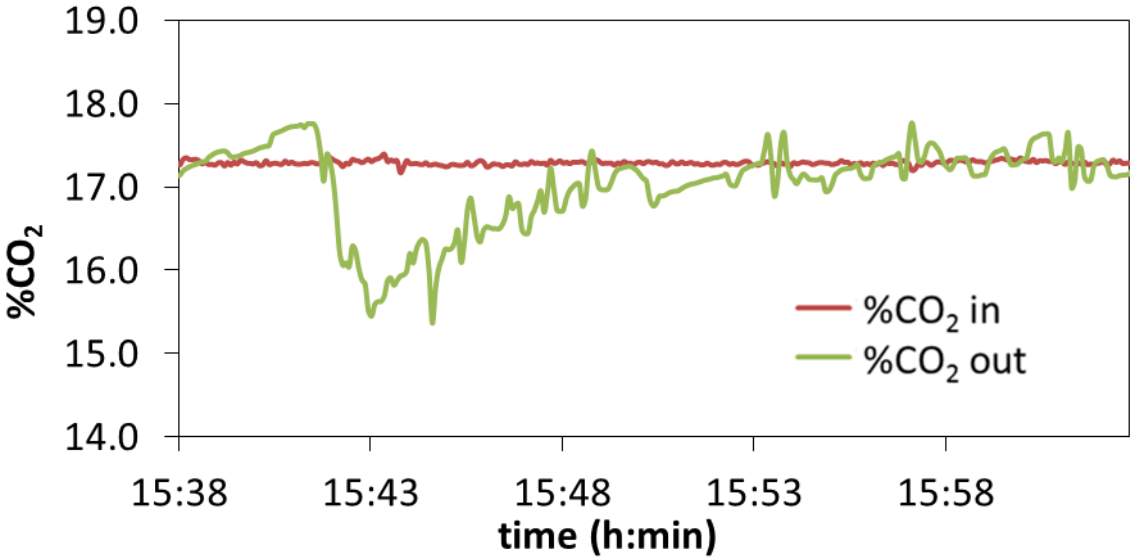

Experiment 2

Solid fed	CaO
Xave	0.25
T (°C)	651
u_{gas} (m/s)	2.16
CO_2 in (vol(%)	24.8
Solid flow (kg/h)	4.1
Total gas flow (m^3/h)	18.0
H_2O (vol%)	0.0

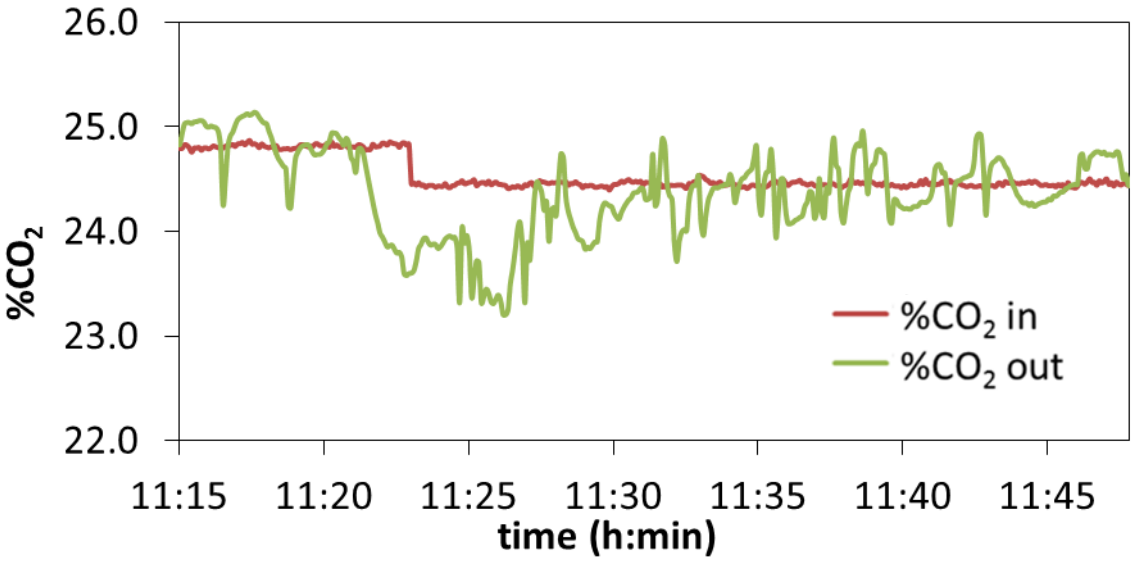

This project has received funding from the European Union's Horizon2020 Research and Innovation Programme under Grant Agreement No 641185

Experiment 3

Solid fed	CaO
Xave	0.25
T (°C)	656
u_{gas} (m/s)	1.84
CO_2 in (vol%)	5.3
Solid flow (kg/h)	4.0
Total gas flow (m^3/h)	15.3
H_2O (vol%)	0.0

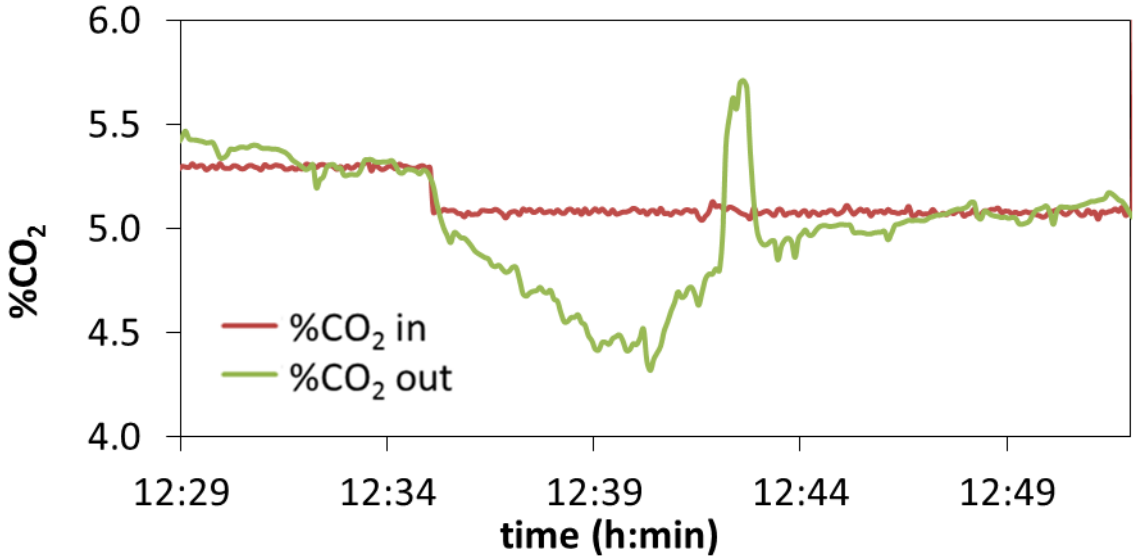

Experiment 4

Solid fed	CaO
Xave	0.25
T (°C)	661
u_{gas} (m/s)	1.96
CO_2 in (vol%)	15.4
Solid flow (kg/h)	3.9
Total gas flow (m^3/h)	16.2
H_2O (vol%)	0.0

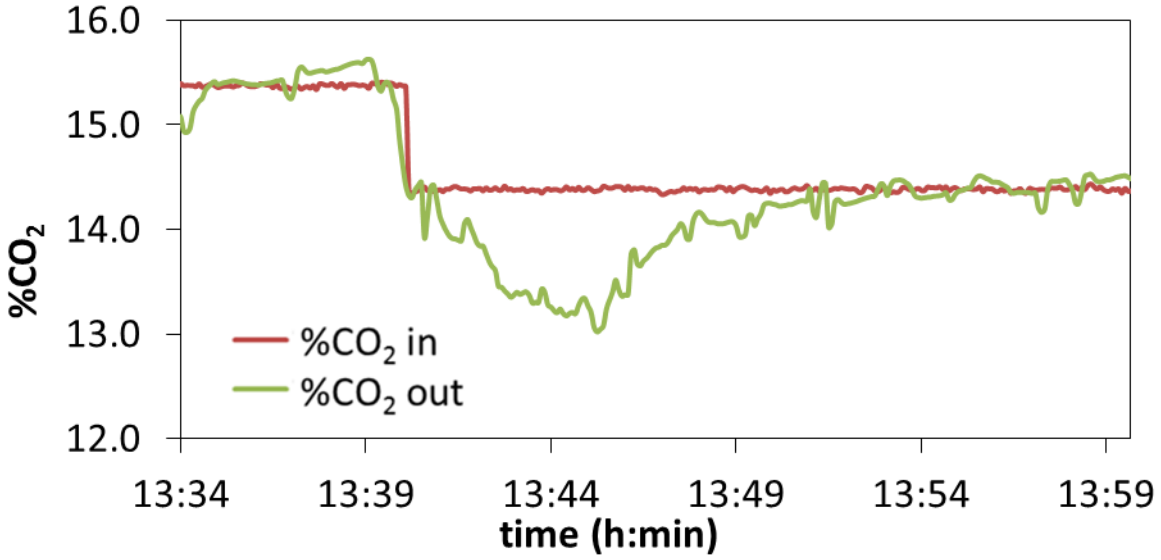

This project has received funding from the European Union's Horizon2020 Research and Innovation Programme under Grant Agreement No 641185

Experiment 5

Solid fed	CaO
Xave	0.25
T (°C)	661
u_{gas} (m/s)	2.01
CO_2 in (vol%)	30.3
Solid flow (kg/h)	3.8
Total gas flow (m^3/h)	16.6
H_2O (vol%)	0.0

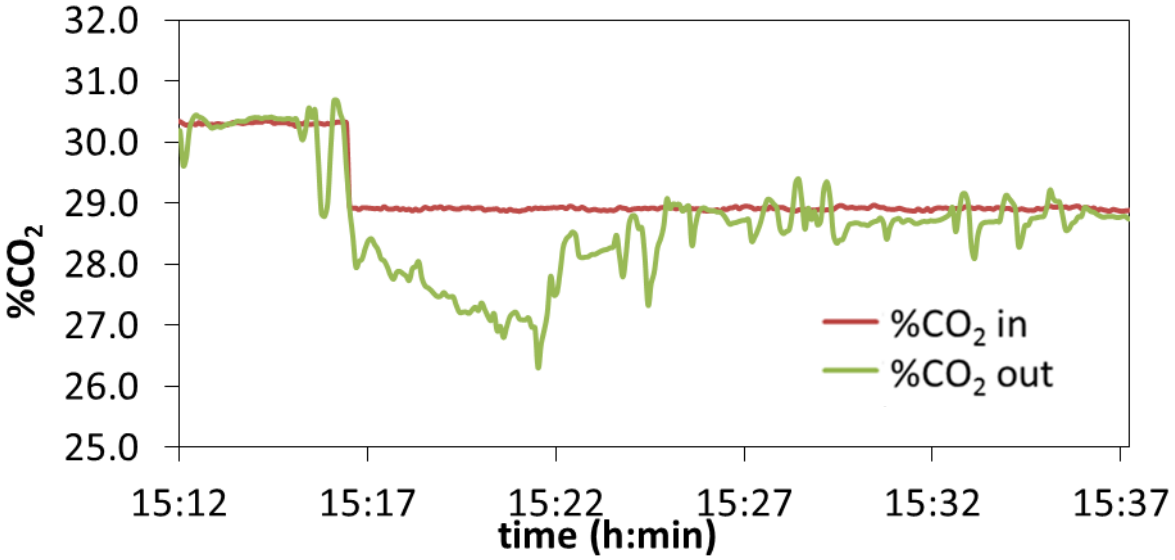

Experiment 6

Solid fed	CaO
Xave	0.25
T (°C)	653
u_{gas} (m/s)	1.95
CO_2 in (vol%)	11.1
Solid flow (kg/h)	4.4
Total gas flow (m^3/h)	16.3
H_2O (vol%)	0.0

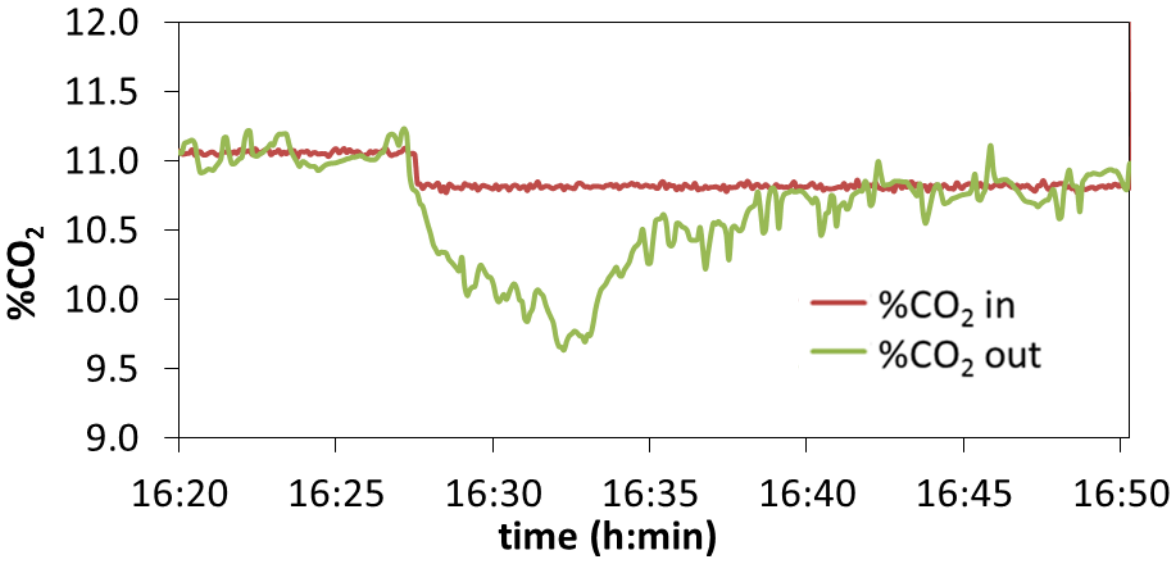

This project has received funding from the European Union's Horizon2020 Research and Innovation Programme under Grant Agreement No 641185

Experiment 7

Solid fed	CaO
Xave	0.25
T (°C)	653
u_{gas} (m/s)	2.14
CO_2 in (vol%)	23.7
Solid flow (kg/h)	3.3
Total gas flow (m^3/h)	17.9
H_2O (vol%)	0.0

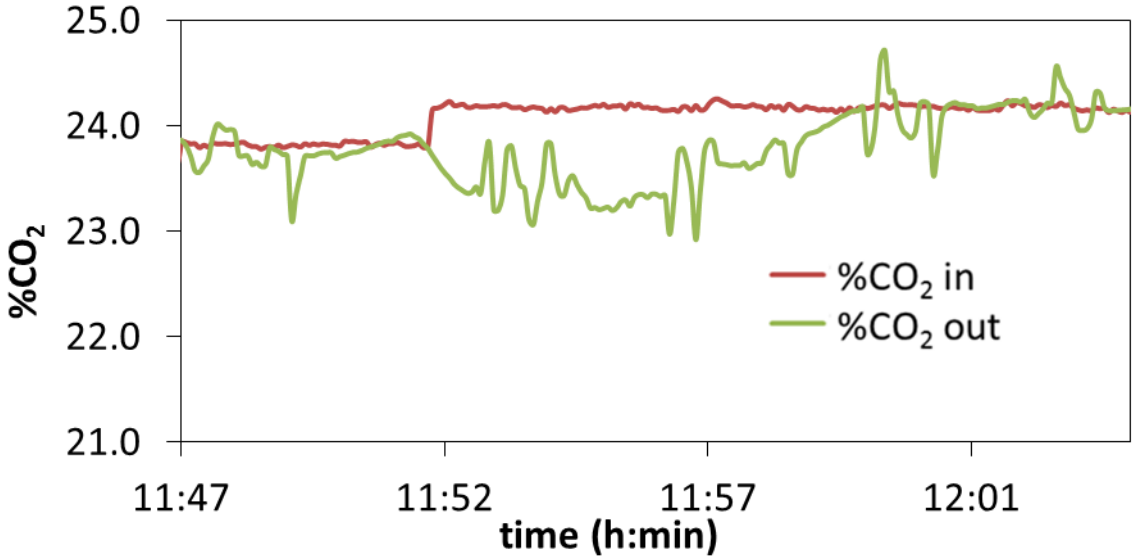

Experiment 8

Solid fed	CaO
Xave	0.25
T (°C)	655
u_{gas} (m/s)	2.20
CO_2 in (vol%)	23.7
Solid flow (kg/h)	6.3
Total gas flow (m^3/h)	18.3
H_2O (vol%)	0.0

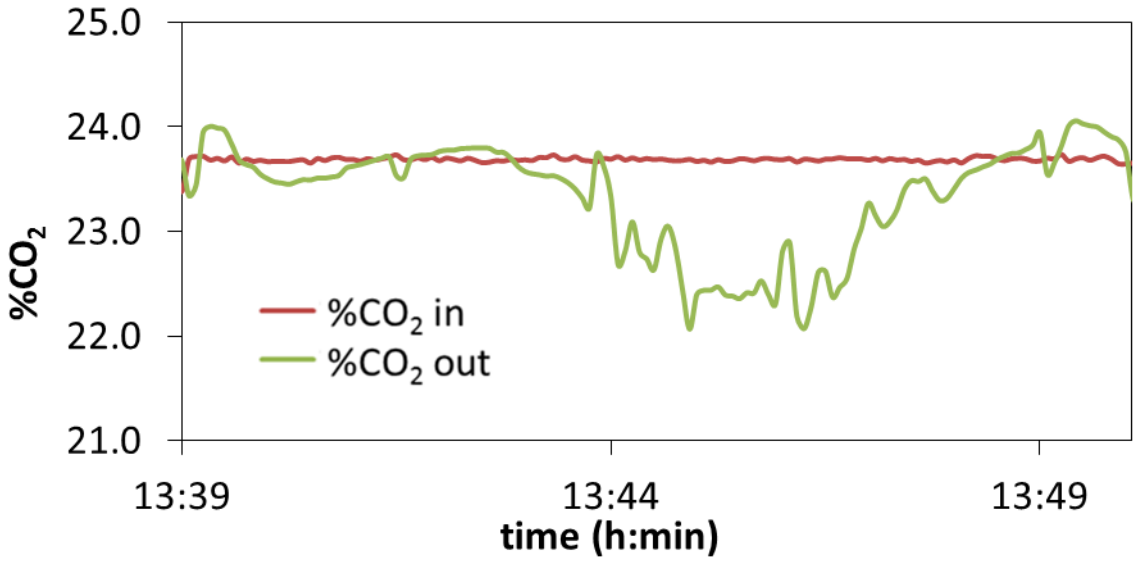

This project has received funding from the European Union's Horizon2020 Research and Innovation Programme under Grant Agreement No 641185

Experiment 9

Solid fed	CaO
Xave	0.25
T (°C)	650
u_{gas} (m/s)	1.88
CO_2 in (vol%)	27.7
Solid flow (kg/h)	3.3
Total gas flow (m^3/h)	15.7
H_2O (vol%)	0.0

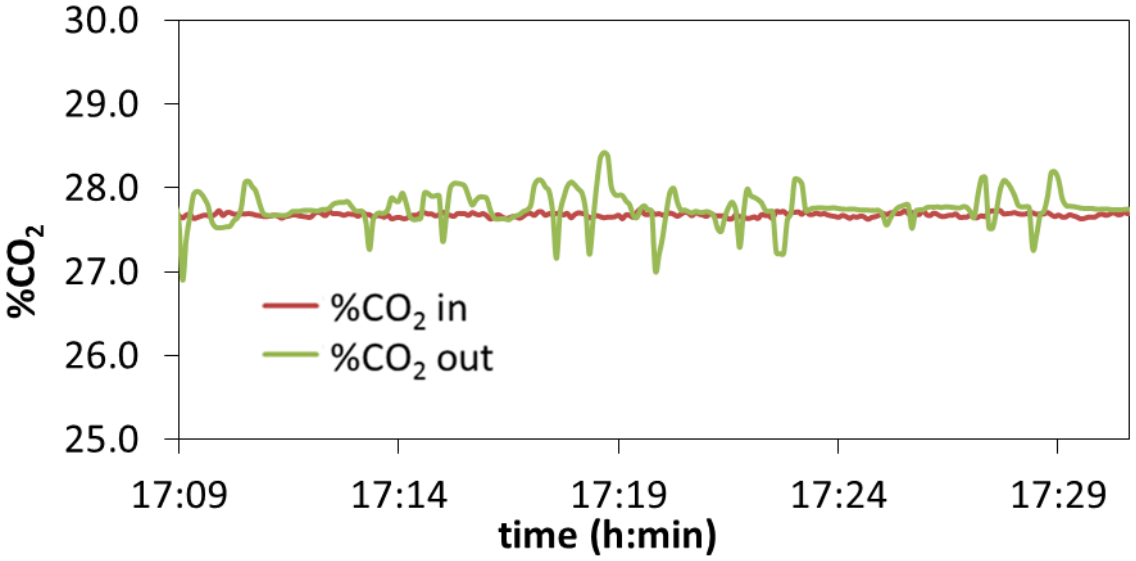

This project has received funding from the European Union's Horizon2020 Research and Innovation Programme under Grant Agreement No 641185

A.5.4 Campaign 4: entrained 'down- flow' testing using the three-pistons solid feeding system

Due to the difficulties on obtaining reliable results with the up-flow configuration, it was decided to change the configuration of the carbonator in order to operate in down-flow. The detail description of this configuration is included in Section 2.3 of this report. The experiments were carried out using the in-house solid feeding system with three injectors described in section A.2.3. The air and CO_2 mix was injected in the pre-heater reactor and carried to the top of the carbonator. Under this configuration, no solids were captured with the cyclone and the carbonation was followed by the CO_2 variations in the gas phase. With this new way of working, the solid deposition problems disappeared but there were still problems with the air leakages in the solid feeding system. In addition, there were some leakages of the CO_2 and air mix in the way from the pre-heater riser to the carbonator.

There were made 4 different experiments using calcined limestone with an average CO_2 carrying capacity of around 0.26. The gas velocity was settled at around 2m/s and the CO_2 concentration at 22%$_v$. The temperature was kept constant at around 640°C.

This project has received funding from the European Union's Horizon2020 Research and Innovation Programme under Grant Agreement No 641185

Experiment 1

Solid fed	CaO
Xave	0.25
T (°C)	642
u_{gas} (m/s)	2.20
CO_2 in (vol%)	22.3
Solid flow (kg/h)	3.0
Total gas flow (m^3/h)	18.6
H_2O (vol%)	0.0

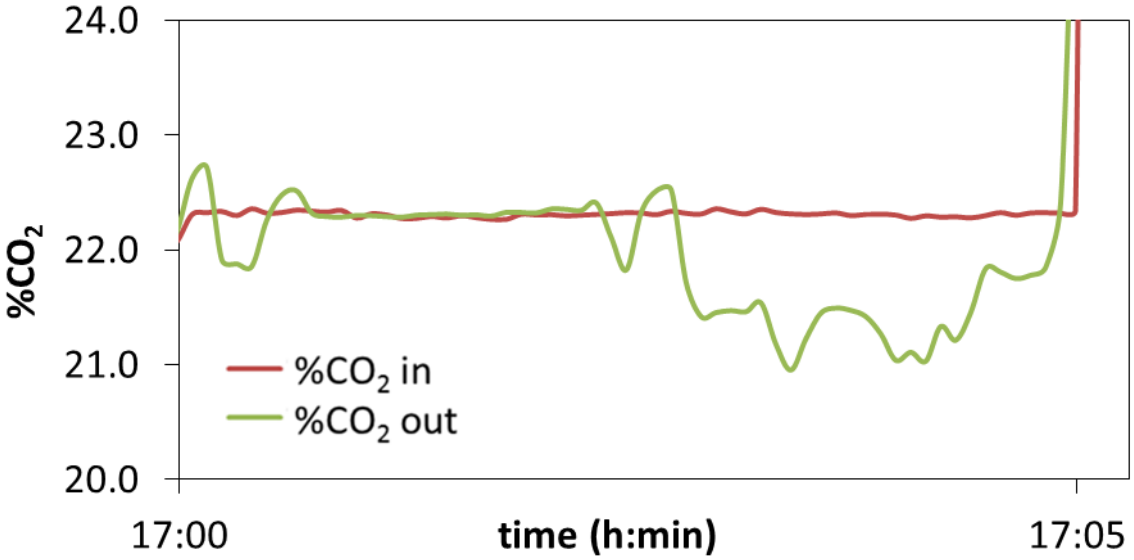

Experiment 2

Solid fed	CaO
Xave	0.25
T (°C)	638
u_{gas} (m/s)	2.22
CO_2 in (vol%)	21.4
Solid flow (kg/h)	8.0
Total gas flow (m^3/h)	18.8
H_2O (vol%)	0.0

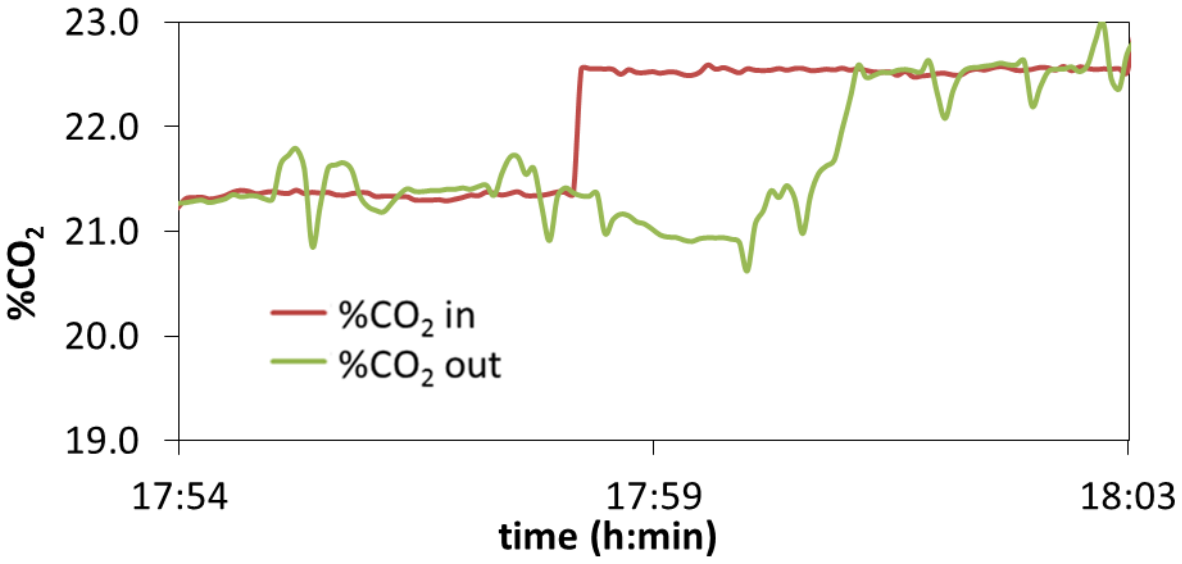

This project has received funding from the European Union's Horizon2020 Research and Innovation Programme under Grant Agreement No 641185

Experiment 3

Solid fed	CaO
Xave	0.25
T (°C)	638
u_{gas} (m/s)	2.33
CO_2 in (vol%)	21.3
Solid flow (kg/h)	6.5
Total gas flow (m^3/h)	19.7
H_2O (vol%)	0.0

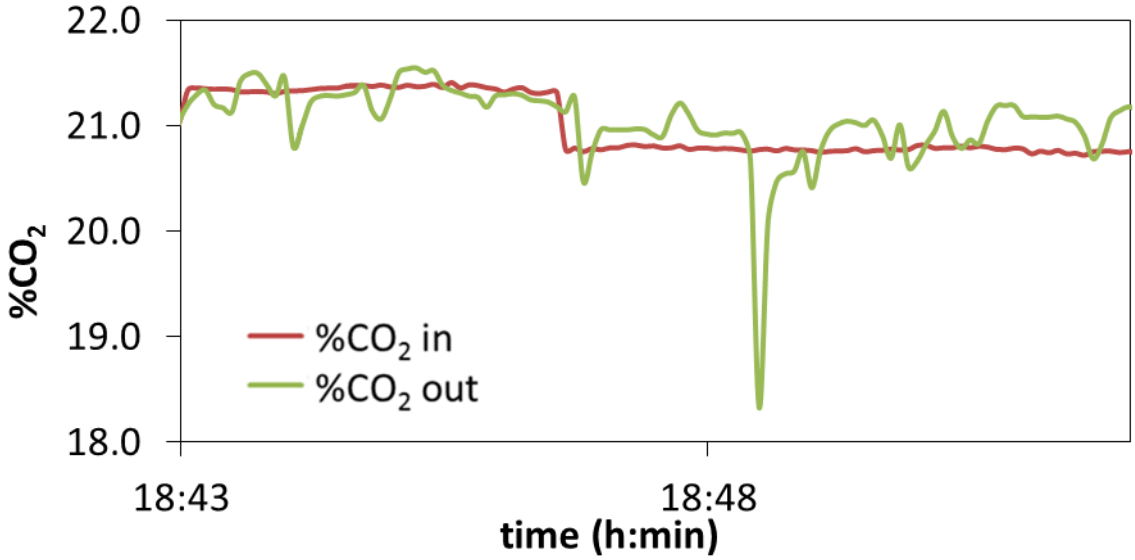

Experiment 4

Solid fed	CaO
Xave	0.25
T (°C)	641
u_{gas} (m/s)	2.10
CO_2 in (vol%)	23.3
Solid flow (kg/h)	4.9
Total gas flow (m^3/h)	17.7
H_2O (vol%)	0.0

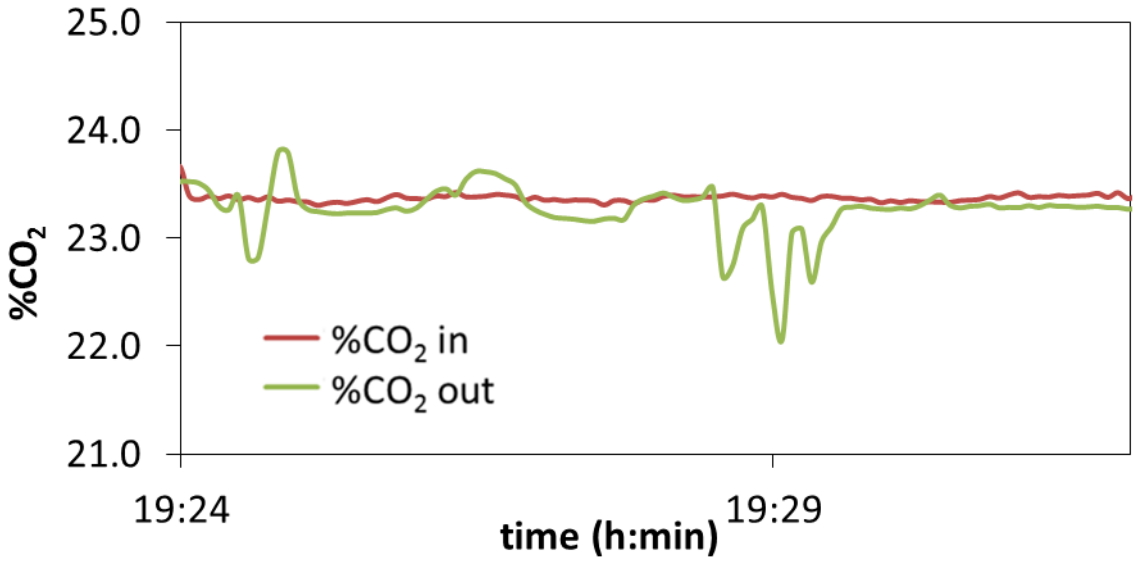

This project has received funding from the European Union's Horizon2020 Research and Innovation Programme under Grant Agreement No 641185

A.5.5 Campaign 5: entrained 'down-flow' testing using the drain-tube solid feeding system and nascent CaO as a sorbent

Due to the problems encountered with the air leakage from the solid feeding system a new design was tested (Configuration 3 described in Section 2.3). One advantage of this design is that the pressure drop across the bed of particles in the reservoir of solids reduces largely the leakage of the carrying air.

The new solid feeding system developed better results than the former one since it allowed feeding high solid flow rates in a more stable way and with controlled air leakages. Therefore the data treatment was easier and the results more reliable. The sorbent used was a nascent calcium oxide with an average CO_2 carrying capacity of around 0.70 that allowed achieving higher CO_2 capture efficiencies.

There were made 31 different experiments at different gas velocities and CO_2 concentrations. The gas velocity varied between 0.5 and 2m/s and the CO_2 concentration between 5%$_v$ and 25%$_v$, with the aim of sweep a wide range of residence times and CO_2 concentrations. The temperature was kept constant at around 675°C.

This project has received funding from the European Union's Horizon2020 Research and Innovation Programme under Grant Agreement No 641185

Experiment 1

Solid fed	CaO
Xave	0.25
T (°C)	659
u_{gas} (m/s)	0.51
CO_2 in (vol%)	24.8
Solid flow (kg/h)	7.6
Total gas flow (m^3/h)	4.3
H_2O (vol%)	0.0

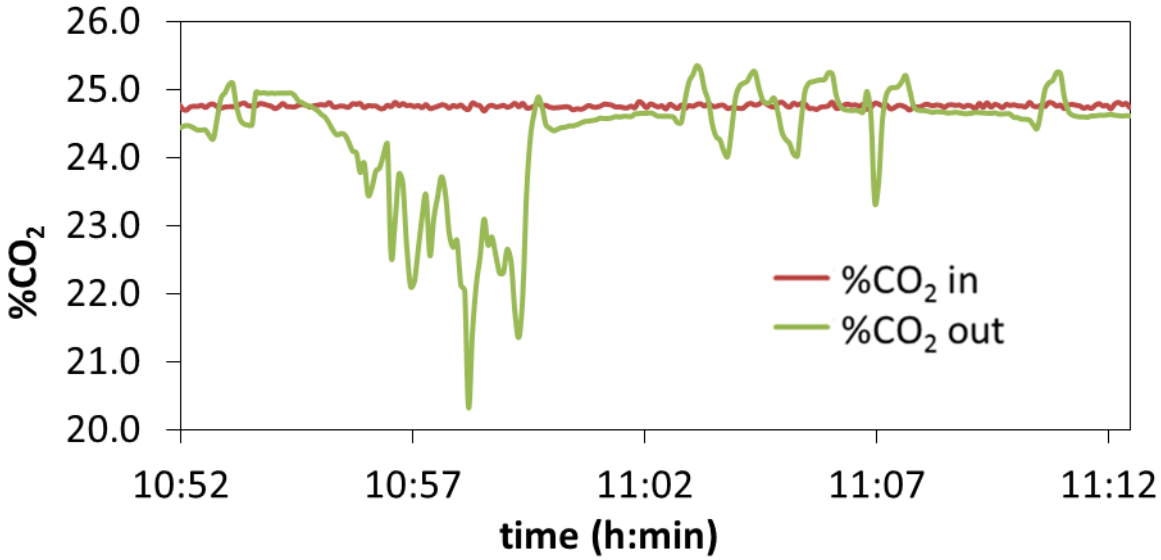

Experiment 2

Solid fed	nascent CaO
Xave	0.70
T (°C)	662
u_{gas} (m/s)	0.50
CO_2 in (vol%)	24.4
Solid flow (kg/h)	4.6
Total gas flow (m^3/h)	4.1
H_2O (vol%)	0.0

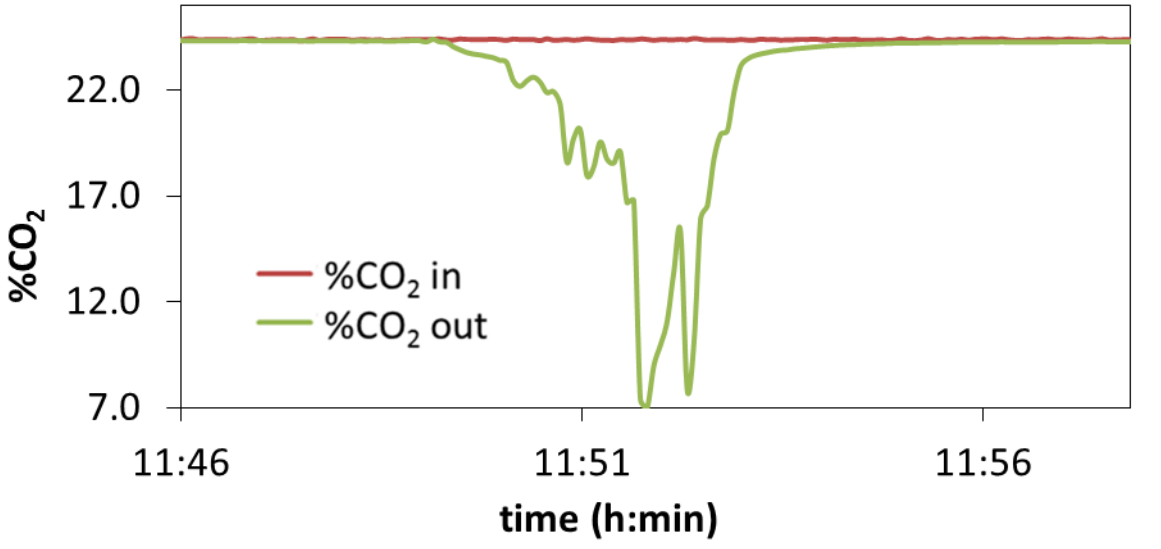

This project has received funding from the European Union's Horizon2020 Research and Innovation Programme under Grant Agreement No 641185

Experiment 3

Solid fed	nascent CaO
Xave	0.70
T (°C)	668
u_{gas} (m/s)	0.49
CO_2 in (vol%)	24.2
Solid flow (kg/h)	0.9
Total gas flow (m^3/h)	4.0
H_2O (vol%)	0.0

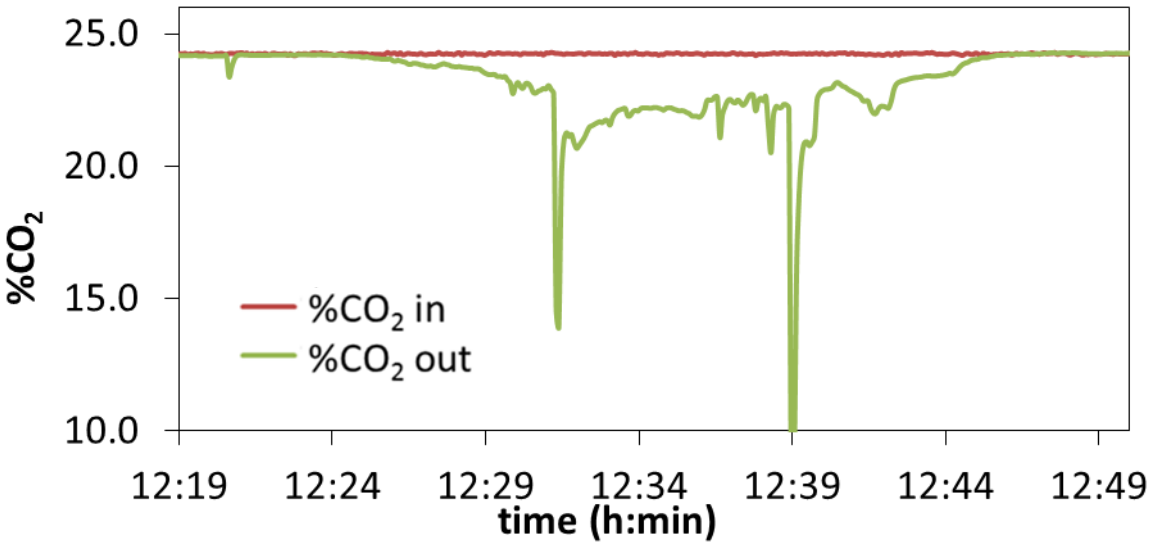

Experiment 4

Solid fed	nascent CaO
Xave	0.70
T (°C)	670
u_{gas} (m/s)	0.49
CO_2 in (vol%)	24.2
Solid flow (kg/h)	3.1
Total gas flow (m^3/h)	4.0
H_2O (vol%)	0.0

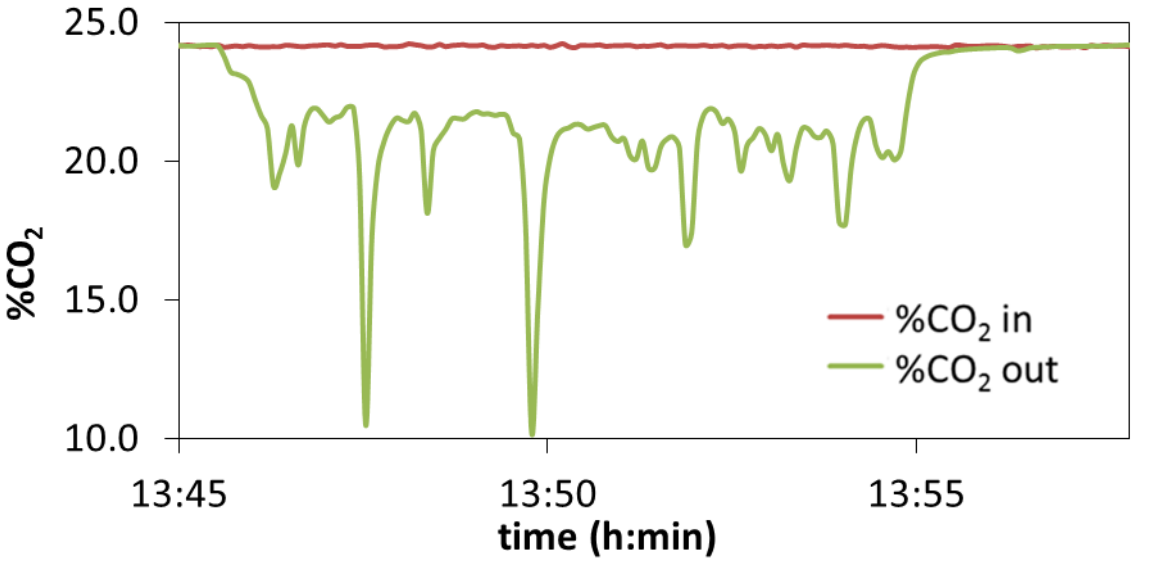

This project has received funding from the European Union's Horizon2020 Research and Innovation Programme under Grant Agreement No 641185

Experiment 5

Solid fed	nascent CaO
Xave	0.70
T (°C)	675
u_{gas} (m/s)	0.40
CO_2 in (vol%)	6.9
Solid flow (kg/h)	3.0
Total gas flow (m^3/h)	3.3
H_2O (vol%)	0.0

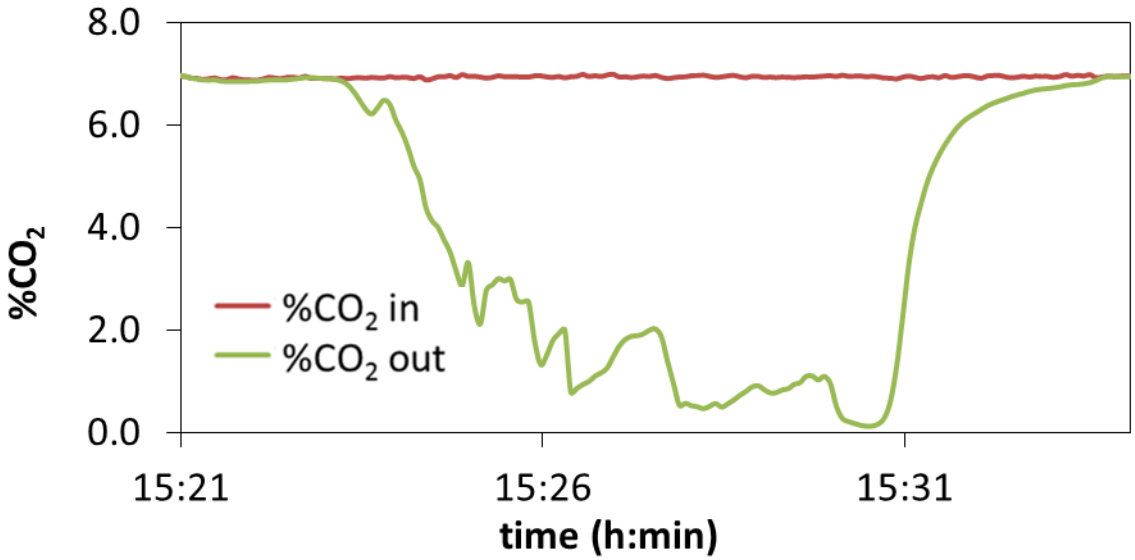

Experiment 6

Solid fed	nascent CaO
Xave	0.70
T (°C)	677
u_{gas} (m/s)	0.31
CO_2 in (vol%)	4.4
Solid flow (kg/h)	2.4
Total gas flow (m^3/h)	2.5
H_2O (vol%)	0.0

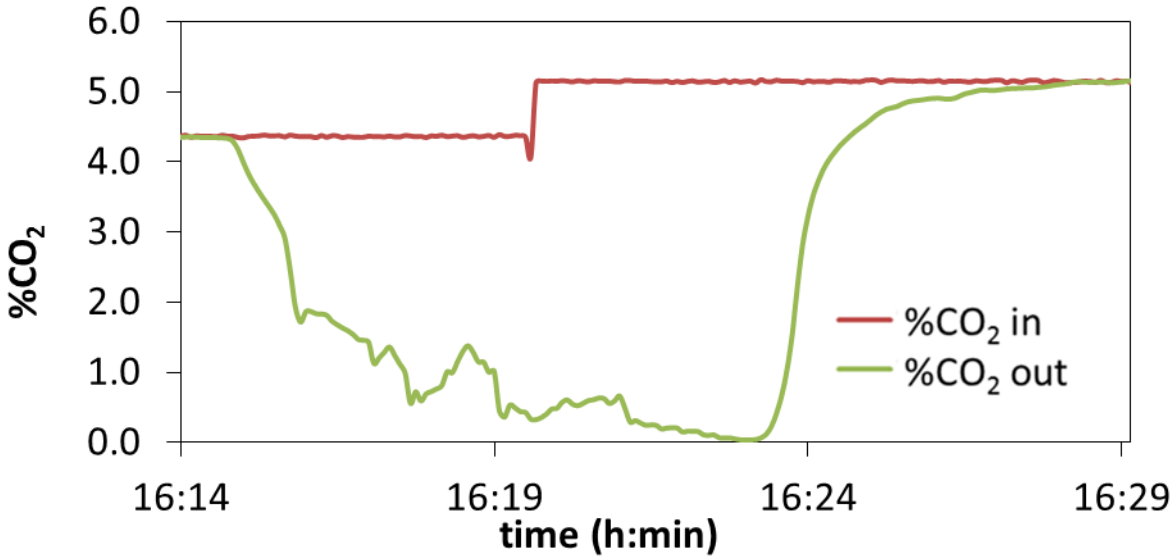

This project has received funding from the European Union's Horizon2020 Research and Innovation Programme under Grant Agreement No 641185

Experiment 7

Solid fed	nascent CaO
Xave	0.70
T (°C)	635
u_{gas} (m/s)	0.82
CO_2 in (vol%)	10.8
Solid flow (kg/h)	3.6
Total gas flow (m^3/h)	6.9
H_2O (vol%)	0.0

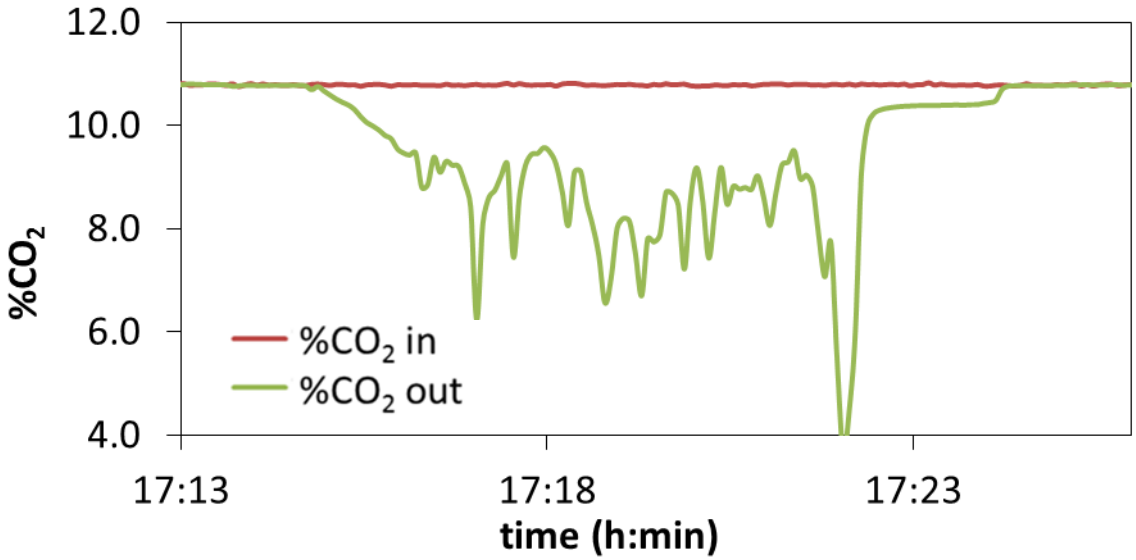

Experiment 8

Solid fed	nascent CaO
Xave	0.70
T (°C)	643
u_{gas} (m/s)	0.60
CO_2 in (vol%)	21.6
Solid flow (kg/h)	3.1
Total gas flow (m^3/h)	5.1
H_2O (vol%)	0.0

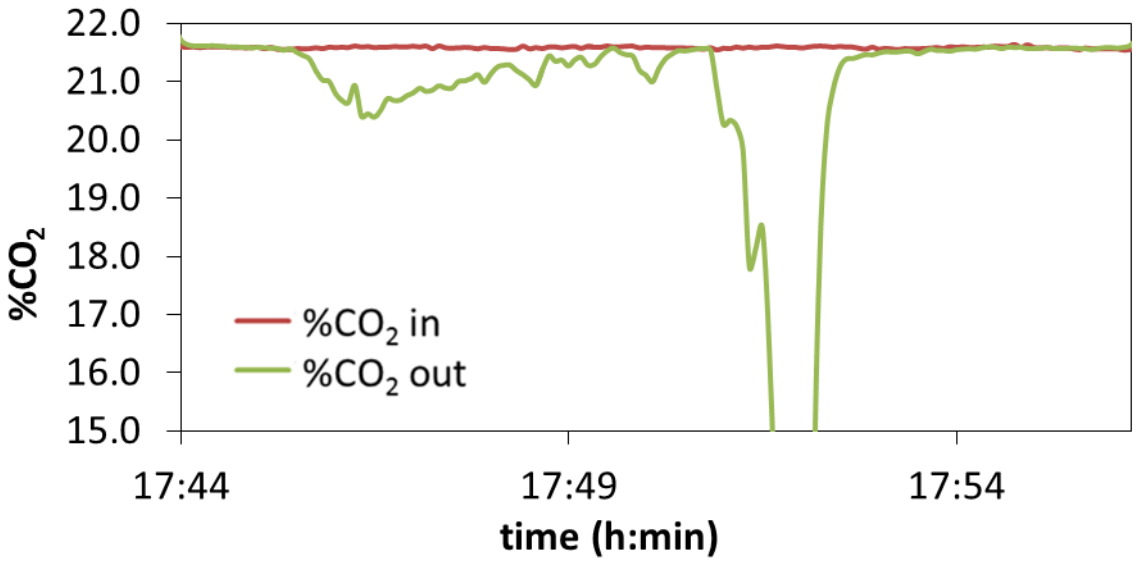

This project has received funding from the European Union's Horizon2020 Research and Innovation Programme under Grant Agreement No 641185

Experiment 9

Solid fed	nascent CaO
Xave	0.70
T (°C)	655
u_{gas} (m/s)	0.61
CO_2 in (vol%)	21.6
Solid flow (kg/h)	2.9
Total gas flow (m^3/h)	5.0
H_2O (vol%)	0.0

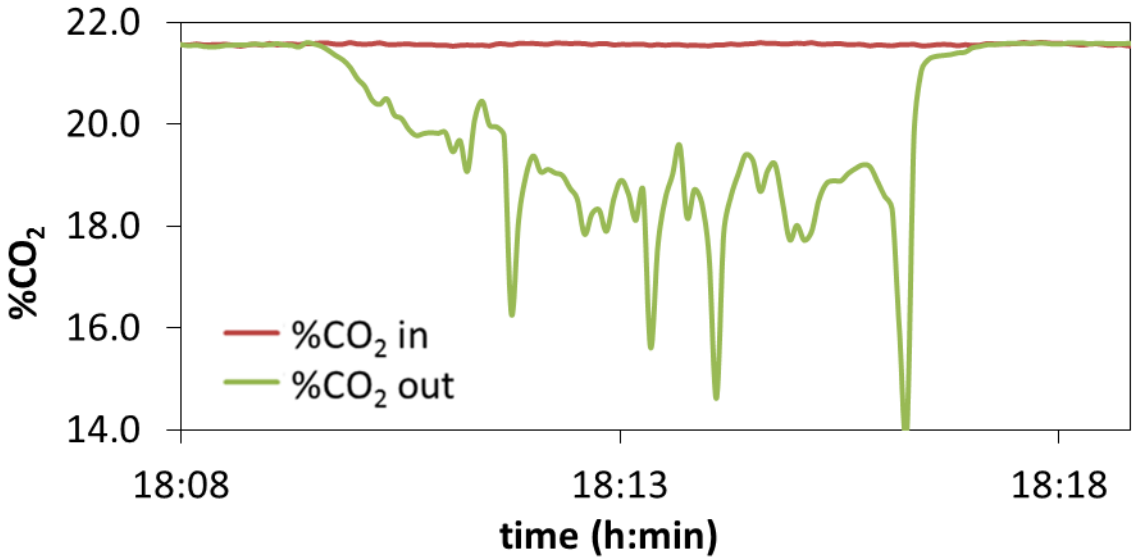

Experiment 10

Solid fed	nascent CaO
Xave	0.70
T (°C)	669
u_{gas} (m/s)	0.70
CO_2 in (vol%)	14.5
Solid flow (kg/h)	1.8
Total gas flow (m^3/h)	5.7
H_2O (vol%)	0.0

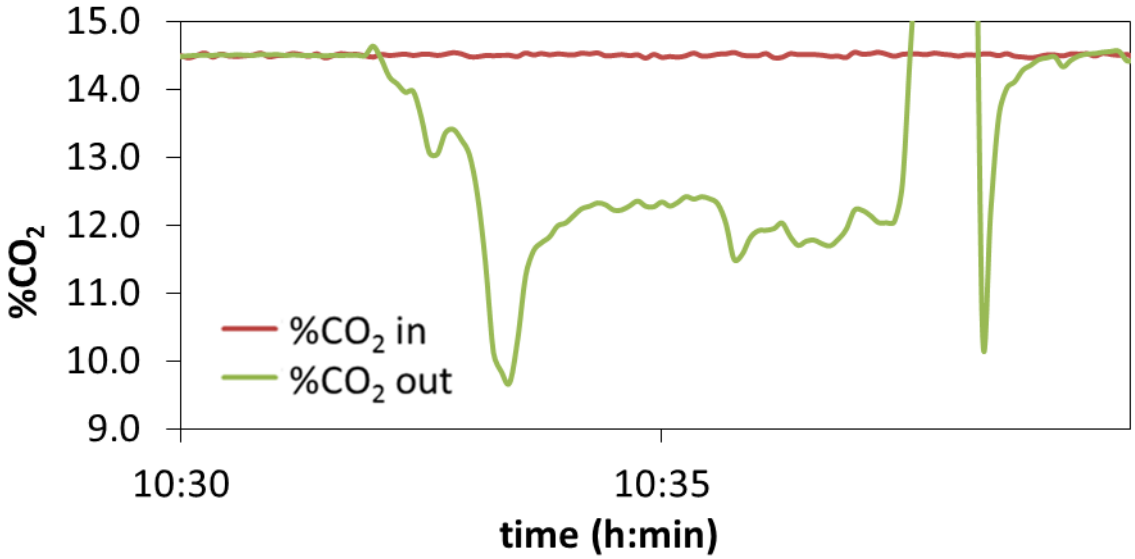

This project has received funding from the European Union's Horizon2020 Research and Innovation Programme under Grant Agreement No 641185

Experiment 11

Solid fed	nascent CaO
Xave	0.70
T (°C)	673
u_{gas} (m/s)	0.69
CO_2 in (vol%)	22.7
Solid flow (kg/h)	1.7
Total gas flow (m^3/h)	5.6
H_2O (vol%)	0.0

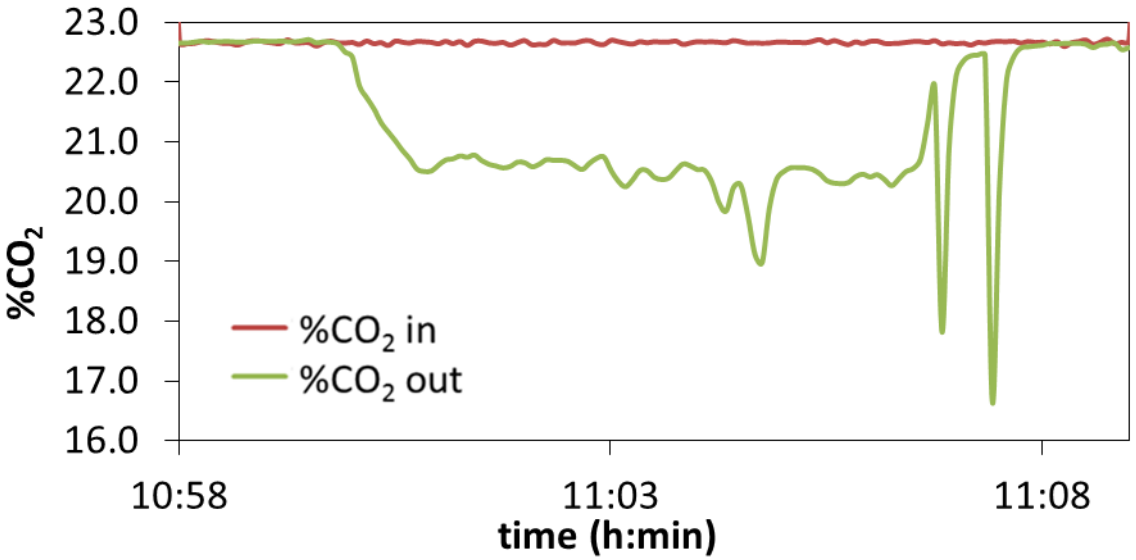

Experiment 12

Solid fed	nascent CaO
Xave	0.70
T (°C)	674
u_{gas} (m/s)	0.96
CO_2 in (vol%)	5.7
Solid flow (kg/h)	1.3
Total gas flow (m^3/h)	7.8
H_2O (vol%)	0.0

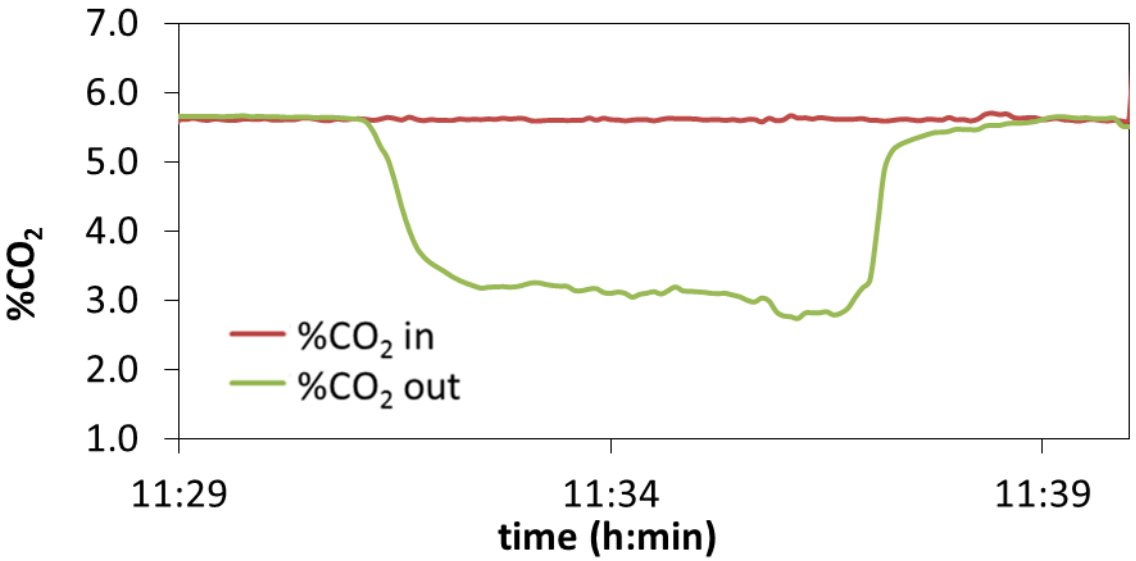

This project has received funding from the European Union's Horizon2020 Research and Innovation Programme under Grant Agreement No 641185

Experiment 13

Solid fed	nascent CaO
Xave	0.70
T (°C)	676
u_{gas} (m/s)	0.73
CO_2 in (vol%)	10.2
Solid flow (kg/h)	1.4
Total gas flow (m^3/h)	6.0
H_2O (vol%)	0.0

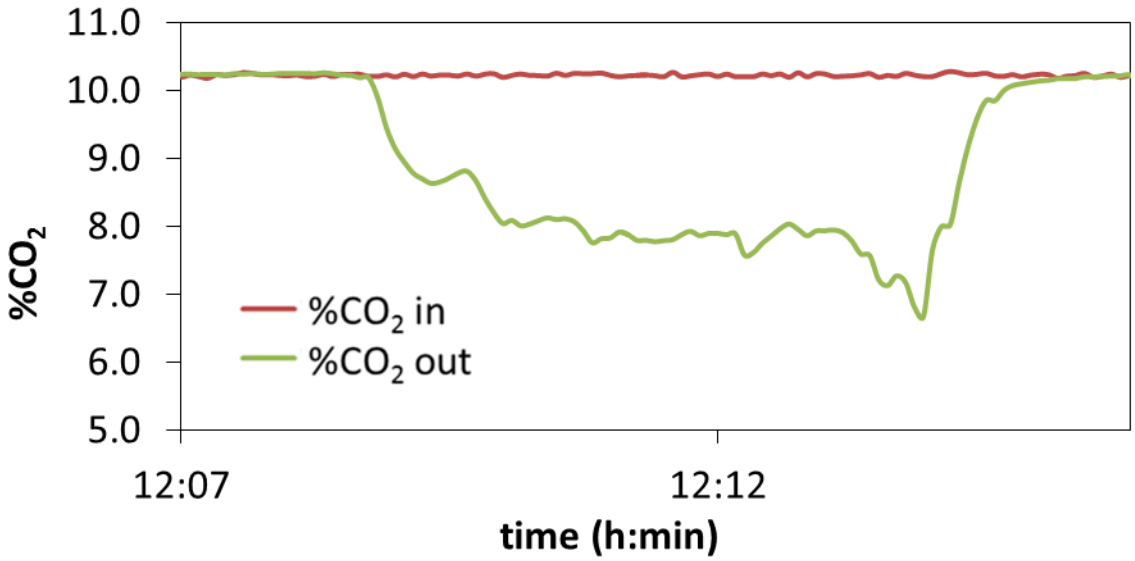

Experiment 14

Solid fed	nascent CaO
Xave	0.70
T (°C)	676
u_{gas} (m/s)	0.68
CO_2 in (vol%)	18.8
Solid flow (kg/h)	1.4
Total gas flow (m^3/h)	5.5
H_2O (vol%)	0.0

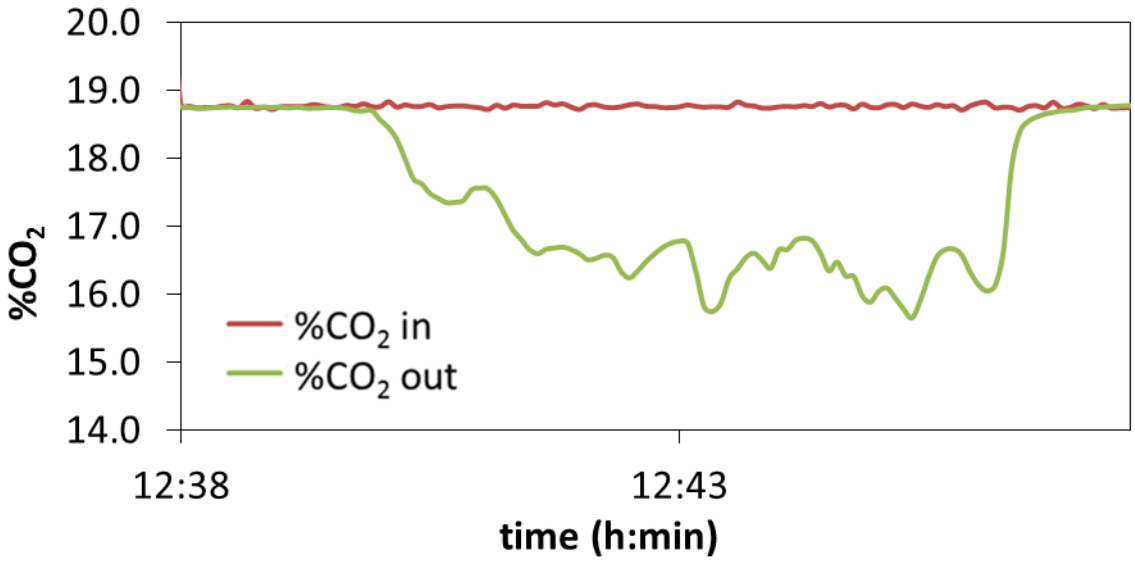

This project has received funding from the European Union's Horizon2020 Research and Innovation Programme under Grant Agreement No 641185

Experiment 15

Solid fed	nascent CaO
Xave	0.70
T (°C)	679
u_{gas} (m/s)	0.52
CO_2 in (vol%)	15.9
Solid flow (kg/h)	1.5
Total gas flow (m^3/h)	4.2
H_2O (vol%)	0.0

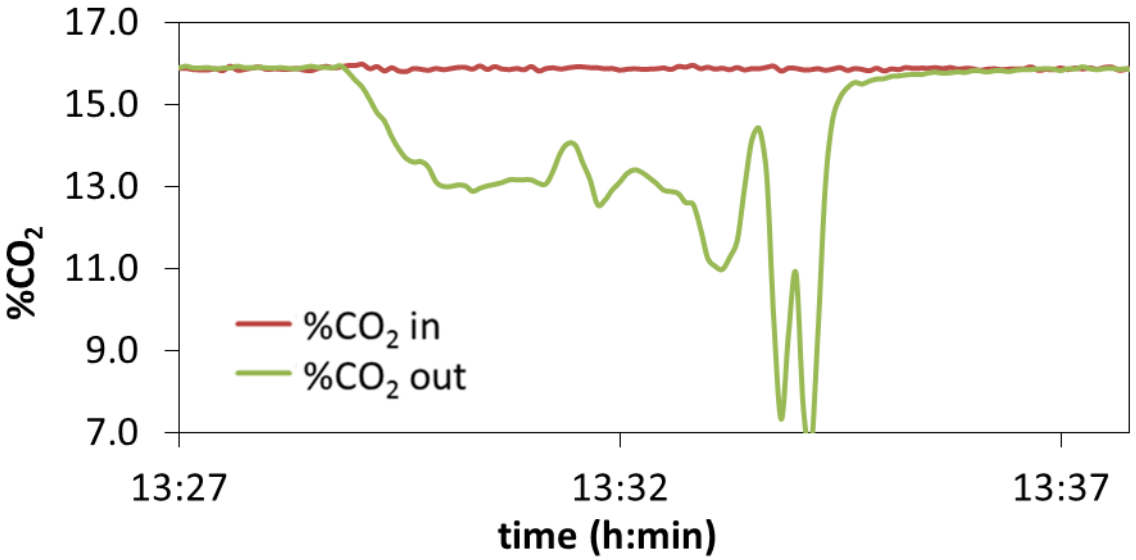

Experiment 16

Solid fed	nascent CaO
Xave	0.70
T (°C)	663
u_{gas} (m/s)	0.93
CO_2 in (vol%)	14.6
Solid flow (kg/h)	1.1
Total gas flow (m^3/h)	7.7
H_2O (vol%)	0.0

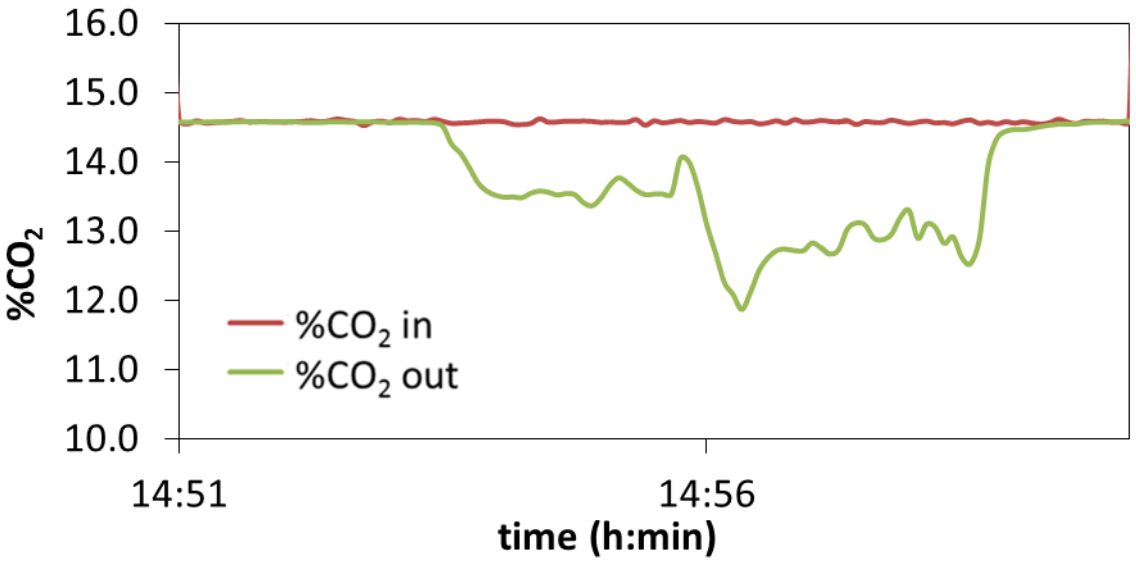

This project has received funding from the European Union's Horizon2020 Research and Innovation Programme under Grant Agreement No 641185

Experiment 17

Solid fed	nascent CaO
Xave	0.70
T (°C)	663
u_{gas} (m/s)	1.70
CO_2 in (vol%)	5.6
Solid flow (kg/h)	1.5
Total gas flow (m^3/h)	14.0
H_2O (vol%)	0.0

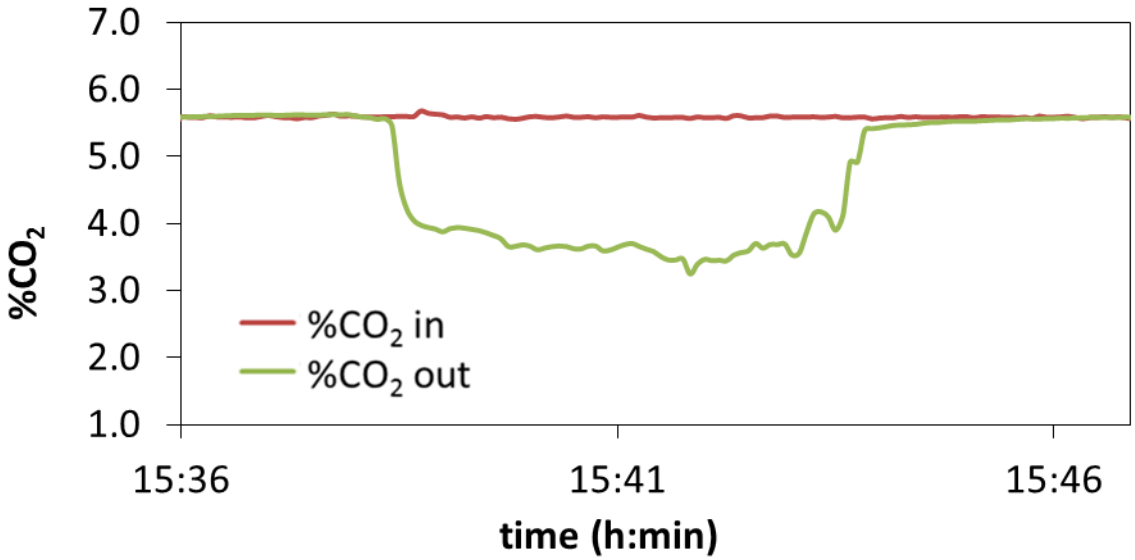

Experiment 18

Solid fed	nascent CaO
Xave	0.70
T (°C)	662
u_{gas} (m/s)	0.99
CO_2 in (vol%)	15.2
Solid flow (kg/h)	1.3
Total gas flow (m^3/h)	8.2
H_2O (vol%)	0.0

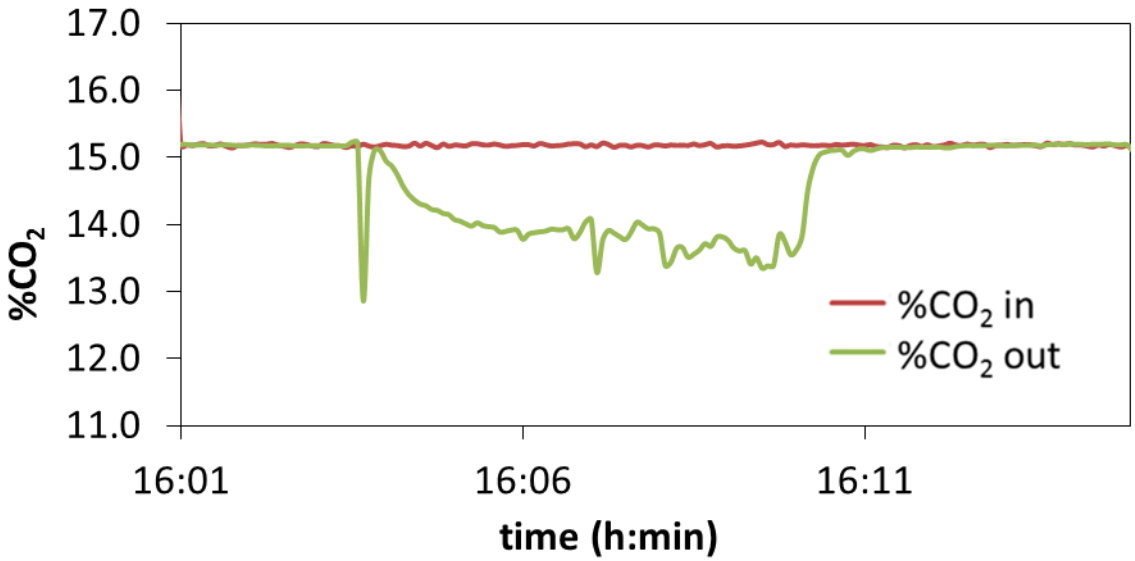

This project has received funding from the European Union's Horizon2020 Research and Innovation Programme under Grant Agreement No 641185

Experiment 19

Solid fed	nascent CaO
Xave	0.70
T (°C)	660
u_{gas} (m/s)	0.87
CO_2 in (vol%)	22.6
Solid flow (kg/h)	1.5
Total gas flow (m^3/h)	7.2
H_2O (vol%)	0.0

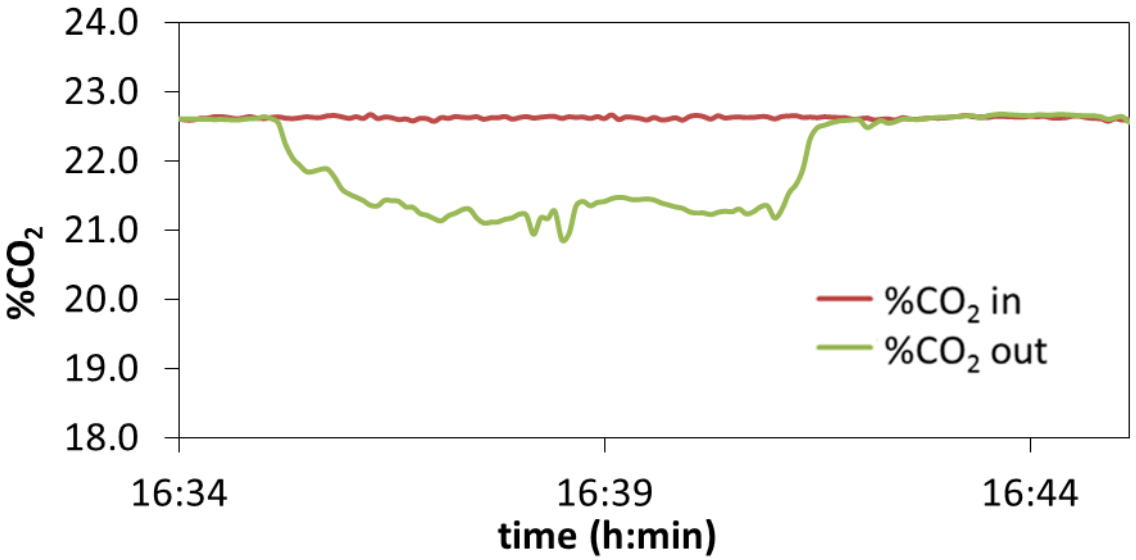

Experiment 20

Solid fed	nascent CaO
Xave	0.70
T (°C)	678
u_{gas} (m/s)	0.46
CO_2 in (vol%)	4.9
Solid flow (kg/h)	1.5
Total gas flow (m^3/h)	3.7
H_2O (vol%)	0.0

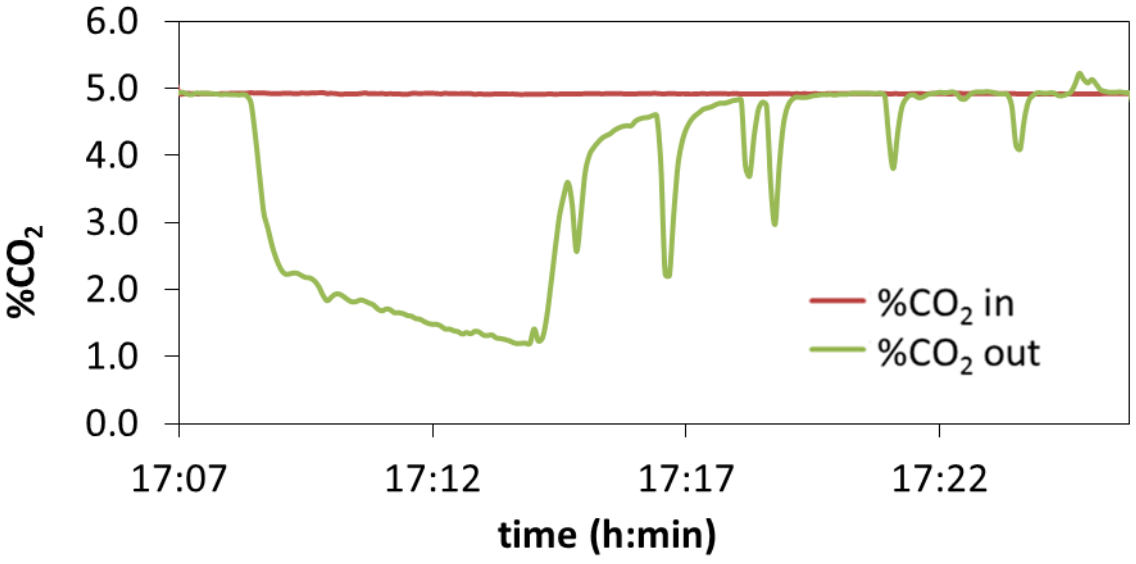

This project has received funding from the European Union's Horizon2020 Research and Innovation Programme under Grant Agreement No 641185

Experiment 21

Solid fed	nascent CaO
Xave	0.70
T (°C)	680
u_{gas} (m/s)	0.57
CO_2 in (vol%)	24.4
Solid flow (kg/h)	1.5
Total gas flow (m^3/h)	4.6
H_2O (vol%)	0.0

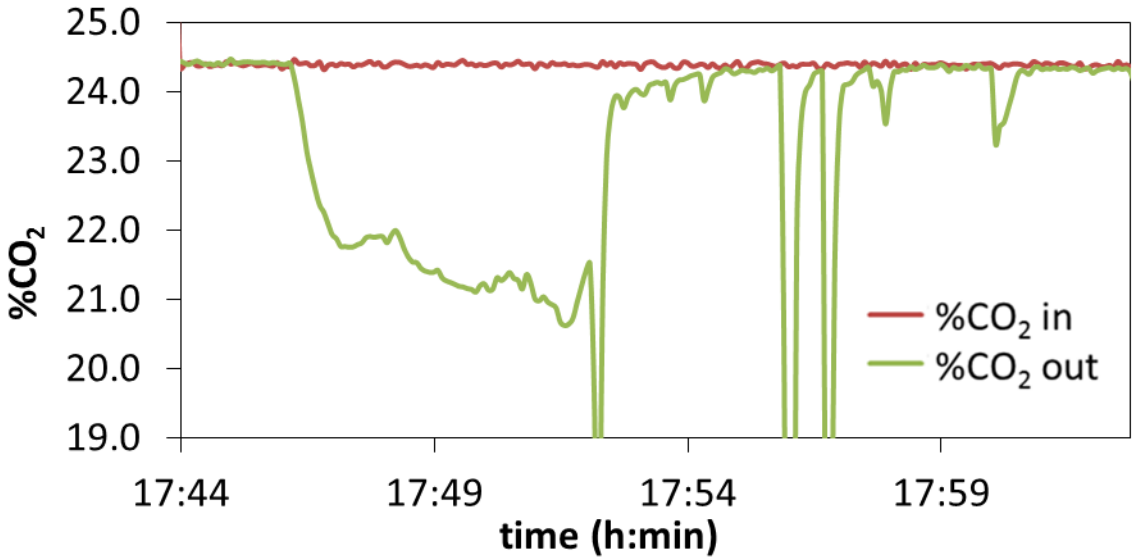

Experiment 22

Solid fed	nascent CaO
Xave	0.70
T (°C)	676
u_{gas} (m/s)	0.72
CO_2 in (vol%)	14.1
Solid flow (kg/h)	1.3
Total gas flow (m^3/h)	5.9
H_2O (vol%)	0.0

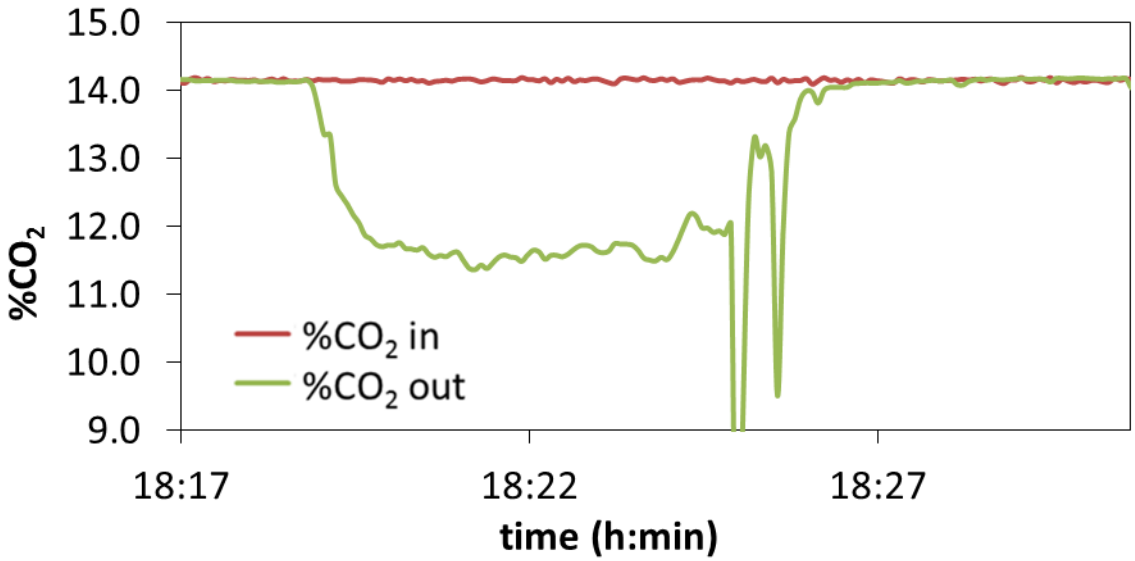

This project has received funding from the European Union's Horizon2020 Research and Innovation Programme under Grant Agreement No 641185

Experiment 23

Solid fed	nascent CaO
Xave	0.70
T (°C)	692
u_{gas} (m/s)	0.73
CO_2 in (vol%)	6.3
Solid flow (kg/h)	1.3
Total gas flow (m^3/h)	5.8
H_2O (vol%)	0.0

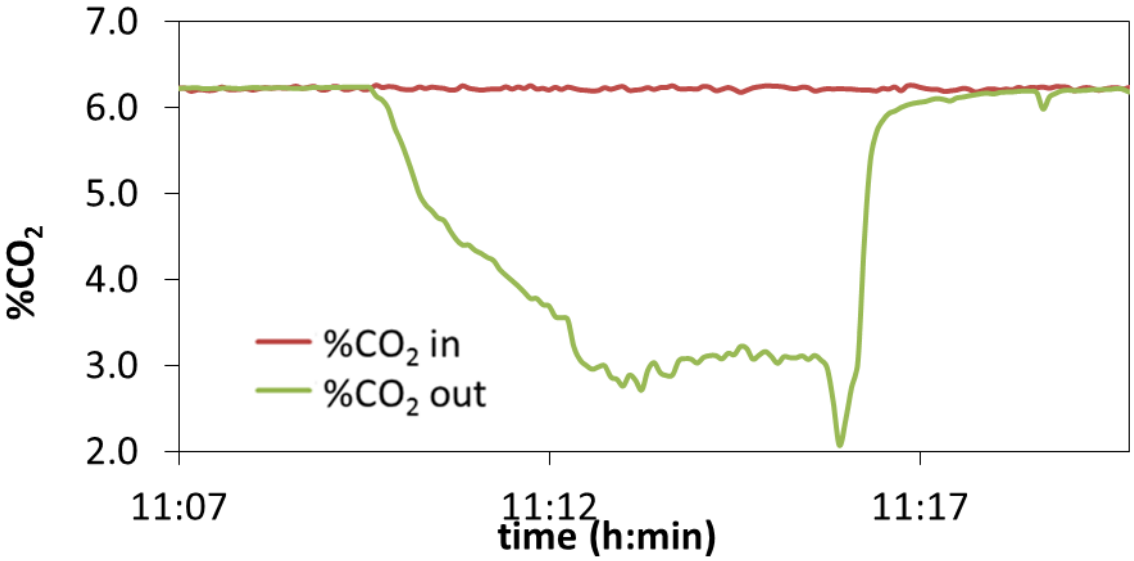

Experiment 24

Solid fed	nascent CaO
Xave	0.70
T (°C)	688
u_{gas} (m/s)	0.71
CO_2 in (vol%)	6.3
Solid flow (kg/h)	0.6
Total gas flow (m^3/h)	5.7
H_2O (vol%)	0.0

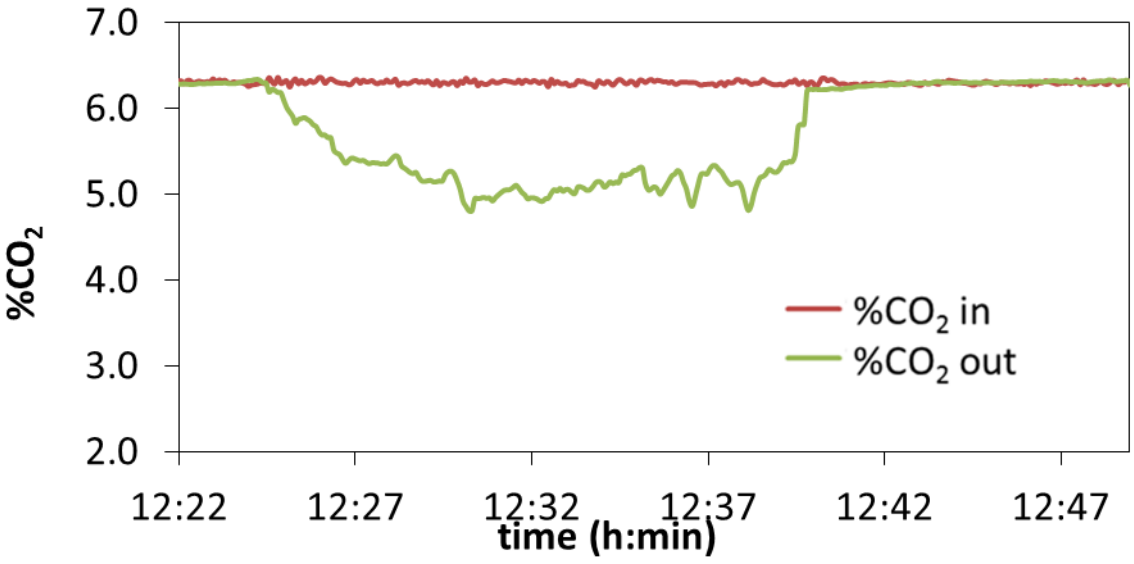

This project has received funding from the European Union's Horizon2020 Research and Innovation Programme under Grant Agreement No 641185

Experiment 25

Solid fed	nascent CaO
Xave	0.70
T (°C)	690
u_{gas} (m/s)	0.71
CO_2 in (vol%)	6.3
Solid flow (kg/h)	1.0
Total gas flow (m^3/h)	5.7
H_2O (vol%)	0.0

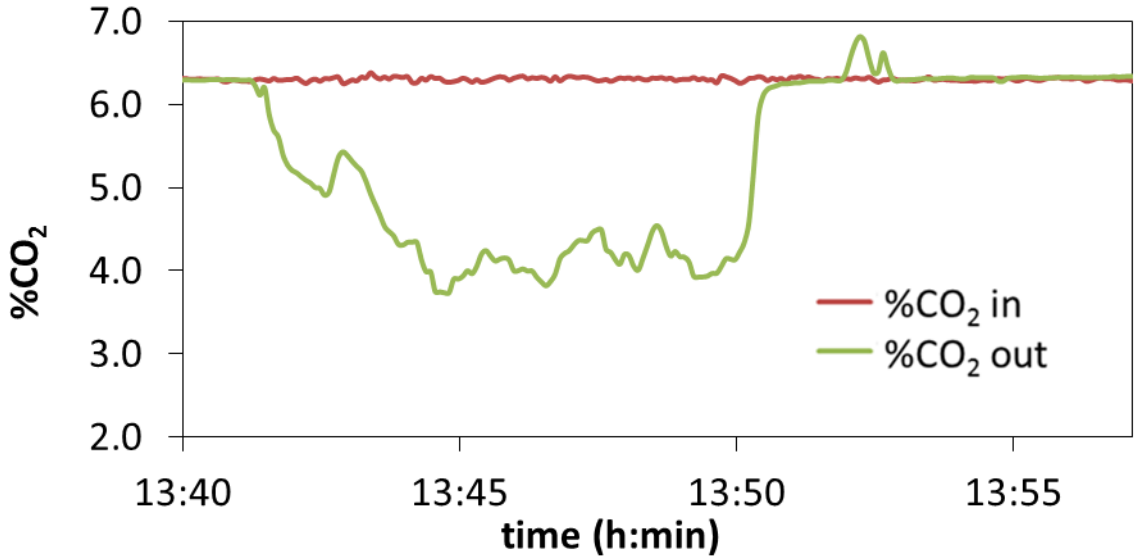

Experiment 26

Solid fed	nascent CaO
Xave	0.70
T (°C)	675
u_{gas} (m/s)	1.81
CO_2 in (vol%)	6.4
Solid flow (kg/h)	1.3
Total gas flow (m^3/h)	14.7
H_2O (vol%)	0.0

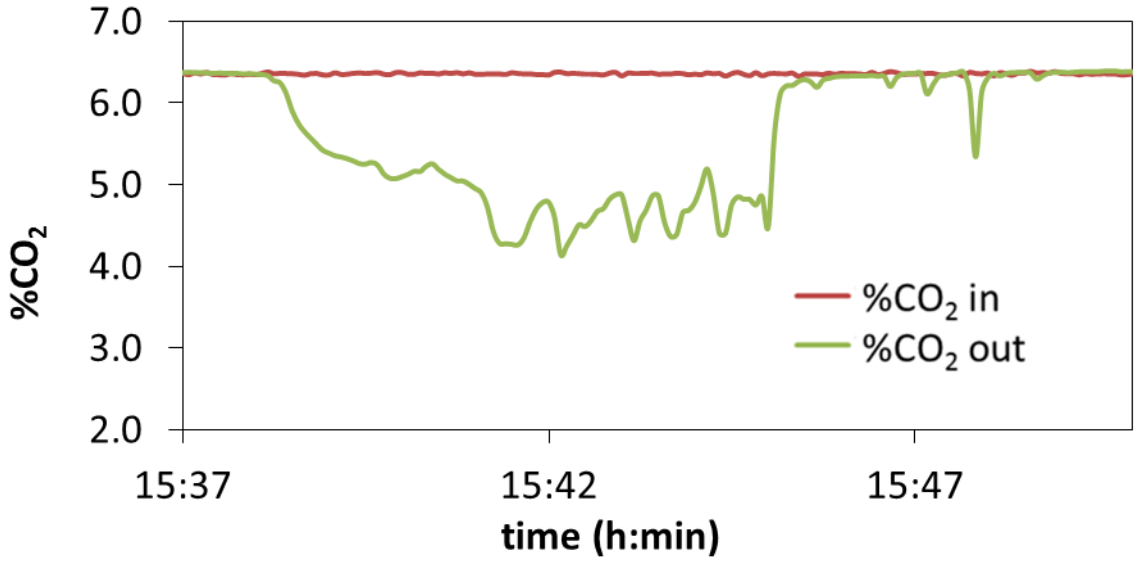

This project has received funding from the European Union's Horizon2020 Research and Innovation Programme under Grant Agreement No 641185

Experiment 27

Solid fed	nascent CaO
Xave	0.70
T (°C)	676
u_{gas} (m/s)	1.77
CO_2 in (vol%)	6.5
Solid flow (kg/h)	0.5
Total gas flow (m^3/h)	14.4
H_2O (vol%)	0.0

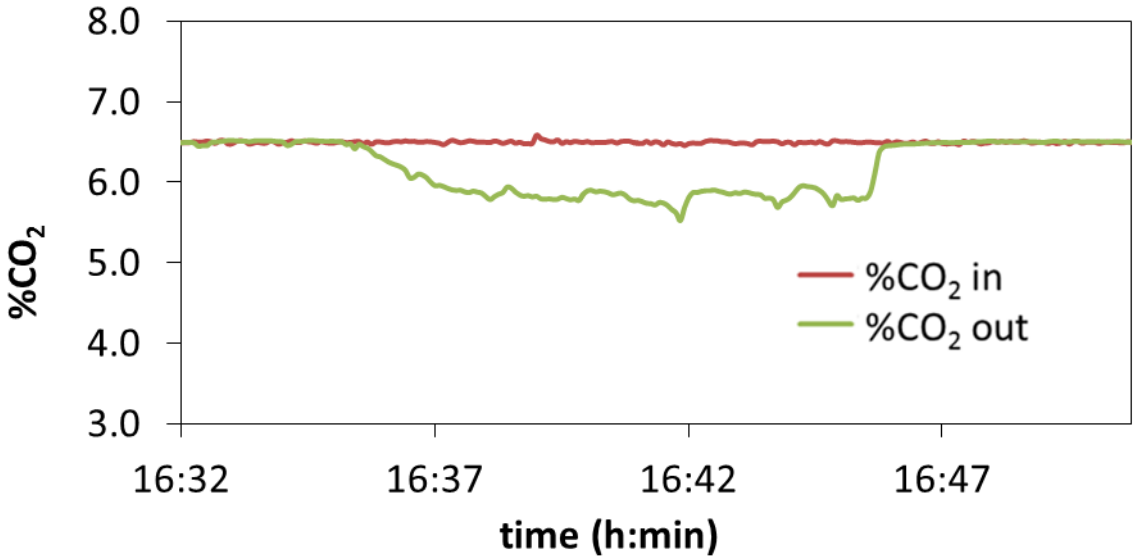

Experiment 28

Solid fed	nascent CaO
Xave	0.70
T (°C)	680
u_{gas} (m/s)	1.78
CO_2 in (vol%)	6.5
Solid flow (kg/h)	1.4
Total gas flow (m^3/h)	14.5
H_2O (vol%)	0.0

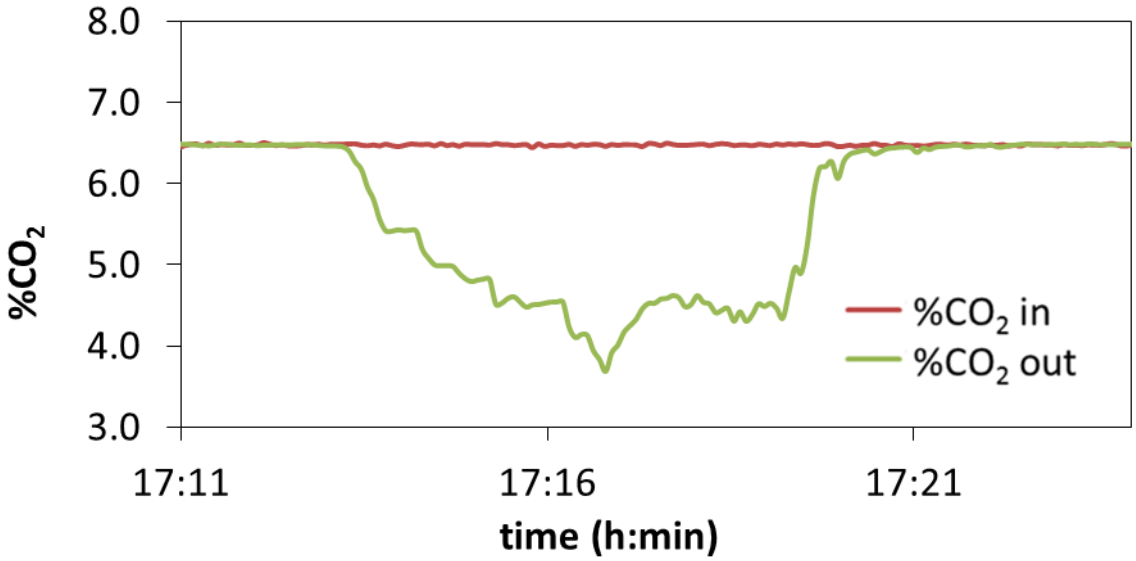

This project has received funding from the European Union's Horizon2020 Research and Innovation Programme under Grant Agreement No 641185

Experiment 29

Solid fed	nascent CaO
Xave	0.70
T (°C)	680
u_{gas} (m/s)	1.80
CO_2 in (vol%)	6.4
Solid flow (kg/h)	0.5
Total gas flow (m^3/h)	14.6
H_2O (vol%)	0.0

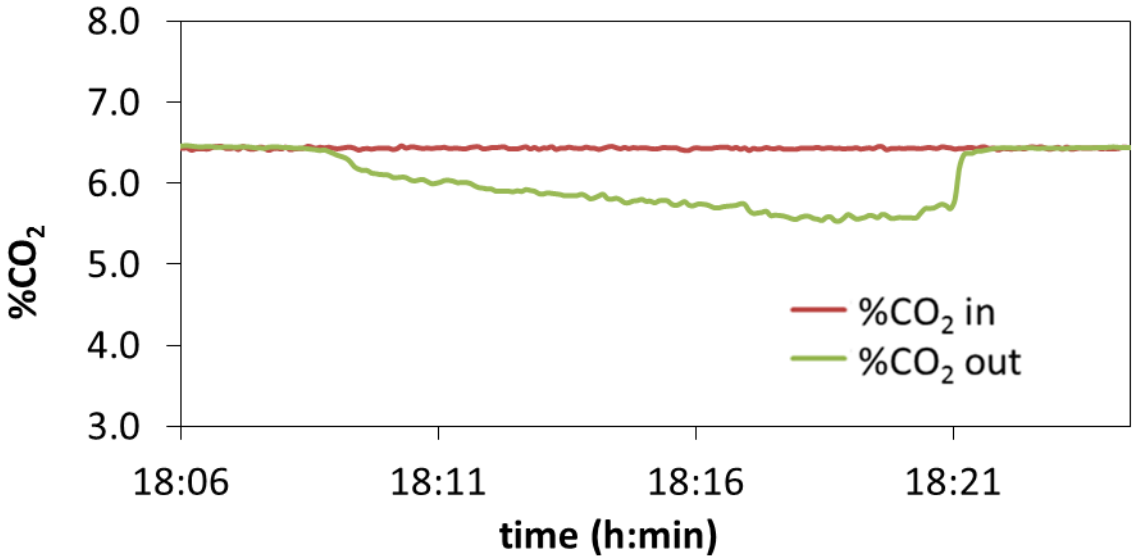

Experiment 30

Solid fed	nascent CaO
Xave	0.70
T (°C)	678
u_{gas} (m/s)	1.83
CO_2 in (vol%)	6.3
Solid flow (kg/h)	1.4
Total gas flow (m^3/h)	14.9
H_2O (vol%)	0.0

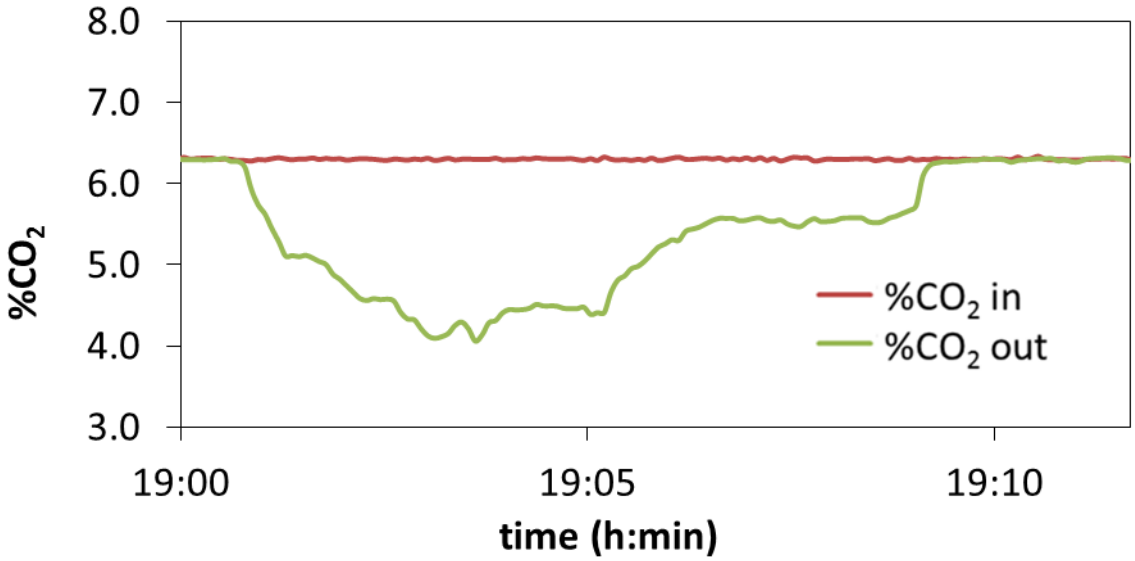

This project has received funding from the European Union's Horizon2020 Research and Innovation Programme under Grant Agreement No 641185

Experiment 31

Solid fed	nascent CaO
Xave	0.70
T (°C)	670
u_{gas} (m/s)	0.81
CO_2 in (vol%)	12.0
Solid flow (kg/h)	1.2
Total gas flow (m^3/h)	6.6
H_2O (vol%)	0.0

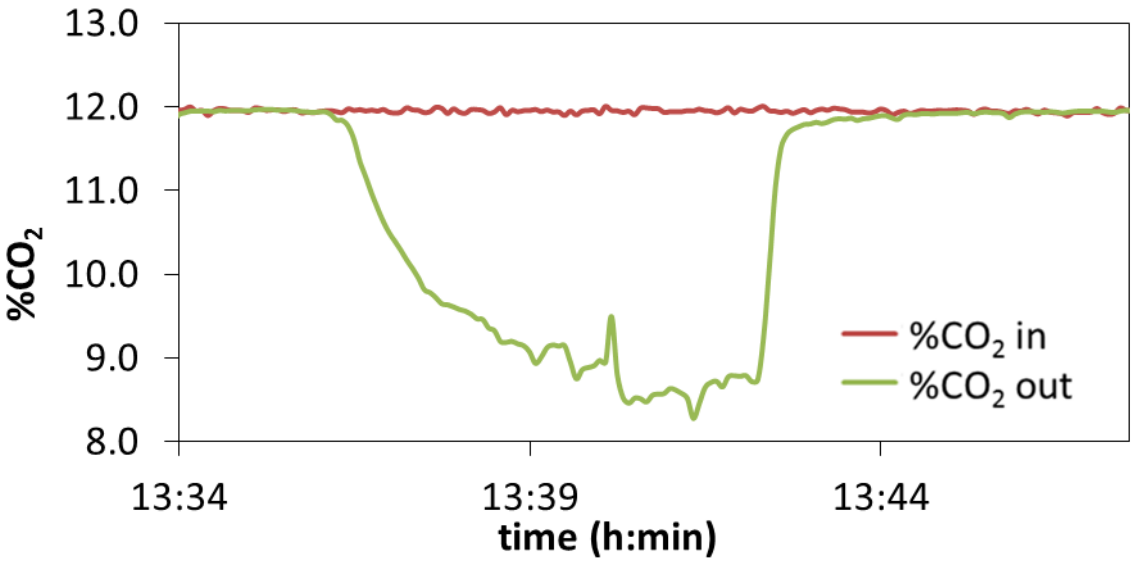

This project has received funding from the European Union's Horizon2020 Research and Innovation Programme under Grant Agreement No 641185

A.5.6 Campaign 6: entrained 'down-flow' testing using the drain-tube solid feeding system and calcined limestone as a sorbent

During this campaign, the same configuration as in Campaign 5 was used. However for this campaign a CaO sorbent derived from a calcined limestone with a Xave of 0.41 was used as indicated in Section 3.2. With the aim of obtaining more information in each experiment, the CO_2 concentration was measured at two heights in the carbonator (at 2.4 and 5.4 m from the sorbent injection point) by using two different analyzers or just one settled in a way that allowed us to change the point of measurement in the middle of the test.

The gas velocity ranged from 0.8 to 2m/s and the CO_2 concentrations from 5%$_v$ to 25%$_v$, in order to sweep as many experimental conditions as possible. The temperature was kept constant at around 660°C.

This project has received funding from the European Union's Horizon2020 Research and Innovation Programme under Grant Agreement No 641185

Experiment 1

Solid fed	CaO
Xave	0.41
T (°C)	670
u_{gas} (m/s)	0.81
CO_2 in (vol%)	11.9
Solid flow (kg/h)	3.2
Total gas flow (m^3/h)	6.6
H_2O (vol%)	0.0

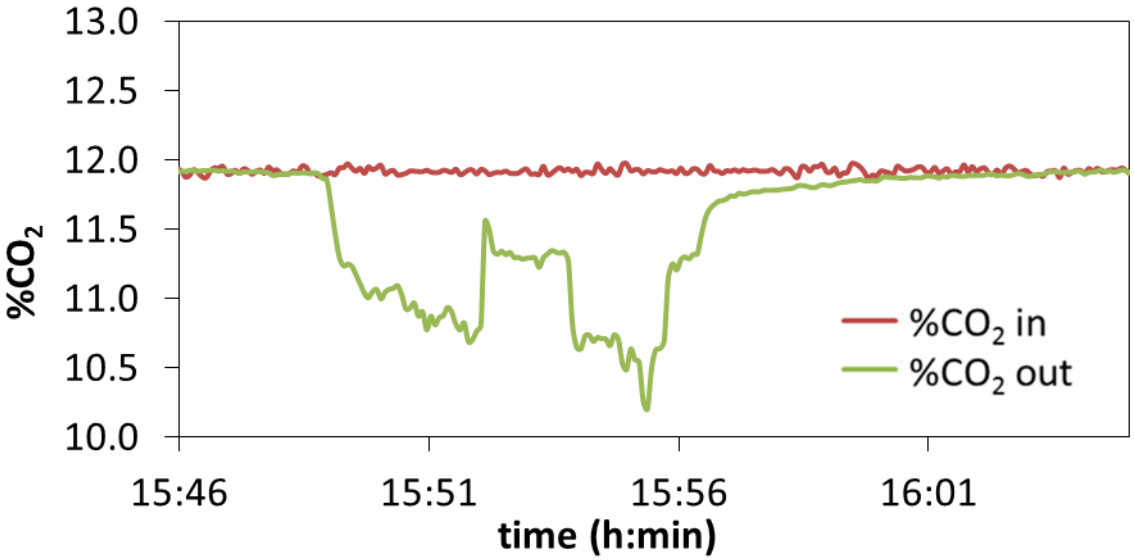

Experiment 2

Solid fed	CaO
Xave	0.41
T (°C)	668
u_{gas} (m/s)	0.96
CO_2 in (vol%)	24.0
Solid flow (kg/h)	3.2
Total gas flow (m^3/h)	7.9
H_2O (vol%)	0.0

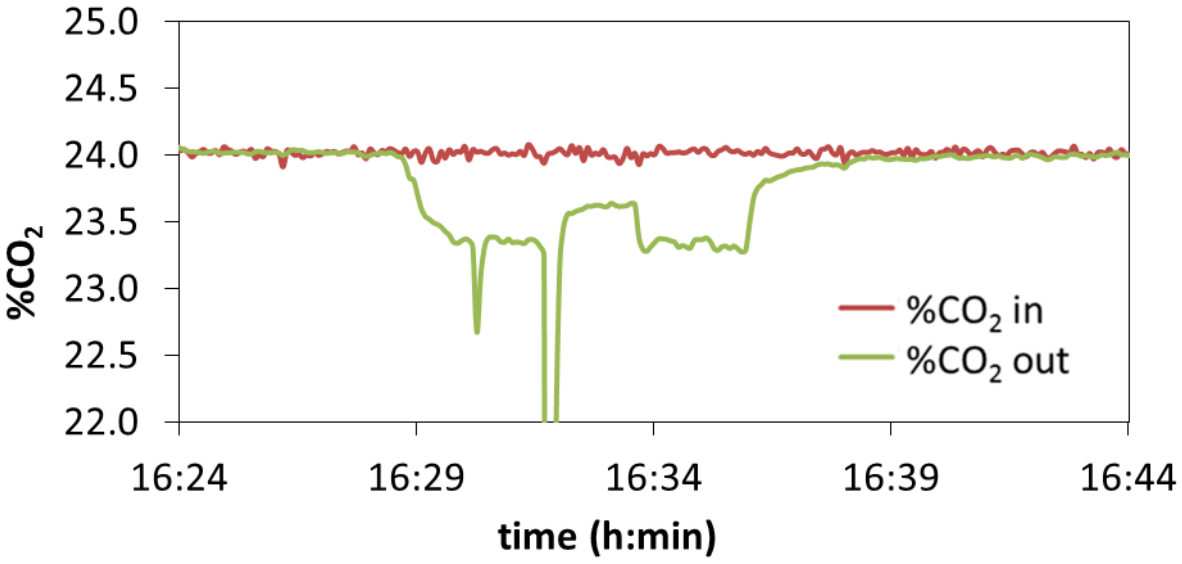

This project has received funding from the European Union's Horizon2020 Research and Innovation Programme under Grant Agreement No 641185

Experiment 3

Solid fed	CaO
Xave	0.41
T (°C)	669
u_{gas} (m/s)	0.88
CO_2 in (vol%)	19.3
Solid flow (kg/h)	3.1
Total gas flow (m^3/h)	7.2
H_2O (vol%)	0.0

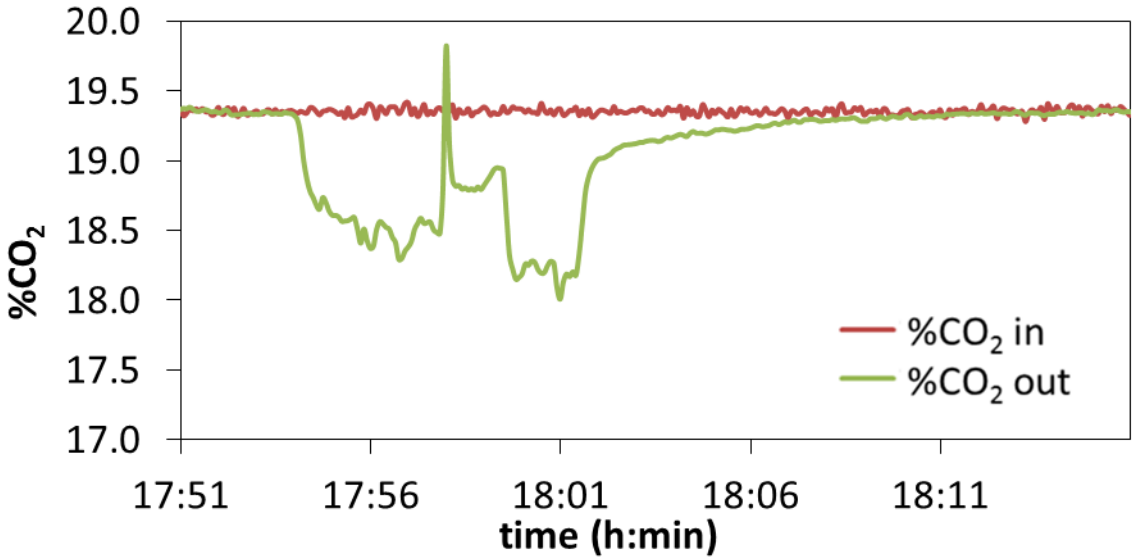

Experiment 4

Solid fed	CaO
Xave	0.41
T (°C)	665
u_{gas} (m/s)	0.90
CO_2 in (vol%)	4.1
Solid flow (kg/h)	3.0
Total gas flow (m^3/h)	7.4
H_2O (vol%)	0.0

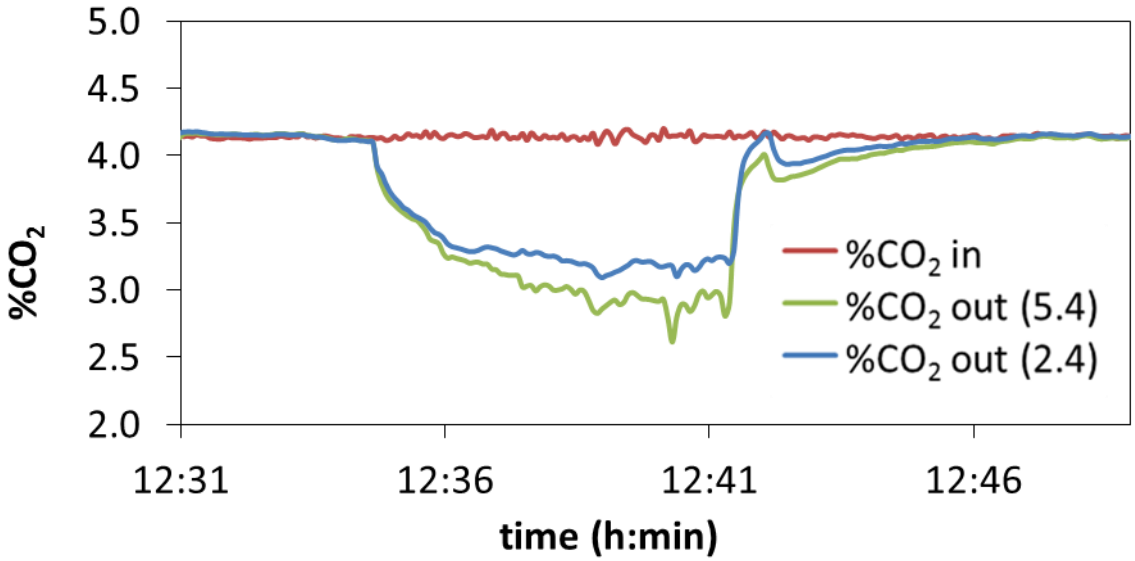

This project has received funding from the European Union's Horizon2020 Research and Innovation Programme under Grant Agreement No 641185

Experiment 5

Solid fed	CaO
Xave	0.41
T (°C)	642
u_{gas} (m/s)	1.68
CO_2 in (vol%)	5.5
Solid flow (kg/h)	3.1
Total gas flow (m^3/h)	14.2
H_2O (vol%)	0.0

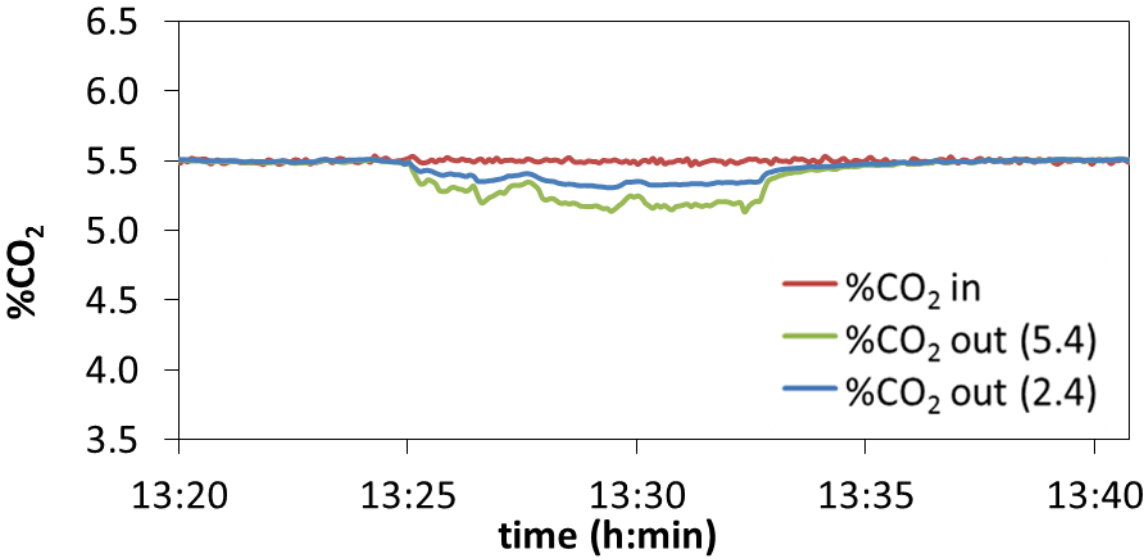

Experiment 6

Solid fed	CaO
Xave	0.41
T (°C)	643
u_{gas} (m/s)	1.96
CO_2 in (vol%)	15.0
Solid flow (kg/h)	3.2
Total gas flow (m^3/h)	16.5
H_2O (vol%)	0.0

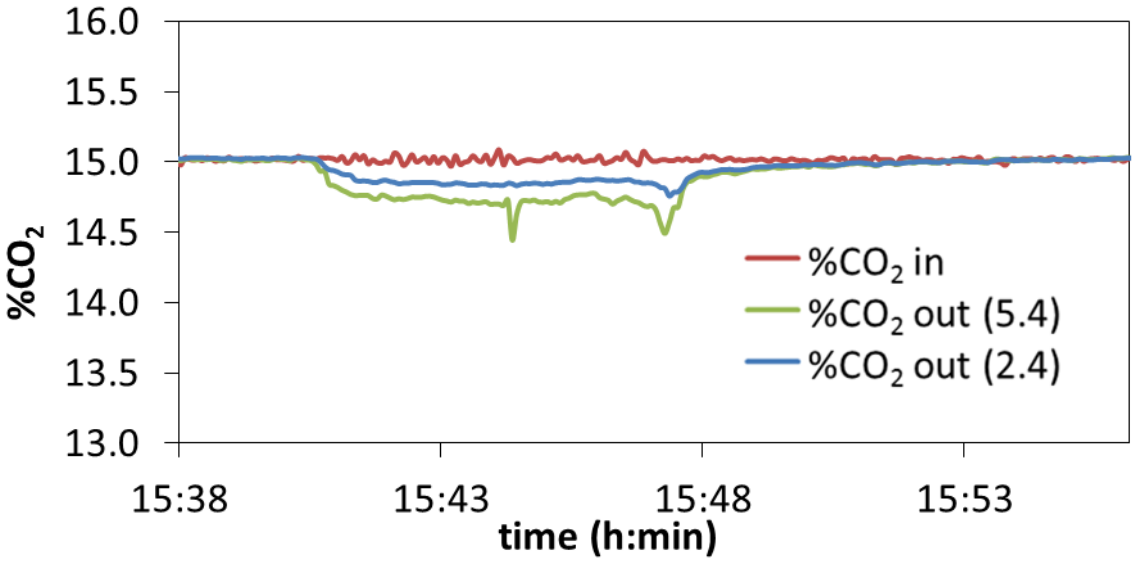

This project has received funding from the European Union's Horizon2020 Research and Innovation Programme under Grant Agreement No 641185

Experiment 7

Solid fed	CaO
Xave	0.41
T (°C)	653
u_{gas} (m/s)	1.98
CO_2 in (vol%)	22.6
Solid flow (kg/h)	3.2
Total gas flow (m^3/h)	16.5
H_2O (vol%)	0.0

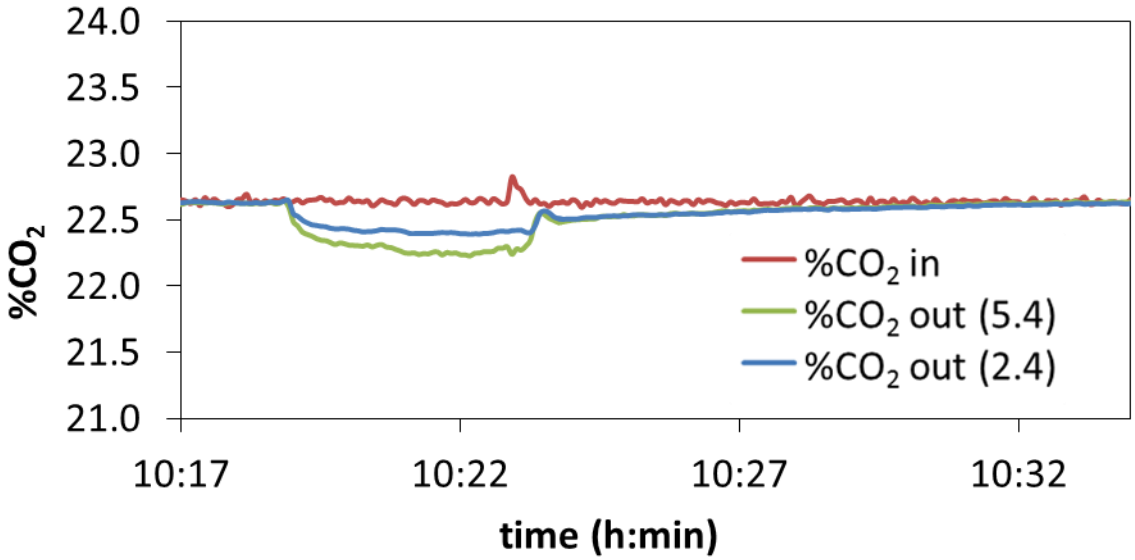

Experiment 8

Solid fed	CaO
Xave	0.41
T (°C)	671
u_{gas} (m/s)	0.72
CO_2 in (vol%)	6.0
Solid flow (kg/h)	3.2
Total gas flow (m^3/h)	5.9
H_2O (vol%)	0.0

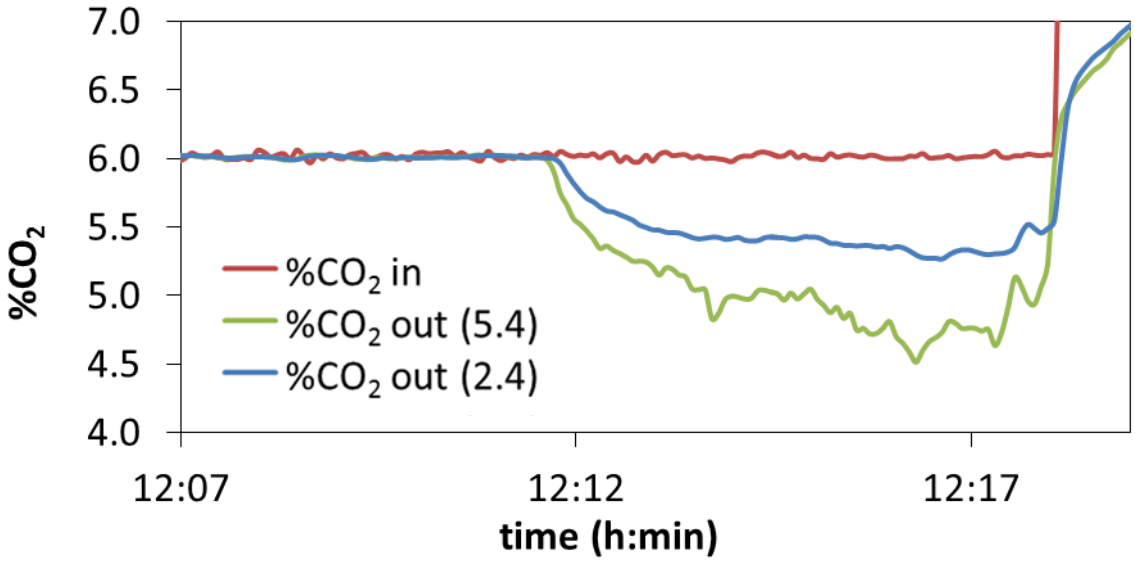

This project has received funding from the European Union's Horizon2020 Research and Innovation Programme under Grant Agreement No 641185

Experiment 9

Solid fed	CaO
Xave	0.41
T (°C)	669
u_{gas} (m/s)	0.85
CO_2 in (vol%)	14.1
Solid flow (kg/h)	3.0
Total gas flow (m^3/h)	7.0
H_2O (vol%)	0.0

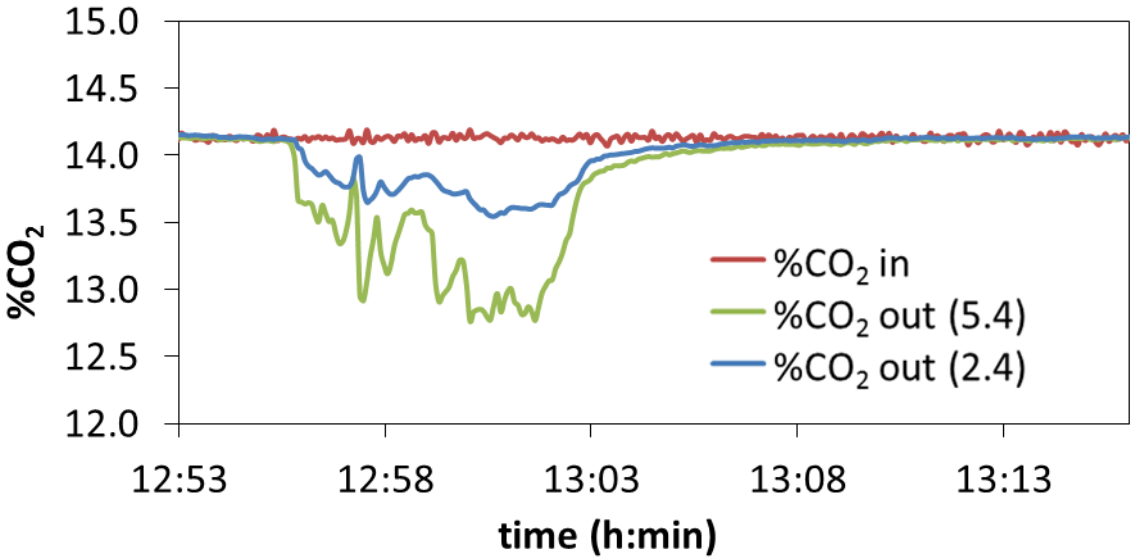

Experiment 10

Solid fed	CaO
Xave	0.41
T (°C)	669
u_{gas} (m/s)	0.86
CO_2 in (vol%)	14.0
Solid flow (kg/h)	2.8
Total gas flow (m^3/h)	7.1
H_2O (vol%)	0.0

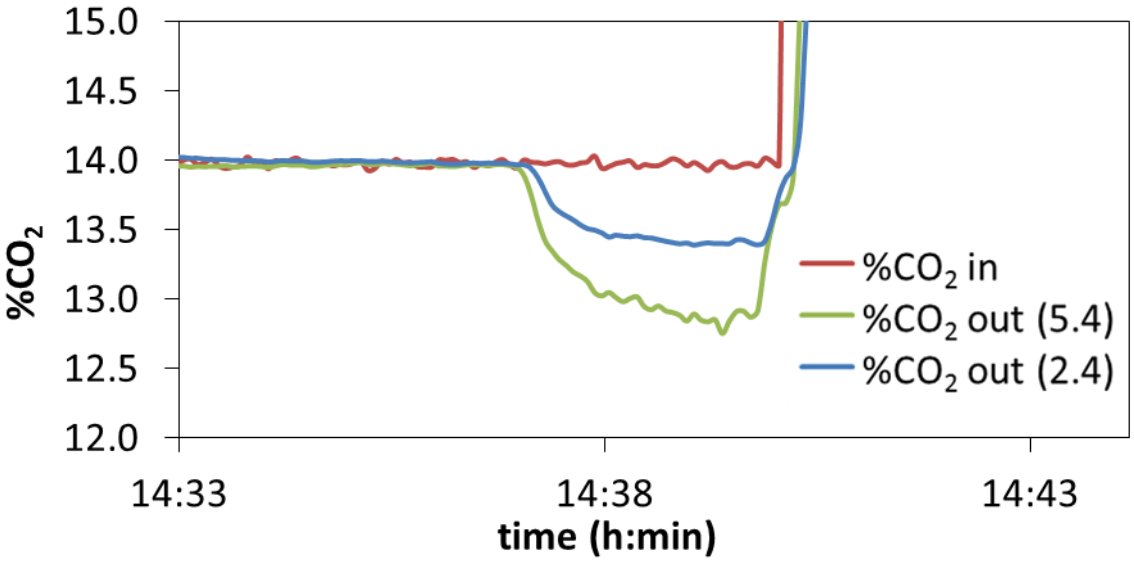

This project has received funding from the European Union's Horizon2020 Research and Innovation Programme under Grant Agreement No 641185

Experiment 11

Solid fed	CaO
Xave	0.41
T (°C)	667
u_{gas} (m/s)	1.06
CO_2 in (vol%)	14.0
Solid flow (kg/h)	3.0
Total gas flow (m^3/h)	8.7
H_2O (vol%)	0.0

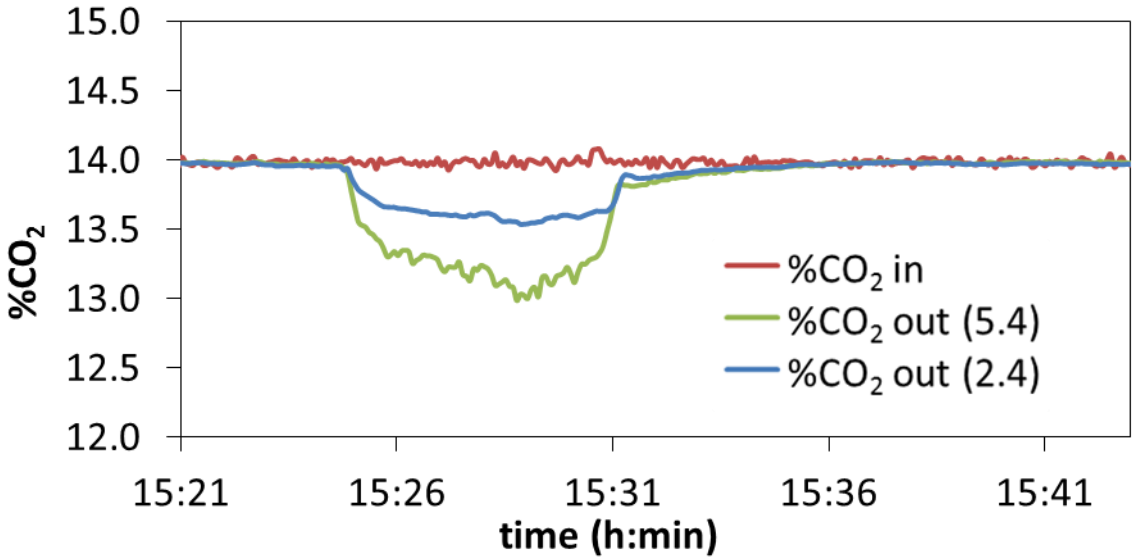

Experiment 12

Solid fed	CaO
Xave	0.41
T (°C)	668
u_{gas} (m/s)	0.88
CO_2 in (vol%)	5.5
Solid flow (kg/h)	3.2
Total gas flow (m^3/h)	7.2
H_2O (vol%)	0.0

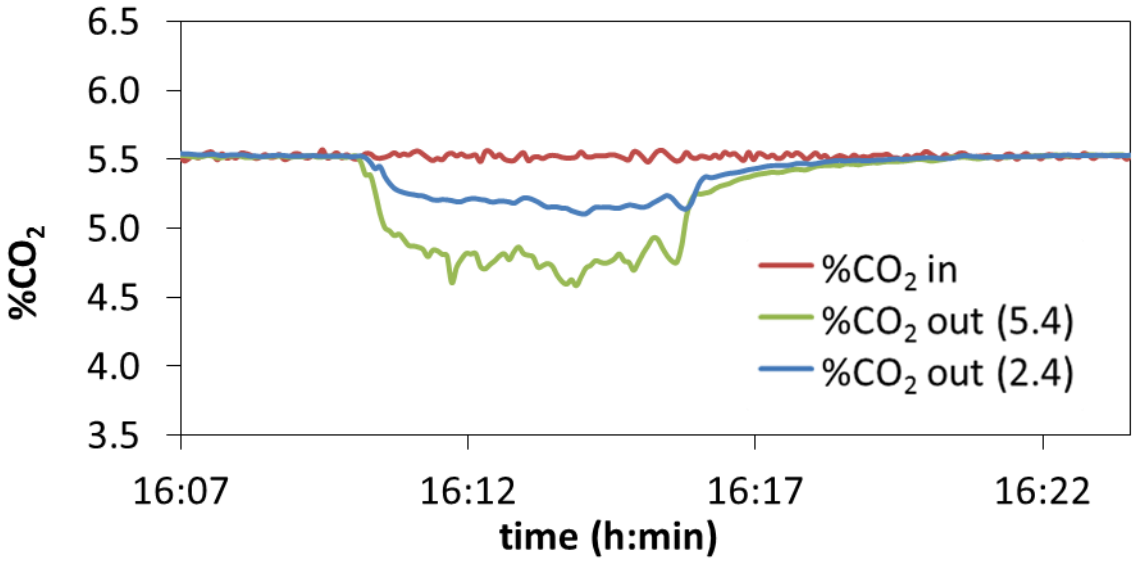

This project has received funding from the European Union's Horizon2020 Research and Innovation Programme under Grant Agreement No 641185

Experiment 13

Solid fed	CaO
Xave	0.41
T (°C)	669
u_{gas} (m/s)	0.97
CO_2 in (vol%)	14.1
Solid flow (kg/h)	3.1
Total gas flow (m^3/h)	8.0
H_2O (vol%)	0.0

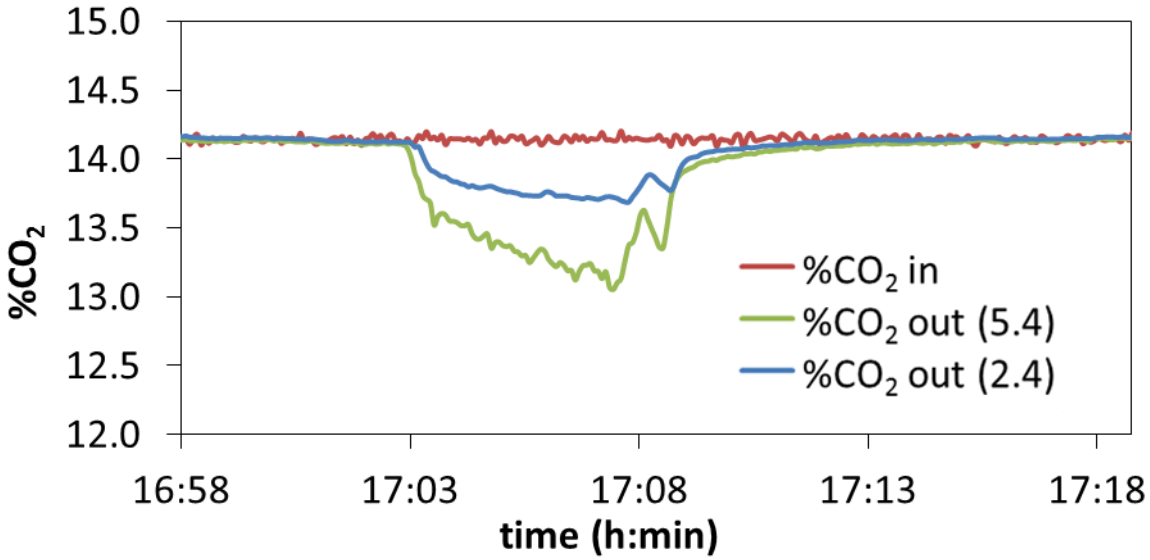

Experiment 14

Solid fed	CaO
Xave	0.41
T (°C)	667
u_{gas} (m/s)	0.95
CO_2 in (vol%)	5.8
Solid flow (kg/h)	2.5
Total gas flow (m^3/h)	7.8
H_2O (vol%)	0.0

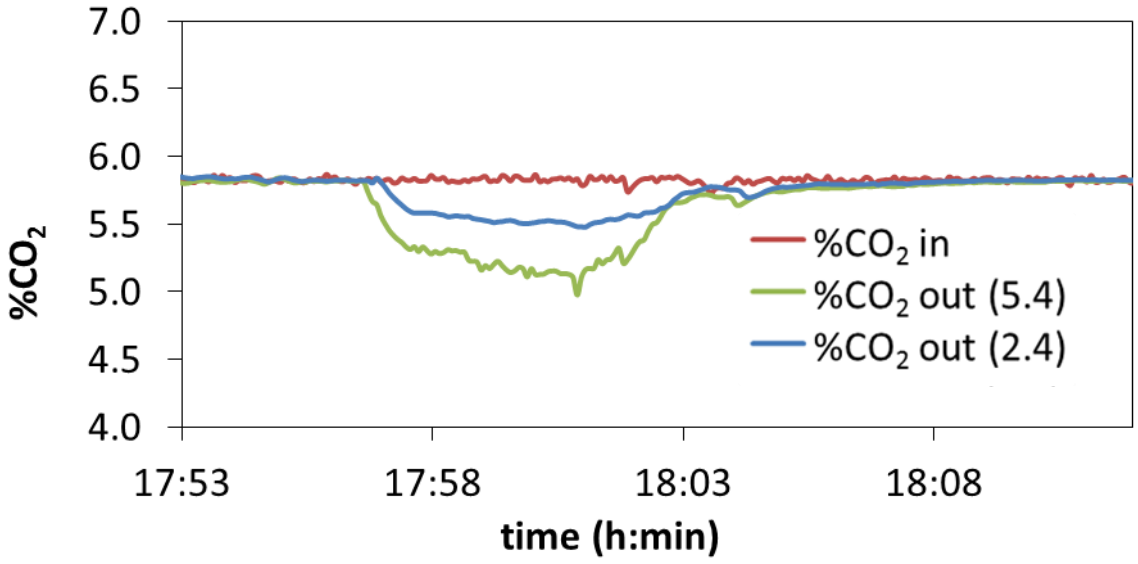

This project has received funding from the European Union's Horizon2020 Research and Innovation Programme under Grant Agreement No 641185

Experiment 15

Solid fed	CaO
Xave	0.41
T (°C)	675
u_{gas} (m/s)	0.98
CO_2 in (vol%)	22.5
Solid flow (kg/h)	3.7
Total gas flow (m^3/h)	8.0
H_2O (vol%)	0.0

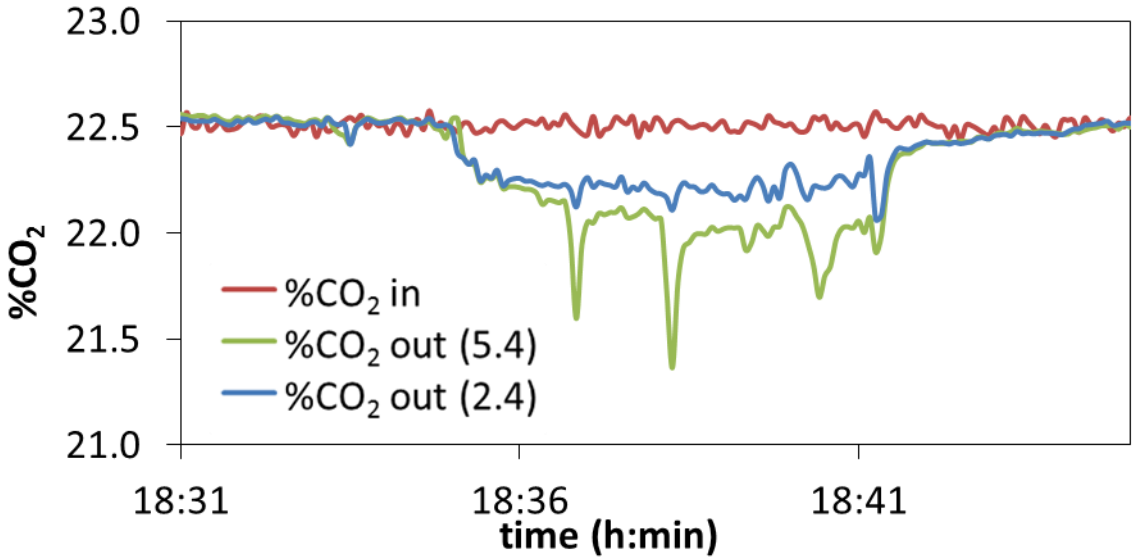

Experiment 16

Solid fed	CaO
Xave	0.41
T (°C)	659
u_{gas} (m/s)	2.21
CO_2 in (vol%)	14.0
Solid flow (kg/h)	3.8
Total gas flow (m^3/h)	18.3
H_2O (vol%)	12.5

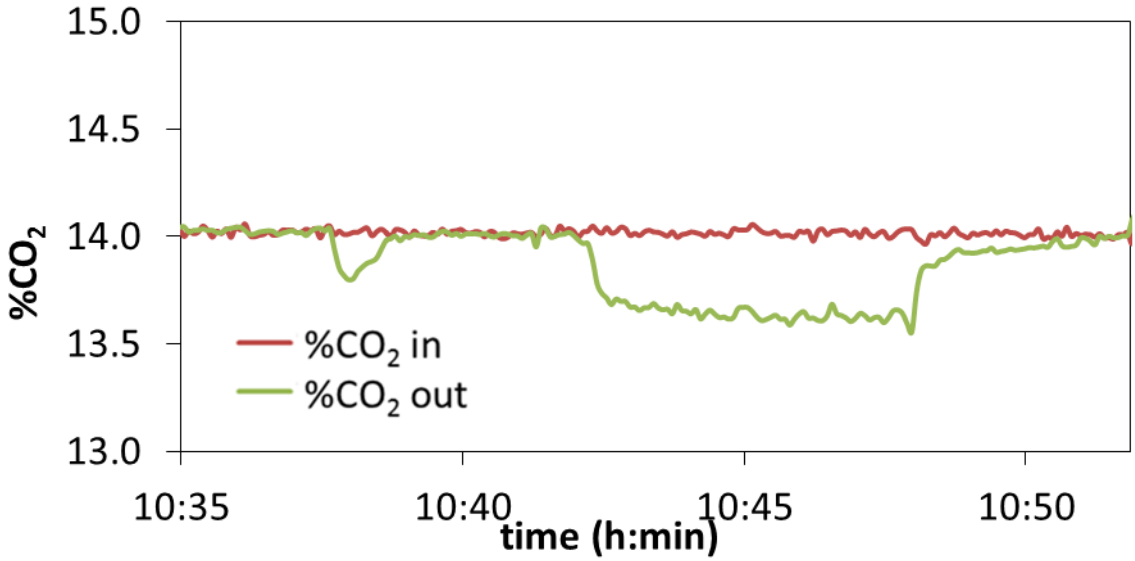

This project has received funding from the European Union's Horizon2020 Research and Innovation Programme under Grant Agreement No 641185

A.5.7 Campaign 7: entrained 'down-flow' testing using the drain-tube solid feeding system and calcined limestone as a sorbent: study of the steam influence

The objective of this campaign was to study the influence of steam on CO_2 capture. The reactors set up and the solid feeding system was the same as the ones used in the former campaign. The steam was injected in the bottom of the gas pre-heater reactor and carried together with the CO_2 and air to the top of the carbonator reactor. The CO_2 concentration was measured at 2.4 and 5.4 m from the injection point by using one analyzer (approximately during the two initial minutes at 5.4m, then 2 minutes at 2.4 m and 2 min at 5.4 m again).

The sorbent used was calcined limestone with 0.41 of CO_2 carrying capacity. The CO_2 concentration was settled on 15%$_v$ but the gas velocity ranged from 0.8 to 2m/s in order to sweep as many residence time as possible. The temperature was kept constant at around 660°C.

This project has received funding from the European Union's Horizon2020 Research and Innovation Programme under Grant Agreement No 641185

Experiment 1

Solid fed	CaO
Xave	0.41
T (°C)	659
u_{gas} (m/s)	2.21
CO_2 in (vol%)	14.0
Solid flow (kg/h)	3.8
Total gas flow (m^3/h)	18.3
H_2O (vol%)	12.5

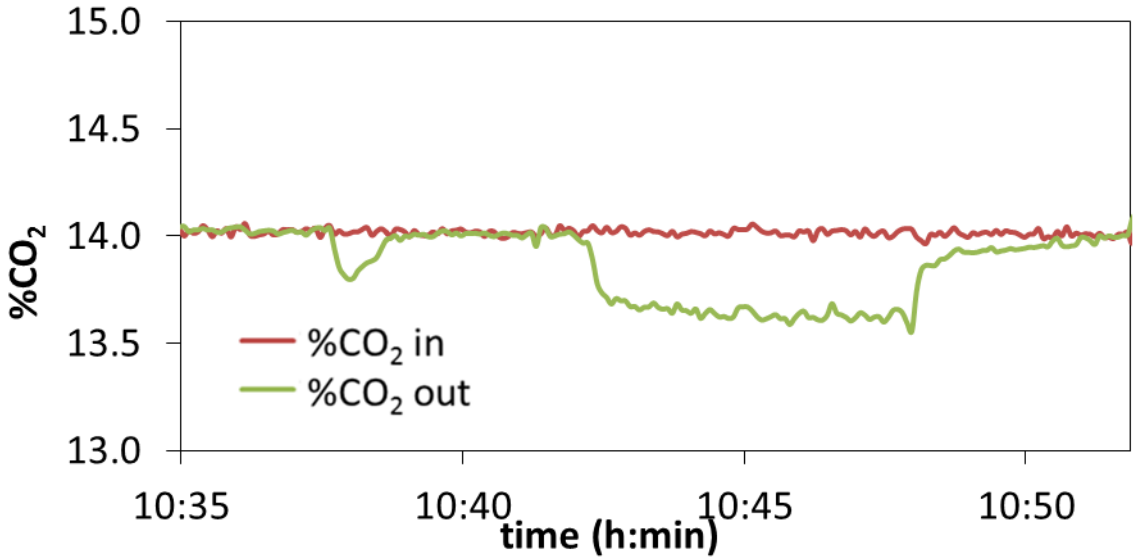

Experiment 2

Solid fed	CaO
Xave	0.41
T (°C)	664
u_{gas} (m/s)	2.26
CO_2 in (vol%)	13.9
Solid flow (kg/h)	3.5
Total gas flow (m^3/h)	18.6
H_2O (vol%)	12.7

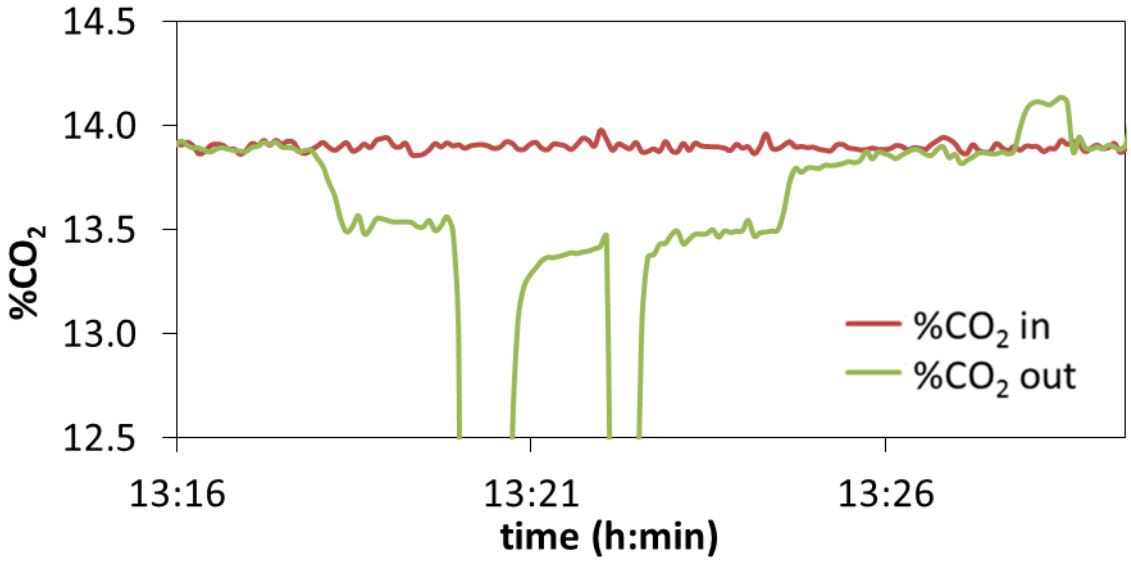

This project has received funding from the European Union's Horizon2020 Research and Innovation Programme under Grant Agreement No 641185

Experiment 3

Solid fed	CaO
Xave	0.41
T (°C)	686
u_{gas} (m/s)	1.32
CO_2 in (vol%)	13.5
Solid flow (kg/h)	3.3
Total gas flow (m^3/h)	10.6
H_2O (vol%)	22.3

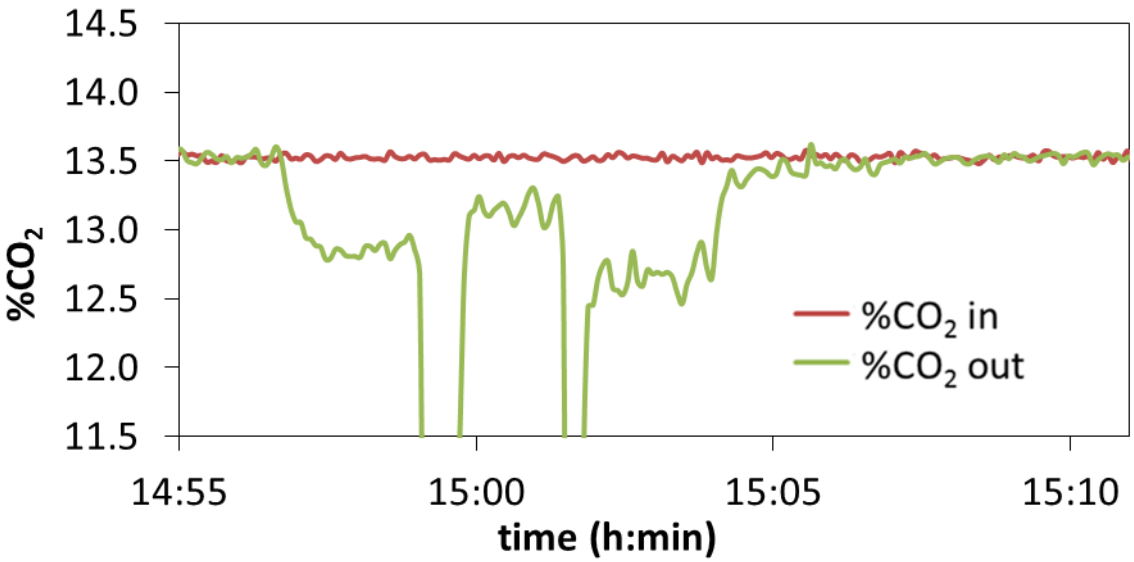

Experiment 4

Solid fed	CaO
Xave	0.41
T (°C)	652
u_{gas} (m/s)	2.37
CO_2 in (vol%)	13.2
Solid flow (kg/h)	3.7
Total gas flow (m^3/h)	19.8
H_2O (vol%)	12.0

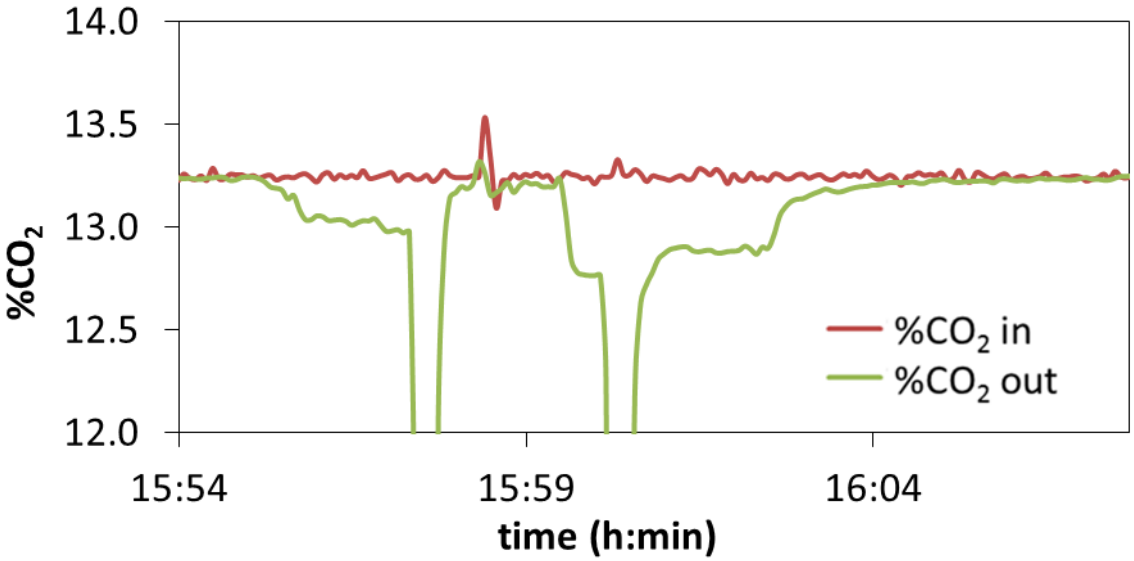

This project has received funding from the European Union's Horizon2020 Research and Innovation Programme under Grant Agreement No 641185

Experiment 5

Solid fed	CaO
Xave	0.41
T (°C)	679
u_{gas} (m/s)	1.27
CO_2 in (vol%)	13.7
Solid flow (kg/h)	3.3
Total gas flow (m^3/h)	10.3
H_2O (vol%)	23.0

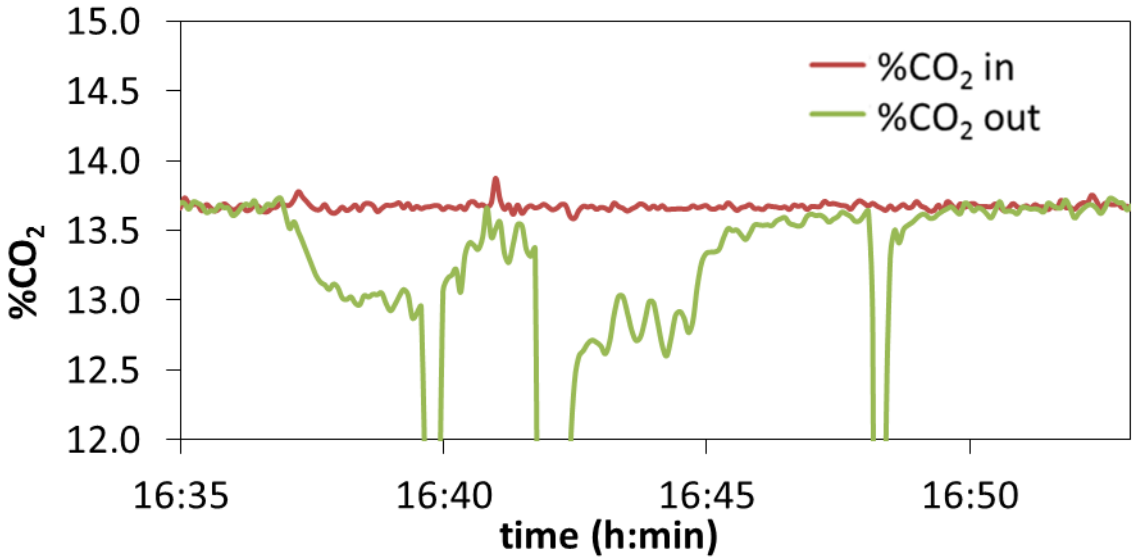

Experiment 6

Solid fed	CaO
Xave	0.41
T (°C)	683
u_{gas} (m/s)	1.05
CO_2 in (vol%)	13.9
Solid flow (kg/h)	3.3
Total gas flow (m^3/h)	8.5
H_2O (vol%)	27.9

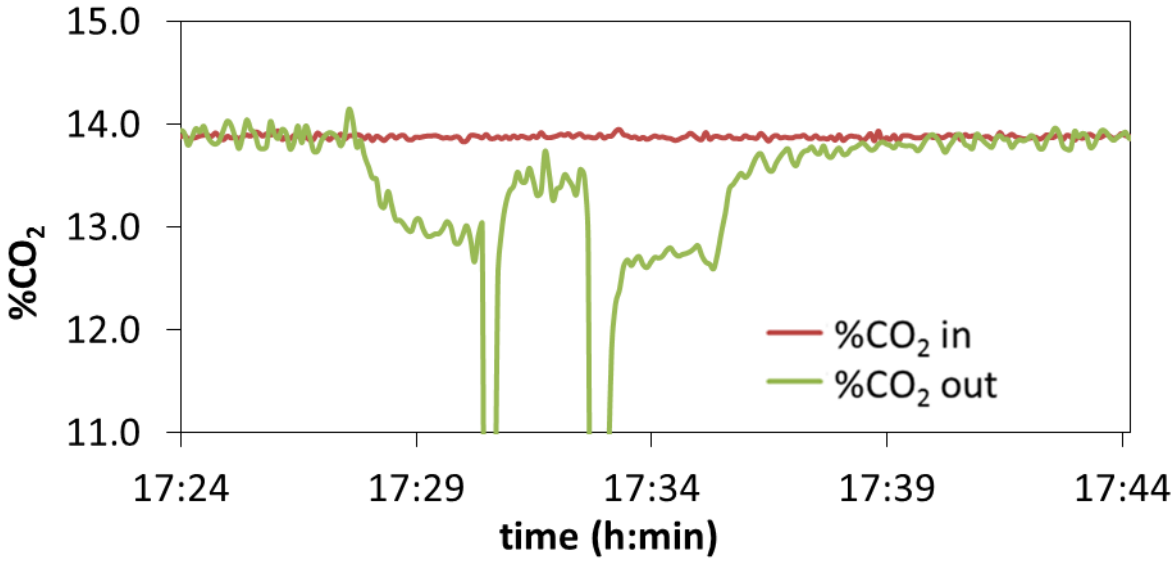

This project has received funding from the European Union's Horizon2020 Research and Innovation Programme under Grant Agreement No 641185

This project has received funding from the European Union's Horizon2020 Research and Innovation Programme under Grant Agreement No 641185